FABRICATION OF DEGRADABLE POLYMER COATED NANOPARTICLES

by

Nora Ejderyan

B.S., Chemistry, Bogazici University, 2018

Submitted to the Institute for Graduate Studies in
Science and Engineering in partial fulfillment of
the requirements for the degree of
Master of Science

Graduate Program in Chemistry

Bogazici University

2020

Dedicated to my mother and father

ACKNOWLEDGEMENTS

First of all, I would like to thank my thesis supervisor Prof. Dr. Amitav Sanyal since he accepted me as his master student and he gave me a great chance for a research experience in Sanyal Group. Throughout the thesis, his endless support and trust motivated me to work in my project with passion. I feel very lucky to work under his supervision in his lab and I am so thankful for the contributions both in theoretical and experimental chemistry and self-improvement in my personal life.

I would like to thank Prof. Dr. Rana Sanyal for being a role model in my life and her contributions in my research.

I wish to extend my thanks to Assist. Prof. Tuğçe Nihal Gevrek Civan for reviewing and improving my thesis. I am thankful that she was my defense jury.

I am so glad to work with encouraging friends. First of all, I want to thank Yavuz Öz for patience, great support and friendship during my research. I would like to thank Filiz Çalık for her great supports and motivation in every aspect of my life. I would like to thank the rest of my friends in Sanyal Lab and my ex-lab mate Dr. Laura Chambre and Görkem Bilgin for their friendship and support from the beginning.

I want to thank my mother and father for their endless love and support.

Finally, I would like to thank The Scientific and Technological Research Council of Turkey (TÜBİTAK) for funding the research (Project No: 217Z072).

ABSTRACT

FABRICATION OF DEGRADABLE POLYMER COATED NANOPARTICLES

In recent years, interest in polymer drug conjugate delivery systems has increased. When these polymer drug conjugate systems are conjugated with magnetic nanoparticles, they can be used as delivery systems by creating magnetic field. In this thesis, firstly monodisperse oleic acid coated, iron oxide nanoparticles were synthesized by thermal decomposition method. By place exchange reaction, these nanoparticles were coated by chain transfer agents which are modified with dopamine and have disulfide bond in their structure. Then PEG based polymer were grafted from the surface of iron oxide nanoparticles by RAFT polymerization in order to make them hydrophilic. In this system, there are disulfide bonds between polymeric brushes and nanoparticles and these bonds can be cleaved by glutathione which is found in excess at diseased tissues. Importantly, it is difficult to characterize the molecular weights of the polymers which were grown from the surface of nanoparticles 'by grafting-from' approach. We envisioned that mild methods to cleave the polymers from nanoparticle surfaces will facilitate their characterization. We demonstrate that treatment with glutathione cleaves the polymeric brushes from nanoparticles under mild conditions. Thus, this study provides an excellent way to analyze molecular weight and molecular weight distributions of polymer brushes. In order to understand the cleavage kinetics, polymer brushes containing fluorescent dye were synthesized. Also, the fluorescent dye acts as a model hydrophobic drug. Incorporation of the dye into polymer brushes provides it with water solubility. Finally, we demonstrated that the trithiocarbonate end groups of polymers can be modified with azo initiators for purposes of attachment of any biomolecules.

ÖZET

KIRILABİLİR POLİMER FIRÇA KAPLI NANOPARÇACIKLARIN FABRİKASYONLARI

Son yıllarda, polimer konjuge ilaç taşıma sistemlerine ilgi artmaktadır. Küçük molekül yapıdaki ilaçlar veya makromoleküler konjugatların manyetik alanla hedeflenen dokulara taşınması, bu ilaçların manyetik nanoparçacıklara konjugasyonları ile mümkündür ve bu konjugasyon için çeşitli yöntemler geliştirilmektedir. Bu tezde, öncelikle oleik asit kaplı demir oksit manyetik nanoparçacıklar termal dekompozisyon metodu ile sentezlenmiştir. Yer değiştirme reaksiyonu ile nanoparçacıklar kırılabilir disülfür bağları içeren, dopamin ile modifiye edilmiş, zincir transfer ajanları ile kaplanmıştır. Daha sonra yüzeyden büyütme yaklaşımı ve RAFT polimerizasyonu ile bu ajanlar üzerinden polimerik fırçalar büyütülmüştür böylece manyetik nanoparçacıklar PEG bazlı hidrofilik polimerler ile kaplanmıştır. Bu sistemde yer alan kırılabilir bağlar redoks ortamına karşı duyarlıdır. Hastalıklı dokularda fazla miktarda bulunan, indirgen madde glutatyon sayesinde polimerler nanoparçacıklardan kolayca ayrılabilmektedir. Polimer zinciri, "yüzeyden büyütme" yaklaşımı kullanılarak bir nanoparçacık yüzeyinden büyütüldüğünde, polimer yüzeyden ayrılamadığı ve analiz edilemediği için moleküler ağırlık ve moleküler ağırlık dağılımları gibi özellikleri tespit etmek oldukça zordur. Burada geliştirilen sistemde, polimerik fırçalar yüzeyden ayrılabildiği için çok ılımlı koşullar altında özelliklerinin verimli bir şekilde belirlenmesi sağlanmıştır. Kontrol grup olarak da kırılabilir disülfür bağı içermeyen system kullanılmıştır. Ayrıca, taşıyıcı olarak kullanılacak sistemde, model ilaç olarak floresan hidrofobik boya molekülü monomer olarak kullanılmıştır. Nanoparçacıklar üzerlerinden floresan boya ve PEG bazlı kopolimerik fırçalar büyütülmüştür böylece hidrofobik olan boya molekülü suda çözünürlük kazanmıştır. Son olarak da polimerlerin tritiyokarbonat uçları NHS gruplarıyla modifiye edilmiştir, böylece polimer nanoparçacık konjuge sistemi biyomoleküllerin bağlanmasına açık hale gelmiştir.

TABLE OF CONTENTS

ACKNOWLEDGEMENTS iv
ABSTRACT v
ÖZET vi
TABLE OF CONTENTS vii
LIST OF FIGURES xii
LIST OF TABLES xvi
LIST OF ACRONYMS/ ABBREVIATIONS xvii
1. INTRODUCTION 1
1.1. Iron Oxide Nanoparticles 1
1.1.1. Types of Iron Oxide Nanoparticles 2
1.1.2. Magnetic Property of Iron Oxide Nanoparticles 4
1.1.3. Synthesis of Iron Oxide Nanoparticles 5
1.2. Coating of Iron Oxide Nanoparticles 8
1.2.1. Anchoring Groups Used in Attaching Protecting Groups 8
1.2.2. Hydrophobic Coating of Iron Oxide Nanoparticles 9
1.2.3. Hydrophilic Coating of Iron Oxide Nanoparticles 10
1.3. Polymer Grafting for Iron Oxide Nanoparticles 10
1.4. Reversible Addition-Fragmentation Chain-Transfer (RAFT) Polymerization 12
1.5. End Group Modification after RAFT Polymerization 14
1.6. Disulfide Cleavage Reaction under Redox Environment 16
2. FABRICATION OF CLEAVABLE POLYMER COATED NANOPARTICLES 18
2.1. Aim of the Study 18
3. EXPERIMENTAL 20
3.1. Materials 20

3.2. Instrumentation 20

3.3. Iron Oxide Nanoparticles Synthesis 21

3.4. Synthesis of Dopamine Modified Chain Transfer Agent (CTA) 21

3.4.1. Synthesis of 2-(((dodecylthio)carbonothioyl)thio)-2-methylpropanoic acid (CTA) 21

3.4.2. Synthesis of 2,5-dioxopyrrolidin-1-yl 2-(((dodecylthio)carbonothioyl)thio)-2-methylpropanoate (CTA-NHS) 21

3.4.3. Synthesis of 1-((3,4-dihydroxyphenethyl)amino)-2-methyl-1-oxopropan-2-yl dodecyl carbonotrithioate (CTA-Dopa) 21

3.5. Synthesis of Disulfide Containing Chain Transfer Agent 22

3.5.1. Synthesis of 2-((2-hydroxyethyl)disulfaneyl)ethyl 2-(((dodecylthio)carbonothioyl)thio)-2-methylpropanoate (CTA-SS-OH) 22

3.5.2. Synthesis of 2- ((2- ((((2,5-dioxopyrrolidin-1-yl)oxy)carbonyl)oxy)ethyl) disulfaneyl)ethyl 2-(((dodecylthio) carbonothioylthio)-2-methylpropanoate (CTA-SS-DSC) 22

3.5.3. Synthesis of 2- ((2- (((3,4- dihydroxyphenethyl)carbamoyl)oxy)ethyl) disulfaneyl)ethyl 2- (((dodecylthio)carbonothioyl)thio)-2-methylpropanoate (CTA-SS-Dopa) 23

3.6. Place Exchange Reaction between Oleic Acid-Coated Nanoparticle and Chain Transfer Agent 23

3.6.1. Place Exchange Reaction between Fe_3O_4@OA and CTA-Dopa (Fe_3O_4@Dopa-CTA) 23

3.6.2. Place Exchange Reaction between Fe_3O_4@OA and CTA-SS-Dopa (Fe_3O_4@Dopa-SS-CTA) 24

3.7. RAFT Polymerization of PEGMEA from the Surface of Fe_3O_4 Nanoparticles 24

3.7.1. Synthesis of Polymer-Coated Fe_3O_4 Nanoparticles (Fe_3O_4 @Dopa-PEGMEA) 24

3.7.2. Synthesis of Degradable Polymer-Coated Fe_3O_4 Nanoparticles (Fe_3O_4 @Dopa-SS-PEGMEA) 25

3.8. Reductive Cleavage of PEGMEA Polymers from Fe_3O_4 Nanoparticles 25
3.9. RAFT Polymerization of PEGMEA from the Surface of Fe_3O_4 Nanoparticles (Fe_3O_4@Dopa-SS-PEGMEA) and Free CTA (Dopa-SS-PEGMEA) 26
3.10. Synthesis of BODIPY Dye Monomer 26
3.10.1. Synthesis of BODIPY Bromide (BODIPY-Br) 26
3.10.2. Synthesis of BODIPY Acetate (BODIPY-OAc) 26
3.10.3. Synthesis of BODIPY Alcohol (BODIPY-OH) 27
3.10.4. Synthesis of BODIPY Acrylate Monomer 27
3.11. RAFT Copolymerization of PEGMEA and BODIPY Acrylate from the Surface of Fe_3O_4 Nanoparticles (Fe_3O_4@Dopa-SS-PEGMEA-r-BODIPY) 27
3.12. Reductive Cleavage of PEGMEA and BODIPY Copolymer Brushes from Fe_3O_4 Nanoparticles 28
3.13. End Group Modification of Polymer-Coated Fe_3O_4 Nanoparticles 28
3.13.1. Synthesis of (E)-bis(2,5-dioxopyrrolidin-1-yl) 4,4'-(diazene-1,2-diyl)bis(4-cyanopentanoate) (NHS-ACVA) 28
3.13.2. End Group Modification of Degradable Polymer-Coated Fe_3O_4 Nanoparticles with NHS activated Carboxylic Acid Containing Azo Initiator (Fe_3O_4@Dopa-SS-PEGMEA-NHS) 29
4. RESULTS AND DISCUSSIONS 30
4.1. Synthesis of Fe_3O_4 Nanoparticles and Characterizations 30
4.2. Synthesis of Dopamine Modified Chain Transfer Agent (CTA) and Characterizations 31
4.2.1. Synthesis of 2-(((dodecylthio)carbonothioyl)thio)-2-methylpropanoic acid (CTA) 31
4.2.2. Synthesis of Dopamine Modified Chain Transfer Agent (CTA-Dopa) 32
4.3. Synthesis of Disulfide Containing Dopamine Modified Chain Transfer Agent (CTA) and Characterizations 33
4.3.1. Synthesis of Chain Transfer Agent Alcohol (CTA-SS-OH) 33

4.3.2. Synthesis of DSC Activated Chain Transfer Agent (CTA-SS-DSC) 34

4.3.3. Synthesis of Dopamine Modified Disulfide Containing Chain Transfer Agent (CTA-SS-Dopa) 35

4.4. Immobilization of Chain Transfer Agent onto Fe_3O_4 Nanoparticles by Ligand Exchange Reaction and Characterizations 37

4.4.1. Immobilization of CTA-Dopa onto Fe_3O_4 Nanoparticles (Fe_3O_4@Dopa-CTA) 37

4.4.2. Immobilization of CTA-SS-Dopa onto Fe_3O_4 Nanoparticles (Fe_3O_4@Dopa-SS-CTA) 39

4.5. Surface Initiated RAFT Polymerization of PEGMEA from the Surface of Fe_3O_4 Nanoparticles and Characterizations 40

4.5.1. Synthesis of Polymer-Coated Fe_3O_4 Nanoparticles (Fe_3O_4@Dopa-PEGMEA) 40

4.5.2. Synthesis of Degradable Polymer-Coated Fe_3O_4 Nanoparticles (Fe_3O_4@Dopa-SS-PEGMEA) 42

4.6. Degradation of PEGMEA Polymeric Brushes from the Surface of Fe_3O_4 Nanoparticles and Characterizations 45

4.6.1. Reductive Cleavage of PEGMEA Polymers from Fe_3O_4 Nanoparticles 45

4.6.2. Molecular Weight and PDI Analysis of Cleaved Polymeric Brushes 48

4.6.3. Polymerization of PEGMEA From the Surface of Nanoparticle (Fe_3O@Dopa-SS-PEGMEA) and From the Free CTA (Dopa-SS-PEGMEA) 49

4.6.4. Polymerization of PEGMEA From the Surface of Nanoparticle (Fe_3O@Dopa-SS-PEGMEA) at Different Conditions 50

4.7. Synthesis of BODIPY Dye Monomer 52

4.7.1. Synthesis of BODIPY Bromide (BODIPY-Br) 52

4.7.2. Synthesis of BODIPY Acetate (BODIPY-OAc) 53

4.7.3. Synthesis of BODIPY Alcohol (BODIPY-OH) 53

4.7.4. Synthesis of BODIPY Acrylate Monomer 54

4.8. RAFT Copolymerization of PEGMEA and BODIPY Acrylate from the Surface of Fe_3O_4 Nanoparticles (Fe_3O_4@Dopa-SS-PEGMEA-r-BODIPY) 55

4.9. Reductive Cleavage of PEGMEA and BODIPY Copolymer Brushes from Fe_3O_4 Nanoparticles 58

4.10. Release Study of PEGMEA and BODIPY Copolymer Brushes from Fe_3O_4 Nanoparticles by Glutathione 59

4.11. Functionalization of Polymer-Coated Fe_3O_4 Nanoparticles by End Group Modifications 60

4.11.1. Synthesis of NHS Containing Carboxylic Acid Functionalized V-501 Azo Initiator (NHS-ACVA) 60

4.11.2. End Group Modification of Polymer-Coated Fe_3O_4 Nanoparticles by NHS Activated Carboxylic Acid Containing Azo Initiator 61

5. CONCLUSION 63

REFERENCES 64

APPENDIX A: COPYRIGHT NOTICES 72

LIST OF FIGURES

Figure 1.1. Types of iron oxide nanoparticles [12]. 3

Figure 1.2. Transformation of iron oxide nanoparticles. 3

Figure 1.3. Magnetization characteristics of magnetic materials [14]. 4

Figure 1.4. The behavior of the size-dependent coercivity of nanoparticles [15]. 5

Figure 1.5. Reactions of co-precipitation method. 6

Figure 1.6. Synthetic pathway of thermal-decomposition method. 7

Figure 1.7. Anchoring groups for iron oxide nanoparticles. 8

Figure 1.8. Grafting-to approach for iron oxide nanoparticles [51]. 11

Figure 1.9. Grafting-from approach for iron oxide nanoparticles [52]. 12

Figure 1.10. Reaction mechanism of RAFT polymerization. 14

Figure 1.11. End group modification of polymer-coated iron oxide nanoparticles with protected maleimide and azide groups by radical exchange reaction. 15

Figure 1.12. Conjugation of cRGDfK to end group modified polymer coated iron oxide nanoparticles. 16

Figure 1.13. Releasing scheme of disulfide bond containing dye loaded mesoporous silica nanoparticles [59]. 17

Figure 2.1. General scheme of the project. 19

Figure 4.1. The synthesis of iron oleate complex. 30

Figure 4.2. Synthesis of iron oxide nanoparticles. 30

Figure 4.3. FT-IR spectrum (top) and DLS analysis (bottom) of Fe_3O_4@OA. 31

Figure 4.4. Synthesis of chain transfer agent (CTA). 32

Figure 4.5. Synthetic pathway of dopamine modified chain transfer agent (Dopa-CTA). 32

Figure 4.6. Synthesis of CTA-SS-OH. 33

Figure 4.7. ^{1}H NMR spectrum of CTA-SS-OH. 34

Figure 4.8. Synthesis of CTA-SS-DSC. 35

Figure 4.9. Synthesis of CTA-SS-Dopa 36

Figure 4.10. ^{1}H NMR spectrum of CTA-SS-Dopa. 36

Figure 4.11. Synthesis of Fe_3O_4@Dopa-CTA. 37

Figure 4.12. FT-IR spectrum (top left), UV spectroscopy (top right) and DLS analysis (bottom) of Fe_3O_4@Dopa-CTA 38

Figure 4.13. Ligand exchange reaction between Fe_3O_4@OA and CTA-SS-Dopa. 39

Figure 4.14. UV spectroscopy (top left), FT-IR spectrum (top right), and DLS analysis (bottom) of Fe_3O_4@Dopa-SS-CTA. 40

Figure 4.15. Surface initiated RAFT polymerization of PEGMEA. 41

Figure 4.16. FT-IR spectrum (top left) and UV-Vis spectroscopy (top right) and DLS analysis (bottom) of Fe_3O_4@Dopa-PEGMEA. 42

Figure 4.17. Synthesis of Fe_3O_4@Dopa-SS-PEGMEA by RAFT polymerization. 43

Figure 4.18. FT-IR spectrum (top left), UV spectroscopy (top right) and DLS analysis (bottom) and of Fe_3O_4@Dopa-SS-PEGMEA 44

Figure 4.19. Dispersibility difference of Fe_3O_4@Dopa-SS-CTA (left) and Fe_3O_4@Dopa-SS-PEGMEA nanoparticles 45

Figure 4.20. Cleavage of disulfide bond in polymer-coated nanoparticles by DTT. 46

Figure 4.21. Dispersibility of Fe_3O_4@Dopa-SS-PEGMEA in water (left), after treatment with DTT and centrifugation. 46

Figure 4.22. UV-Vis spectra of cleaved iron oxide nanoparticles (upper-left), polymeric brushes (upper-right) and Fe_3O_4@Dopa-SS-PEGMEA (without DTT exposure) upon treatment with Ellman's reagent. 47

Figure 4.23. Synthesis of Fe_3O_4@Dopa-SS-PEGMEA by RAFT polymerization with Free CTA. 49

Figure 4.24. Synthesis of BODIPY bromide (BODIPY-Br). 52

Figure 4.25. Synthesis of BODIPY acetate (BODIPY-OAc). 53

Figure 4.26. Synthesis of BODIPY alcohol (BODIPY-OH). 54

Figure 4.27. Synthesis of BODIPY acrylate monomer. 54

Figure 4.28. ^{1}H NMR spectrum of BODIPY acrylate monomer. 55

Figure 4.29. Synthesis of Fe_3O_4@Dopa-SS-PEGMEA-r-BODIPY by RAFT Polymerization. 56

Figure 4.30. UV-vis Spectrum of Fe_3O_4@Dopa-SS-PEGMEA-r-BODIPY 57

Figure 4.31. Dispersibility difference of BODIPY monomer (left) and Fe_3O_4@PEGMEA-r-BODIPY nanoparticles. 57

Figure 4.32. Cleavage of disulfide bond in copolymer-coated nanoparticles by DTT. 58

Figure 4.33 Dispersibility of Fe_3O_4@Dopa-SS-PEGMEA-r-BODIPY in water (left), after treatment with DTT and centrifugation. 59

Figure 4.34. Release of Fe_3O_4-Dopa-SS-PEGMEA-r-BODIPY by glutathione. 60

Figure 4.35. Synthesis of NHS-ACVA radical initiator. 61

Figure 4.36. End group modification of polymer-coated iron oxide nanoparticles by NHS-activated carboxylic acid group. 61

Figure 4.37. FT-IR spectrum (top) and UV-Vis spectra (bottom) of Fe_3O_4@Dopa-SS-PEGMEA-NHS nanoparticles. 62

Figure A.1. Copyright license of [12] 73

Figure A.2. Copyright license of [14]. 74

Figure A.3. Copyright license of [15]. 75

Figure A.4. Copyright license of [51]. 76

Figure A.5. Copyright license of [52]. 77

Figure A.6. Copyright license of [59]. 78

LIST OF TABLES

Table 4.1. Molecular weights and PDI values of polymer-coated iron oxide nanoparticles having different time polymerizations. 48

Table 4.2. Molecular weights and PDI values of polymer-coated iron oxide nanoparticles having different conditions. 51

LIST OF ACRONYMS/ ABBREVIATIONS

AcOH	Acetic Acid
ACVA	4’4-Azobis(4-cyanovaleric acid)
AIBN	2,2’-azobisisobutyronitrile
ATRP	Atom Transfer Radical Polymerization
BODIPY	4,4-difluoro-4-bora-3a,4a-diaza-s-indacene
CTA	Chain Transfer Agent
DCC	N,N'-Dicyclohexylcarbodiimide
DCM	Dichloromethane
DLS	Dynamic Light Scattering
DMAP	4-Dimethylaminopyridine
DMF	Dimethylformamide
Dopa	Dopamine
DSC	Disuccinimidyl carbonate
DTT	Dithiothreitol
EDCI	1-Ethyl-3-(3-dimethylaminopropyl)carbodiimide
EtOAc	Ethyl Acetate
EtOH	Ethanol
FT-IR	Fourier-transform infrared
GPC	Gel Permeation Chromatography
GSH	Glutathione
kDa	Kilodalton

LiOH	Lithium hydroxide
MeOH	Methanol
MNP	Magnetic Nanoparticle
NHS	N-Hydroxysuccinimide
NMR	Nuclear Magnetic Resonance
OA	Oleic Acid
PDI	Polydispersity Index
PdS	Pyridyl disulfide
PEG	Poly(ethylene glycol)
PEGMEA	Poly(ethylene glycol) methyl ether acrylate
RAFT	Reversible Addition Fragmentation Chain Transfer
rt	Room Temperature
TEA	Triethyl Amine
THF	Tetrahydrofuran
UV	Ultra-Violet

1. INTRODUCTION

1.1. Iron Oxide Nanoparticles

In the past decades, utilization of iron oxide nanoparticle has considerably increased since they can be used in many biomedical applications because of their properties. For instance, iron oxide nanoparticles are biocompatible [1], so they do not have toxic effect on body and hence can be used in *in-vivo* applications. Due to their magnetic property they can be used as magnetically guided delivery systems [2]. While several methods have been reported for their synthesis, most of these methods yield nanoparticles coated with hydrophobic monolayers. The hydrophobic layer installed during their synthesis prevents the aggregation of nanoparticles and provides them with stability [3]. As synthesized iron oxide nanoparticles can be obtained in monodisperse fashion, which means each of them have same chemical and physical properties such as size and shape, so they can be controlled according to desired applications. Control over the size and composition of nanoparticles is very important because it affects their magnetic property [4]. However, for most biomedical applications, iron oxide nanoparticles should be water dispersible. Usually these hydrophobic coatings can be replaced with hydrophilic ligands or polymer through place exchange reactions.

Due to the above-mentioned features of iron oxide nanoparticles, they play an important role in biomedical area such as drug delivery systems. Iron oxide nanoparticles can be coated with polymers or proteins such as human albumin, then drug can be loaded on them [5]. Due to their inherent magnetic property, these nanoparticles can be used as MRI agents [6]. In addition, since they are magnetically addressable, these nanoparticles can be used for bio-separation of proteins and other biomolecules [7]. Another interesting property of magnetic nanoparticles are that they undergo heating when placed in an alternating magnetic field [8]. Magnetic hyperthermia provides an alternative approach for treatment of cancer compared to traditional modalities such as chemotherapy and radiotherapy. Iron

oxide nanoparticles can be used for multimodal cellular imaging. For instance, after polymerization on surface of nanoparticles, dye molecule can be attached onto them, and their interaction with cells can be monitored [9].

1.1.1. Types of Iron Oxide Nanoparticles

There are many types of magnetic nanoparticles such as metal nanoparticles, alloys, oxides and ferrites [10]. Commonly, oxide forms of metals are used as magnetic nanoparticles for example iron, cobalt and nickel oxides. Nickel and cobalt are highly magnetic, however they are not preferred for biomedical applications because they are toxic and undergo facile oxidation [11]. In contrast, iron oxide nanoparticles are preferred for biomedical purposes since they are not as toxic as other magnetic materials. There are two forms of iron oxide nanoparticles found in nature. One of them is magnetite (Fe_3O_4), and the other one is maghemite (γ-Fe_2O_3). The magnetic property of magnetite is higher than that of maghemite. Also, γ-Fe_2O_3 undergoes easier oxidation compared to Fe_3O_4 [12]. When γ-Fe_2O_3 gets oxidized during the clinical applications, it would cause some undesirable results, so Fe_3O_4 is mostly preferred. In addition, there is a hematite form of Fe_2O_3, it is also called as α-Fe_2O_3. According to arrangement in their structure, they can easily be distinguished from the each other (Figure 1.1).

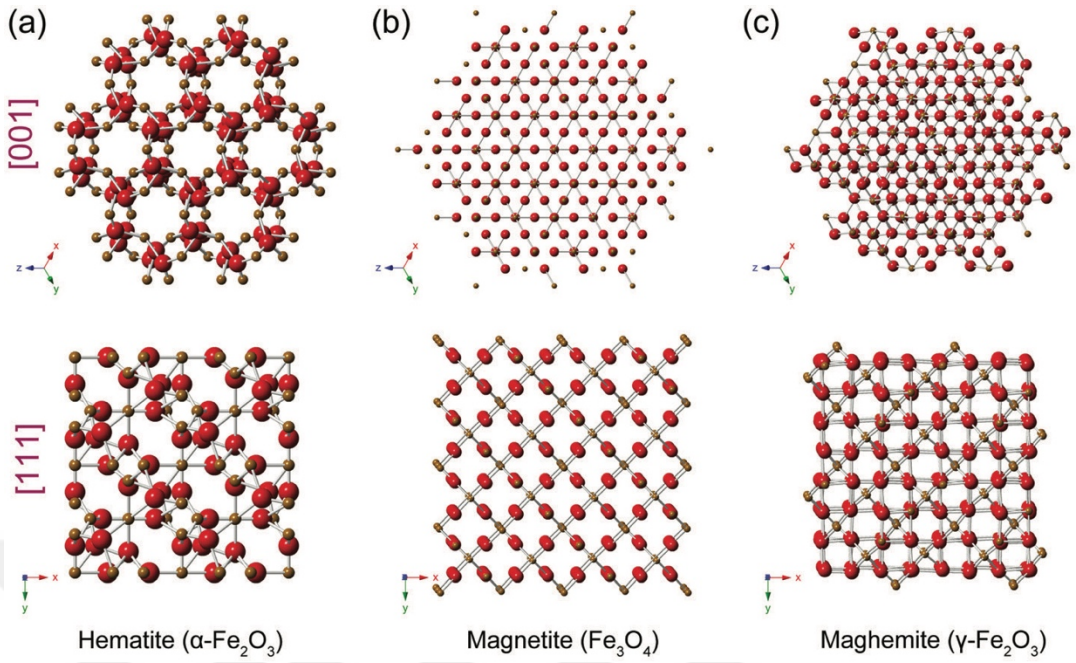

Figure 1.1. Types of iron oxide nanoparticles [12].

By increasing temperature, there can be form transformation between magnetite, maghemite and hematite. Magnetite and maghemite types of iron oxides have similar crystal structure so transformation between them requires temperature about 200 °C. However, crystal structure of hematite is completely different, and its formation requires an elevated temperature of about 500 °C (Figure 1.2) [13].

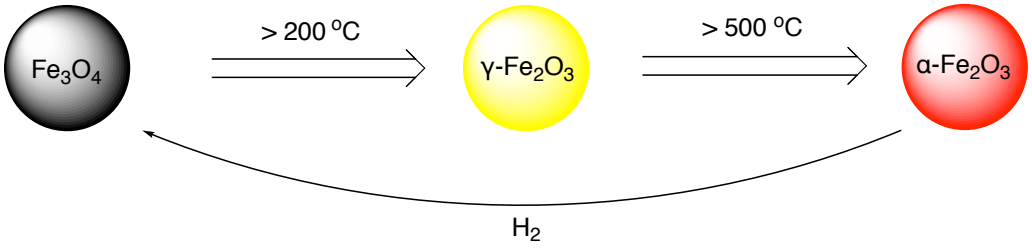

Figure 1.2. Transformation of iron oxide nanoparticles.

1.1.2. Magnetic Property of Iron Oxide Nanoparticles

Iron oxide nanoparticles are magnetic nanoparticles which can be attracted to due to magnetic field. Some materials which are called as ferromagnetics are strongly attracted by magnetic field and they can stay as attracted. On the other hand, paramagnetic materials are weakly attracted by applied magnetic field and they do not show permanent magnetization after the removal of the magnetic field contrary to ferromagnetics [14]. The remaining magnetization of materials after the removal of external magnetic field is called as remanence. In addition, coercivity, which is an ability of magnetics to resist an external magnetic field, is another important property of magnetic materials. The magnetic property of iron oxide nanoparticles can be changed according to their remanence and coercivity balance as shown in Figure 1.3.

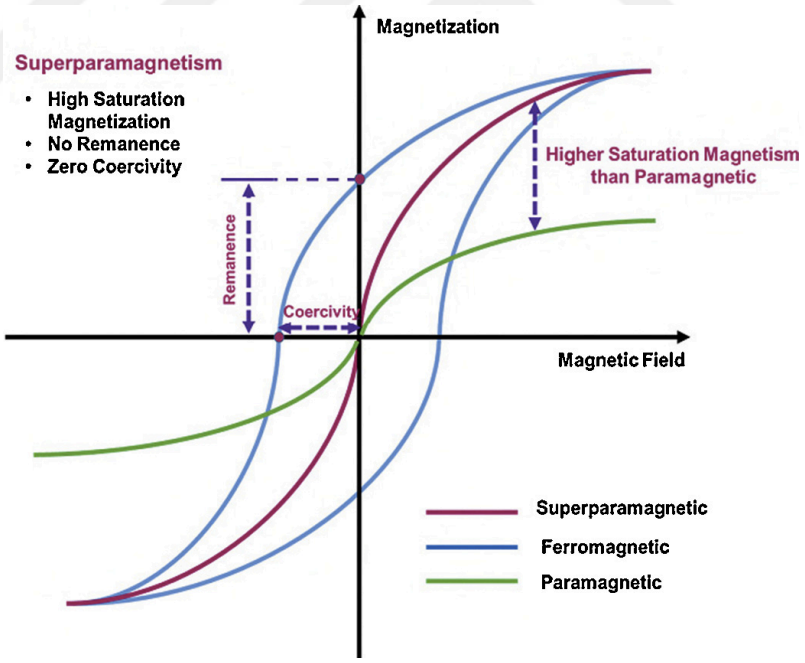

Figure 1.3. Magnetization characteristics of magnetic materials [14].

Ferromagnetics can have single or multiple domain and when the magnetic field is applied on them, their direction of polarization becomes same with external field. When the size of nanoparticles decreases, nanoparticles turn to single domain and they reach high

saturation of magnetization. These types of nanoparticles are referred as superparamagnetic nanoparticles. Magnetic iron oxide nanoparticles which have diameter smaller than 20 nm exhibit superparamagnetic behavior (Figure 1.4) [15]. Overall, the magnetic properties of iron oxide nanoparticles are based on its size, shape, structure and synthesis.

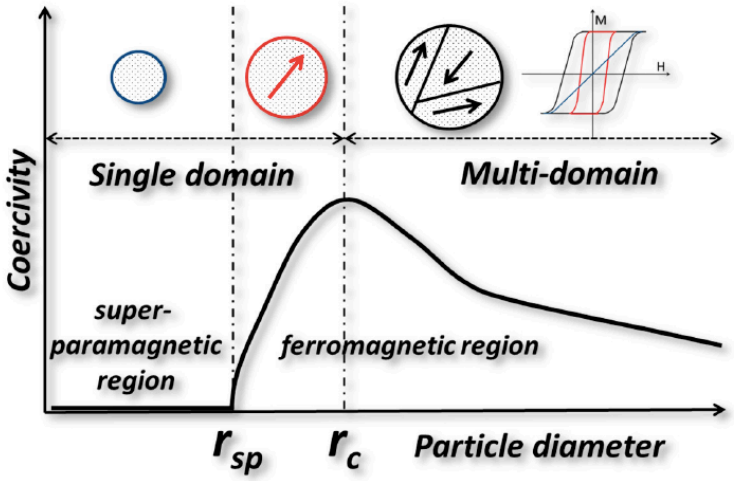

Figure 1.4. The behavior of the size-dependent coercivity of nanoparticles [15].

1.1.3. Synthesis of Iron Oxide Nanoparticles

There are several ways to synthesize iron oxide nanoparticles such as co-precipitation [16], micro-emulsion [17], sol-gel [18], hydrothermal synthesis [19] and thermal decomposition [20].

Co-precipitation method is used to synthesize iron oxide nanoparticles by precipitation of Fe^{2+} and Fe^{3+} ions [21]. This method can be applied at room temperature or higher. By this method, iron oxide nanoparticles can be synthesized in a large scale however size control is low [22]. With different size distributions, Fe_3O_4 and Fe_2O_3 magnetic nanoparticles can be obtained by using this technique. The reactions involved are shown in Figure 1.5.

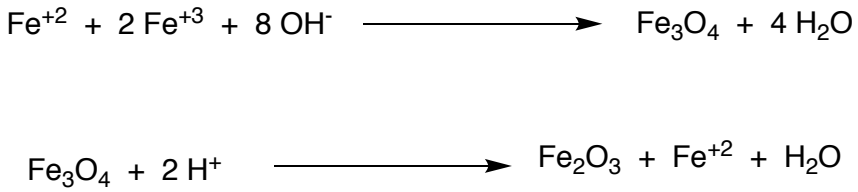

Figure 1.5. Reactions of co-precipitation method.

Another way to synthesize iron oxide nanoparticles is the micro-emulsion method. This method is also referred as wet chemical method. It involves formation of nanoparticles in micelles. Surfactants play an important role in this method, since usually a mixture of water and oil are used as the medium. In this method, although the size control is good, obtained yields are considerably low [23].

A sol-gel method has been developed for the synthesis of magnetic iron oxide nanoparticles. This method involves four steps: hydrolysis, condensation, drying and thermal treatment. Metal alkoxides are hydrolyzed and condensed, and then metal oxides are dispersed in a sol. Finally, metal oxides are dried or gelled by removing solvent from the media or through chemical reactions [24].

Hydrothermal synthesis is another method to synthesize iron oxide nanoparticles under high pressure and temperature [25]. In this strategy, ethylene glycol, which has high boiling point, is used as the solvent. Polyethylene glycol is used as the surfactant and sodium acetate is used for the creating charge on nanoparticles, so they cannot aggregate. The increase in volume of solvent and longer reaction times generally lead to increase in size of iron oxide nanoparticles, thus providing size control [26].

In recent years, the thermal decomposition based synthesis of iron oxide nanoparticle has evolved as one of the most widely used methods. This technique provides very good size control and high yield of reaction [27]. Hence, using this method mono-disperse magnetic nanoparticles can be synthesized. As a result, these magnetic nanoparticles have well-

defined physical and chemical properties [28]. Thermal decomposition method utilizes metal-oleate complex, obtained using metal chloride and sodium oleate. The metal-oleate complex decomposes to yield mono-disperse nanoparticles at very high temperature (Figure 1.6). For the synthesis of iron oxide nanoparticles, salts of iron such as $FeCl_3.H_2O$ are used to make iron oleate complex. The salt is mixed with sodium oleate in a solvent mixture including water, ethanol and hexane. The mixture is to obtain the iron oleate complex. This iron oleate complex decomposes, in the presence of a surfactant such as oleic acid and 1-octadecene which is used as a solvent. The mixture is heated to approximately 300 °C under a nitrogen blanket [29]. The temperature of reaction is very high, so using a high boiling solvent such as 1-octadecene is very important. Spherical iron oxide nanoparticles with narrow polydispersity and controlled size can be synthesized using this approach. In this method, concentration of reagents, type of solvents, reaction time and temperature affect the size and the physical appearance of iron oxide nanoparticles. For instance, to control the increase in temperature provide the size control [30]. In addition, more concentrated reactions cause iron oxide nanoparticles with bigger sizes.

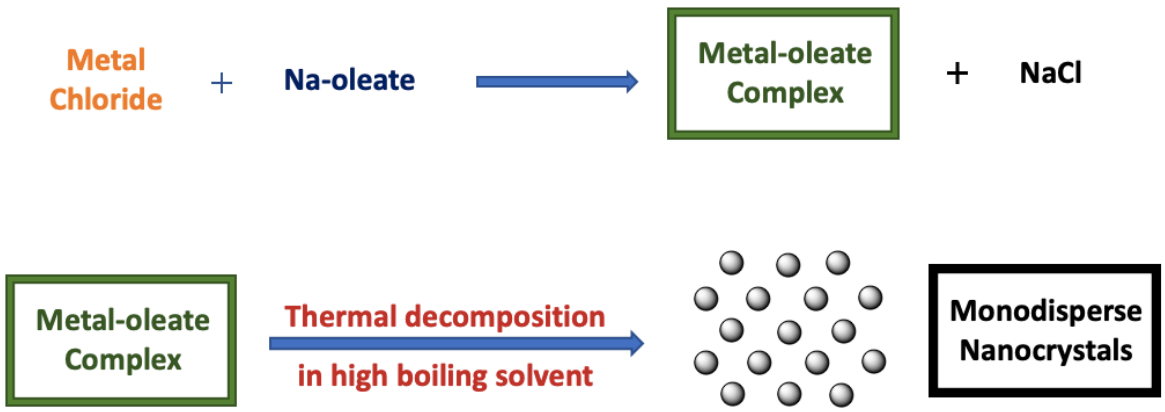

Figure 1.6. Synthetic pathway of thermal-decomposition method.

1.2. Coating of Iron Oxide Nanoparticles

1.2.1. Anchoring Groups Used in Attaching Protecting Groups

An anchoring group is needed for the attachment of the protecting organic ligands onto the inorganic nanoparticle surface. For magnetic nanoparticles, these anchoring groups can be carboxylic acid [31], phosphonic acid [32], trimethoxy silane [33] and a catechol group [34] as shown in Figure 1.7.

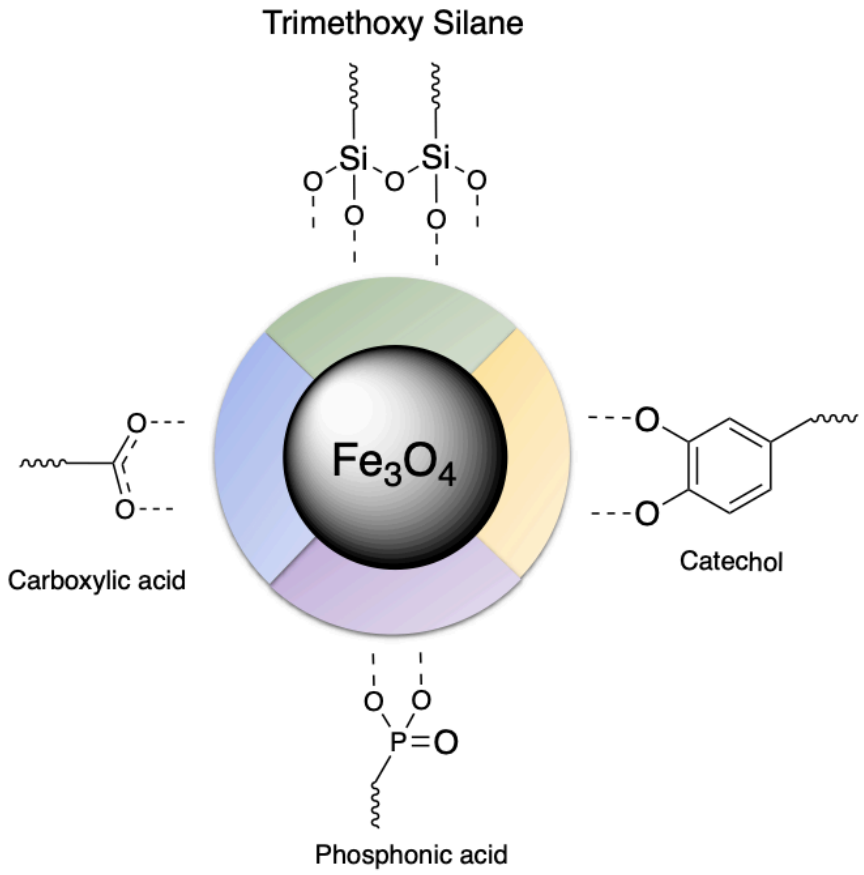

Figure 1.7. Anchoring groups for iron oxide nanoparticles.

Among these anchoring groups, catechol has emerged as one of the most widely used groups in recent years. It can bind to surface of nanoparticles easily and remain stable on it for a long time even at high temperatures. In nature, mussels have adhesive proteins to bind

different surfaces via the special amino acid derivatives which contain catechol group in its structure [35]. Because of an enhanced overlap of the five-membered ring, dopamine group can coordinate with the surface of iron oxide nanoparticles and this results in a strong and stable attachment between dopamine and iron oxide nanoparticles [36]. According to Langmuir isotherms, it was analyzed that dopamine attachment to iron oxide surface is desirable than its detachment [37]. In addition, the amine group in dopamine allows facile attachment of various functional units, such as polymerization initiators to this anchoring group.

1.2.2. Hydrophobic Coating of Iron Oxide Nanoparticles

Iron oxide nanoparticles have strong magnetic properties according to their sizes, so they tend to aggregate with each other. It is important to synthesize mono-dispersed particles, to use them biomedical applications. However, it is also important to save them stable and mono dispersed. Usually, to prevent the agglomeration, iron oxide nanoparticles are synthesized with hydrophobic coating.

In order to eliminate this agglomeration, they are coated by hydrophobic surfactants during their synthesis. The coating materials have long alkyl chains in their structure and these long alkyl chains increase the distance between nanoparticles. They have also anchoring groups such as dopamine, carboxylic acid etc. at the end of their structure, so these anchoring groups provide the attachment of surfactants onto the surface of iron oxide nanoparticles. For the hydrophobic coating, oleic acid is generally used because of its both long alkyl chain and a polar carboxylic acid group [38]. The use of oleic acid as a surfactant, helps to obtain stable, biocompatible monodisperse iron oxide nanoparticles with low toxicity when they are synthesized by thermal decomposition method [39].

1.2.3. Hydrophilic Coating of Iron Oxide Nanoparticles

Iron oxide nanoparticles which have hydrophobic coatings on them cannot be used for biomedical applications, so these hydrophobic coatings of iron oxide nanoparticles need to be replaced by hydrophilic coatings. In addition, iron oxide nanoparticles are more stable with hydrophilic coatings for a long time [40]. Therefore, coating nanoparticles with hydrophilic polymers has been evaluated to make them water dispersible. For example, dextran [41], starch [42], gelatin [43] or chitosan [44] have been used as natural hydrophilic polymers. Alternatively, poly(ethylene glycol) (PEG) [45], poly(ethyleneimine) (PEI) [46], poly(N-isopropylacrylamide) (PNIPAM) [47], polymethylmethacrylate (PMMA) [48] and polyacrylic acid (PAA) [49] derivatives have been employed for coating magnetic nanoparticles.

In recent years, a lot of research has focused on coating of iron oxide nanoparticles with PEG based polymers. PEG is a very hydrophilic material, so it provides iron oxide nanoparticles desirable water dispersibility, which is very important for biomedical applications. Furthermore, PEG based polymers are also biocompatible, and hence their utilization does not show any toxicity during the treatment or delivery [50].

1.3. Polymer Grafting for Iron Oxide Nanoparticles

There are two major approaches for the coating iron oxide nanoparticles with polymers. One of them is the ‘grafting-to’ approach and the other one is the ‘grafting-from’ approach.

In the ‘grafting-to’ approach, polymers are synthesized and subsequently attached to the iron oxide nanoparticles. In the ‘grafting-to’ approach, polymers need to possess an anchoring group so that they can be attached onto the surface of nanoparticle. However, in the ‘grafting-to’ approach, usually the extent of binding is low. Initially tethered polymers, on the surface of nanoparticles, possess a mushroom-like conformation and create a steric

hindrance for the incoming polymer chains. This steric hindrance causes low density of polymer coating on the surface of nanoparticles. On the other hand, the main advantage of this approach is that one can thoroughly characterize the polymers before attachment to nanoparticle surface. A recent example by Sanyal and coworkers demonstrated how the 'grafting-to' approach works for obtaining polymer coated magnetic nanoparticles which are dispersible in aqueous media (Figure 1.8) [51]. First, polymers containing a dopamine based anchoring groups were synthesized. Thereafter, a place exchange reaction between the hydrophobic coating on the nanoparticle surface and dopamine-containing polymers, yielded magnetic nanoparticles suitable for biomedical applications.

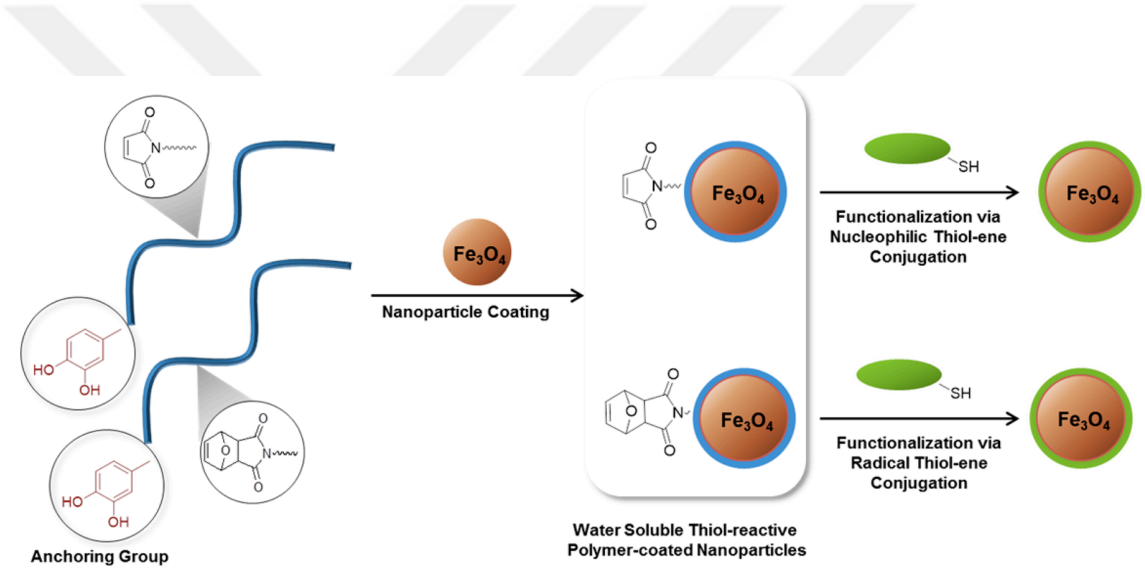

Figure 1.8. 'Grafting-to' approach for iron oxide nanoparticles [51].

Contrary to the 'grafting-to' approach, surface of iron oxide nanoparticles can be coated with polymers with high density through the 'grafting-from' approach. Using this approach, polymers can be directly grown from the surface of magnetic nanoparticles. Polymerization starts with the initiator which is already immobilized to the nanoparticle surface. Growth of polymer chains from surface immobilized initiators leads a to high chain density on the surface. However, characterization of these polymeric brushes be difficult and challenging. For instance, determination of the molecular weight of surface tethered polymer chains is not trivial. A recent example of 'grafting-from' method from Sanyal and coworkers is depicted in Figure 1.9 [52]. First, the oleic acid coating on nanoparticle surface is replaced with a chain transfer agent required for RAFT polymerization. Hydrophilic polymers are

grown from the surface of nanoparticle so there is brush like coating on the surface with high chain density. In addition, the size of polymer coated nanoparticles using the 'grafting-from' approach was higher than ones obtained using the 'grafting-to' approach, presumably due to the brush like nature of the polymer coating.

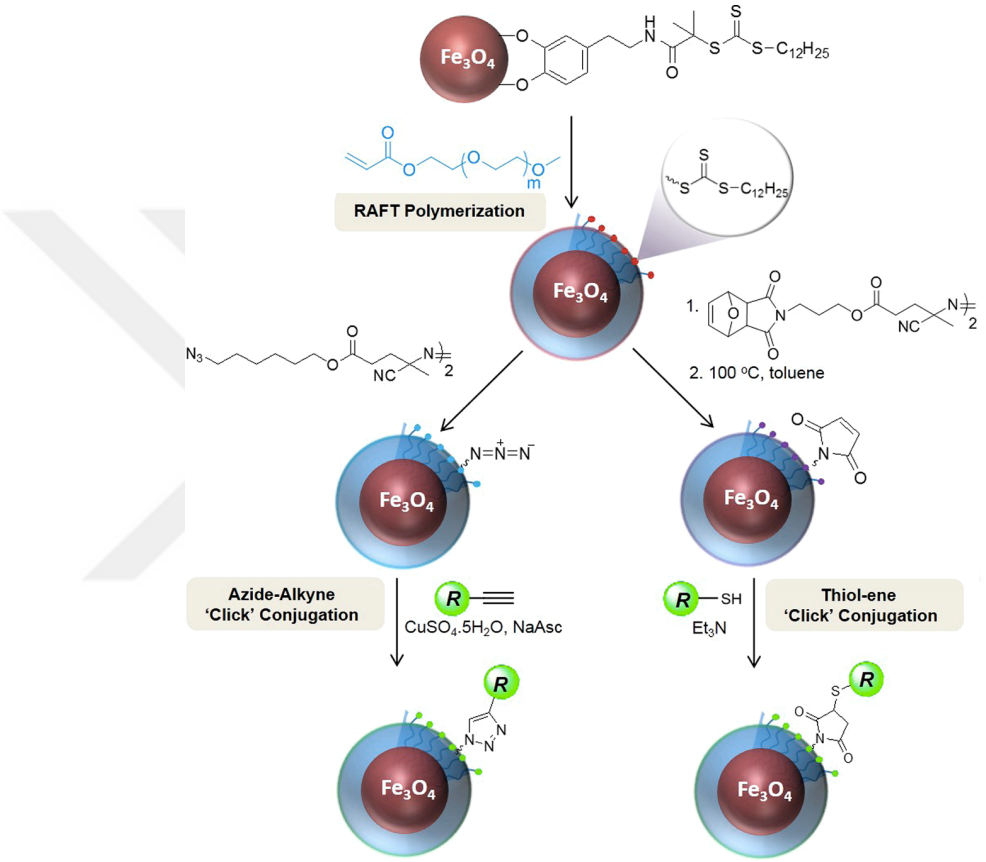

Figure 1.9. 'Grafting-from' approach for iron oxide nanoparticles [52].

1.4. Reversible Addition-Fragmentation Chain-Transfer (RAFT) Polymerization

Polymers grafted onto nanoparticle surfaces have been synthesized using a variety of polymerization techniques, such as, atom transfer radical polymerization (ATRP), nitroxide-mediated radical polymerization and RAFT polymerization. However, when polymers are grafted from the surface of nanoparticles, RAFT polymerization is commonly preferred since it has some advantages, e.g. it can proceed under mild conditions and there is no metal catalyst required. So, purification of polymers obtained using this polymerization is very

easy [53]. Also, use of relatively low temperatures and lack of metal catalyst makes this polymerization technique suitable for a wide range of functional monomers [54].

In addition, RAFT polymerization requires a suitable chain transfer agent with a dithioester group which provides a living polymerization. By this dithioester group, end-group modification can be done by radical exchange reaction [55]. There are many steps to RAFT polymerization takes place. These steps are initiation, propagation, pre-equilibrium, re-initiation, main equilibrium. In conclusion, polymerization stops with termination process [56].

In the initiation step, the initiator is decomposed by temperature to give radicals. Usually, AIBN is used as the radical. The radical attacks on the monomer to continue with the propagation. This propagation step is also referred as chain growth step because the radical formed after initiation step reacts with number of monomers to propagate the polymer chain. Thereafter, RAFT pre-equilibrium step where the growing chain reacts with the dithioester groups of RAFT agent to produce RAFT radical comes. In this step, polymeric unit or the reactive groups of RAFT radical can be cleaved, and these cleaved groups can attack again on the RAFT group, so this is an equilibrium reaction. The previously cleaved reactive group also reacts with number of monomers, so this step is referred as re-initiation step. After re-initiation step, main RAFT equilibrium step follows where growth polymer chain shares its radicals. Finally, the last step is termination where the radical ends of the polymers react with each other to terminate the polymerization. The reaction mechanism of RAFT polymerization is shown below in Figure 1.10.

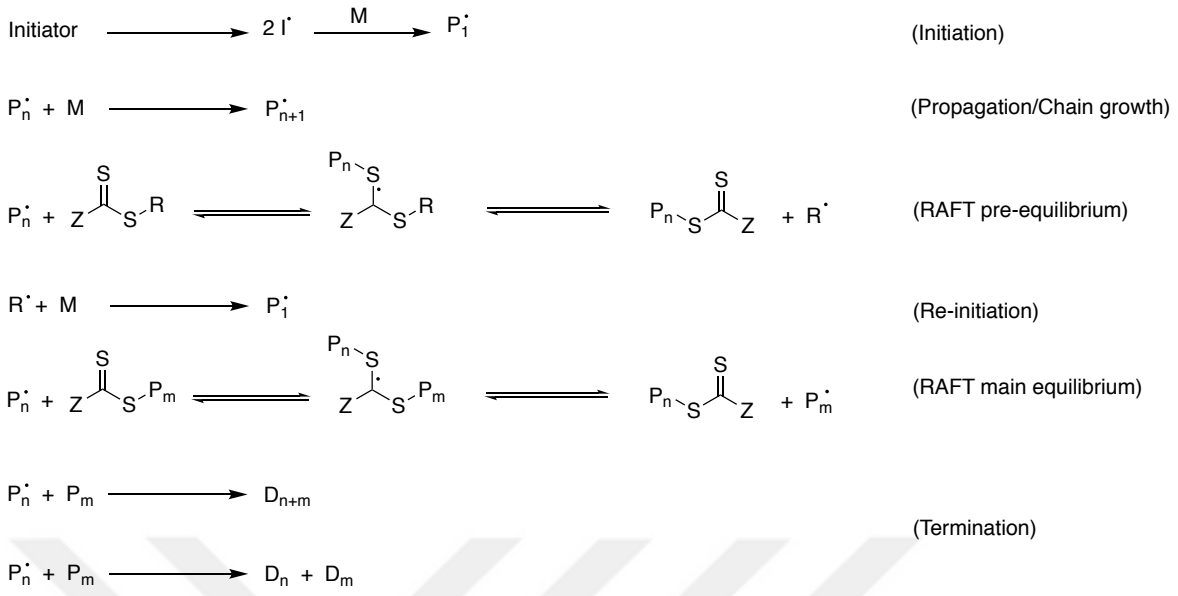

Figure 1.10. Reaction mechanism of RAFT polymerization.

1.5. End Group Modification after RAFT Polymerization

After the synthesis of polymers by RAFT polymerizations, the end groups of these polymers can be dithioester or trithiocrabonate group according to type of chain transfer agent used. These groups are removable i.e. they can be replaced by other functional groups using various chemical transformations. Thus, end group modification is a one of the advantages of RAFT polymerization. One of the widely employed method utilizes modification of end-groups using radical cross coupling reaction [55].

For the radical exchange based end-group modifications, an azo initiator is needed as a radical source. If these azo initiators are modified with functional groups such as N-hydroxysuccinimide (NHS) or maleic anhydride, they create highly reactive site for attachment of functional molecules. For instance, maleic anhydride groups are thiol reactive agents and biomolecules usually have thiol in their structures, so they are available for the conjugation. In addition, end-group modifications require carboxylic acid activating agents to increase percentage of conjugation. For these purposes, NHS activated carboxylic acid containing azo initiator can be synthesized. In literature example, trithiocarbonate groups of iron oxide nanoparticles were replaced using furan-protected maleimide and azide

functionalized azo initiators. After radical exchange reaction, the protected maleimide was deprotected by heating to render chain ends of polymers amenable for thiol-mediated conjugations (Figure 1.11) [52].

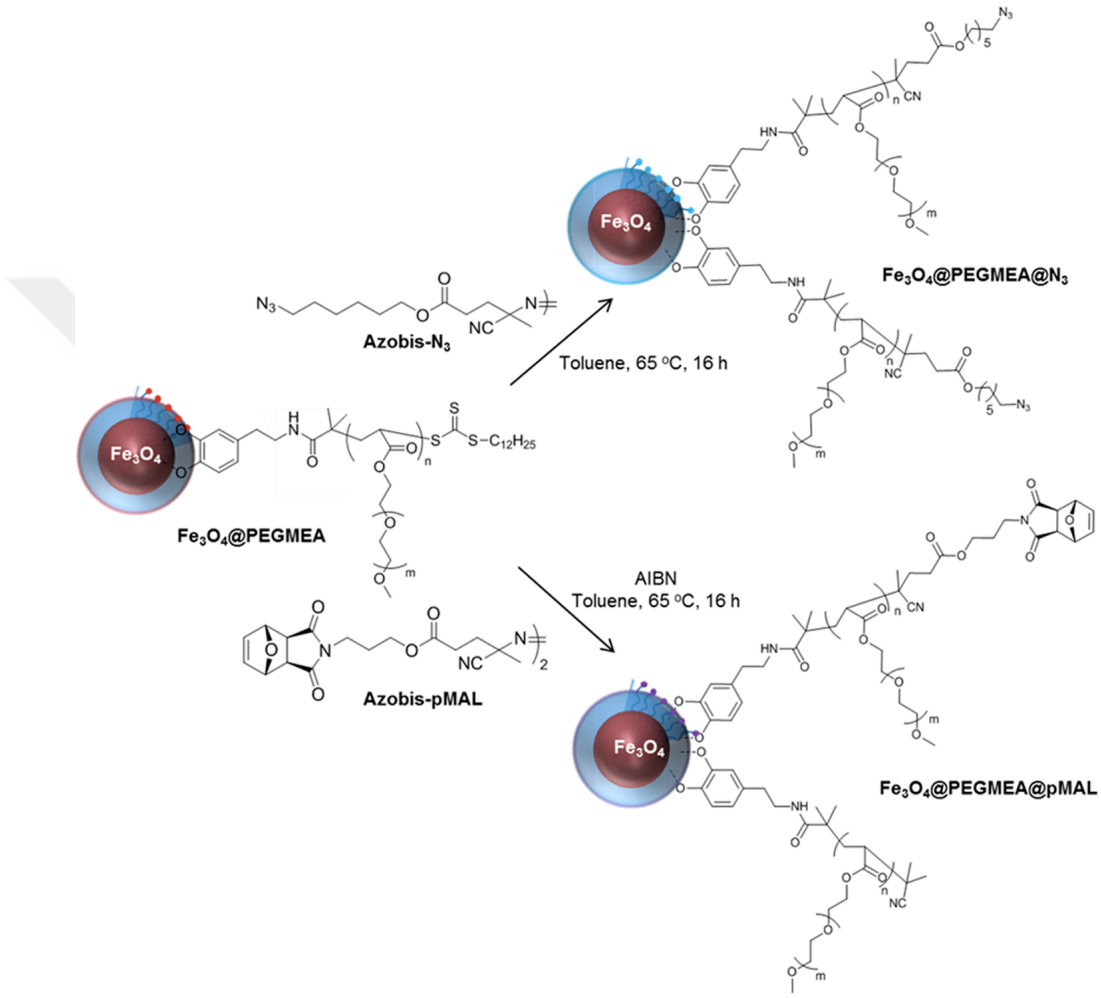

Figure 1.11. End group modification of polymer-coated iron oxide nanoparticles with protected maleimide and azide groups by radical exchange reaction [52].

End group post-polymerization modifications provide an effective strategy for the bioconjugation [57]. When the end groups of polymeric brushes are functionalized, some biomolecules such us drug or peptides can easily attached to the polymers. In a recent example by Sanyal and coworkers, this strategy was used to install maleimide and azide group at chain end of polymer brushes. c-RGDfK peptide which is a targeting group and

BODIPY-SH, a fluorescent dye molecule was attached to the polymer coated nanoparticles (Figure 1.12) [52].

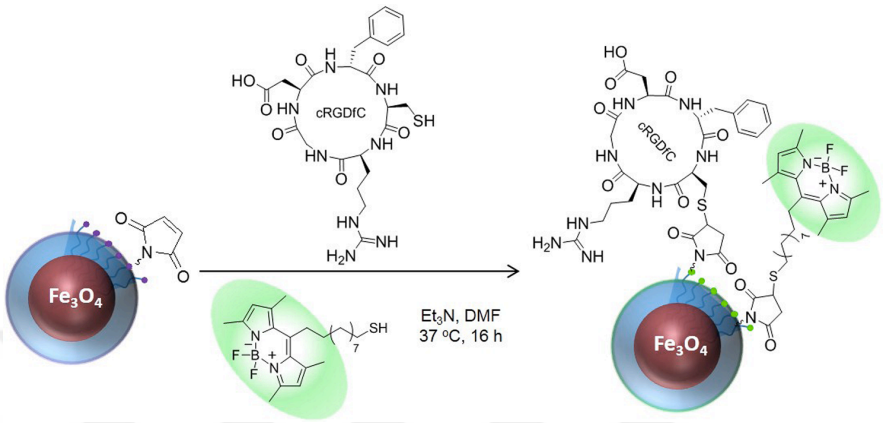

Figure 1.12. Conjugation of cRGDfK to end group modified polymer coated iron oxide nanoparticles [52].

1.6. Disulfide Cleavage Reaction under Redox Environment

In recent years, the focus on disulfide groups in biological applications has increased considerably since they can react with thiol containing compounds such as a protein, drug or targeting group to form an another disulfide bond after conjugation [58]. Whether the conjugation of a compound to polymers is reversible or irreversible is important since it provides release of that compound. The disulfide bonds are commonly preferred in biological applications because of their advantages, e.g. it provides the reversible conjugation. A drug/peptide conjugated to polymers can be released in the presence of a reducing agents shown with an example in Figure 1.13 [59].

It is important to conjugate a biological compound that is proposed to be released from a polymer with disulfide bond. Disulfide bonds are sensitive to redox media and can be cleaved by reducing agents such as glutathione and DTT. Glutathione is a naturally occurring tripeptide which has a free thiol in its structure. Also, the amount of glutathione found in diseased cells is higher than that of normal cells [60]. It gives resistance to cancer

cells to protect themselves from cancer drugs and creates a redox environment in cells. This redox environment can lead to release of drugs from polymeric carriers, and because of this attribute disulfide groups containing systems have gained attention for biomedical applications.

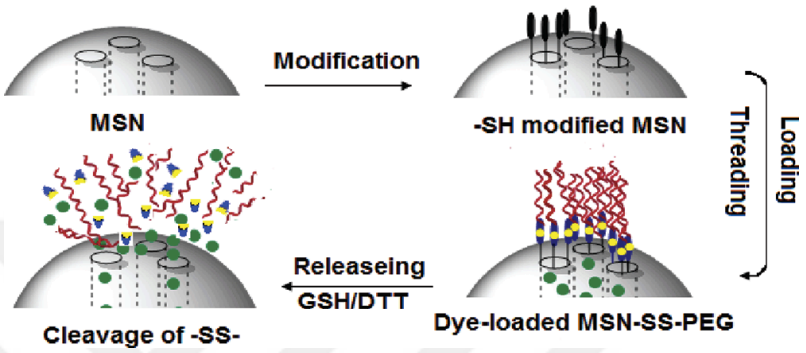

Figure 1.13. Releasing scheme of disulfide bond containing dye loaded mesoporous silica nanoparticles [59].

2. FABRICATION DEGRADABLE POLYMER COATED NANOPARTICLES

2.1. Aim of the Study

The aim of this project is to synthesize and characterize polymer-nanoparticle conjugate that responds to external stimuli like magnetic field and the redox environment found in diseased tissues. Firstly, polymer coated iron oxide nanoparticles without cleavable bond which exist in literature were synthesized as a control system. By RAFT polymerization and 'grafting-from' approach, PEG and fluorescent dye based polymeric brushes were polymerized from the nanoparticle surfaces. Thus, by this method nanoparticles and fluorescent dye were gained solubility. However, it is difficult to analyze molecular weight and polydispersity index of these surface tethered polymer chains by 'grafting-from' approach. The novelty of this project is that nanoparticles were coated with disulfide cleavable bond containing chain transfer agents, so polymeric brushes were cleaved from the surface of nanoparticles under mild condition by reducing agents and cleaved polymeric brushes could be characterized.

First, monodisperse iron oxide nanoparticles were synthesized by thermal decomposition method. Dopamine modified chain transfer agents with and without disulfide bonds were synthesized, characterized and immobilized onto iron oxide nanoparticle surfaces. After immobilization, PEG based hydrophilic polymers were directly grown from the surface of magnetic nanoparticles. In disulfide containing system, polymeric brushes were cleaved and detached from the magnetic nanoparticles in the presence of a reducing agent. Then, nanoparticles were coated with fluorescent dye and PEG based copolymeric brushes. Finally, since RAFT agents install trithiocarbonate groups at the end of polymer chains, it was demonstrated that these removable end groups can be replaced with amine-reactive NHS-based activated ester groups by post-polymerization modifications.

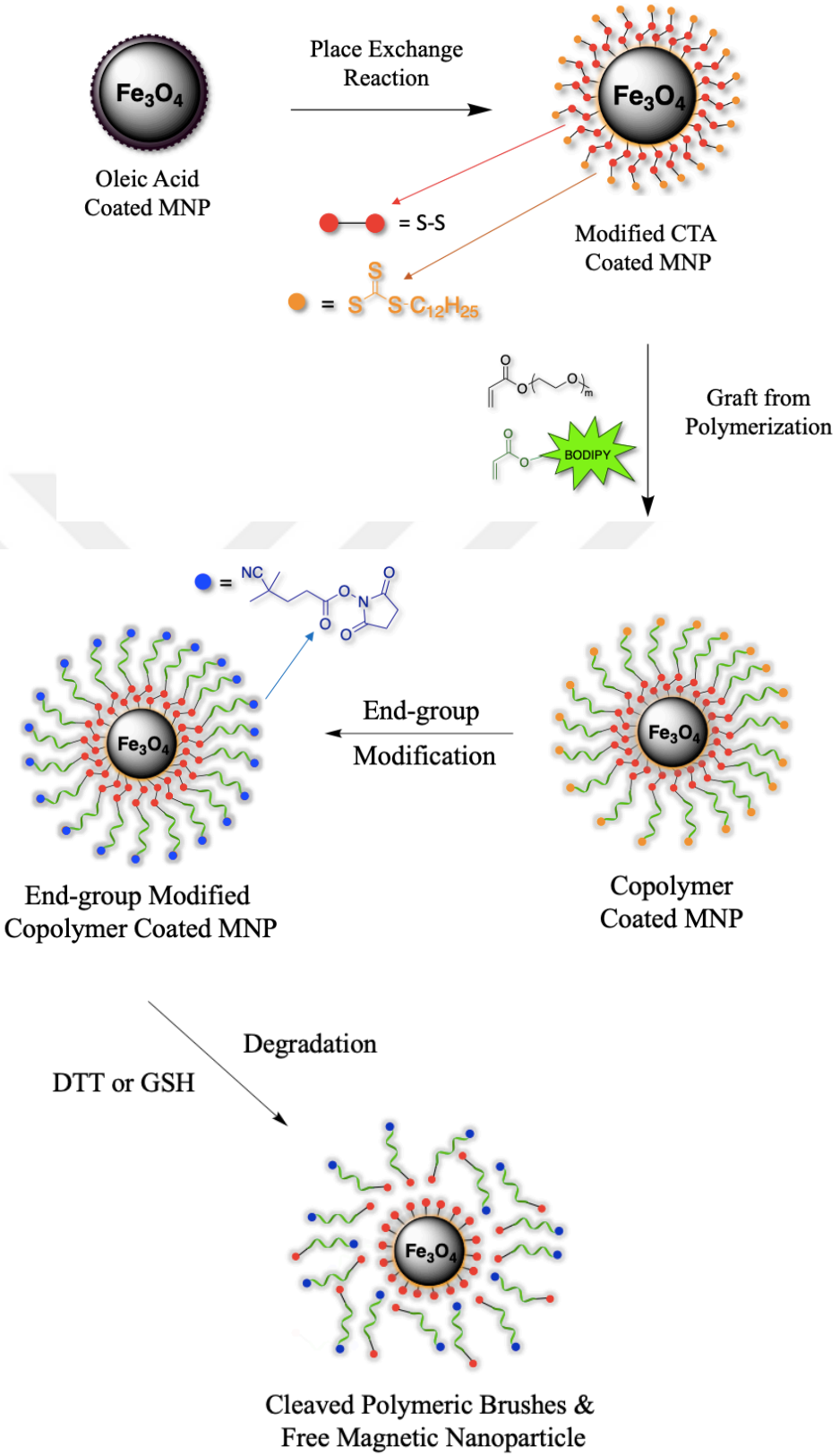

Figure 2.1. General scheme of the project.

3. EXPERIMENTAL

3.1. Materials

Oleic acid, dopamine hydrochloride, 1-dodecanethiol, iron (III) chloride hexahydrate, DMAP, DSC (>95%), and L-Glutathione reduced were purchased from Sigma-Aldrich. No purification was needed for these compounds. Sodium oleate was purchased from TCI. Triethylamine, 2,2'-disulfanediyldiethanol, EDCI, AIBN (recrystallization in ethanol before use), DTT, 1-octadecene, DCC and NHS were purchased from Alfa-Aesar. Poly (ethylene glycol) methyl ether acrylate (PEGMEA), 3-ethyl-2,4-dimethylpyrrole and boron trifluoride dimethyl etherate were purchased from Sigma-Aldrich and V-501 and CS_2 were purchased from Fluka. CTA [61], CTA-Dopa [52], BODIPY Bromine (BODIPY-Br), BODIPY acetate (BODIPY-OAc) and BODIPY alcohol (BODIPY-OH) [62] were synthesized according to the literature examples. Lithium hydroxide, toluene, THF, EtOAc, methanol, DMF, DCM, chloroform, hexane and ethanol were purchased from Merck.

3.2. Instrumentation

^{1}H NMR spectra were obtained using 400 MHz Bruker spectrometer at 25 ^oC. Deuterated chloroform was used as the NMR solvent. Fourier transform infrared (FT-IR) spectra were obtained by using Thermo Scientific Nicolet 380. Gel permeation chromatography with a PSS-SDV column (Gram linear, length/ID 8x300 mm, 10 µm particle size) was used to analyze the molecular weights and PDI values of the grafted polymers. Dimethylacetamide was used as the eluent. UV-visible spectra were obtained using Varian Cary 100 Scan spectrophotometer. Malvern Zetasizer Nano ZS photometer was used to obtain dynamic light scattering (DLS) results. Hexane and DMF were used as the solvents at 20 ^oC.

3.3. Iron Oxide Nanoparticles Synthesis

Iron oxide nanoparticles are synthesized in two steps and the procedure of this reaction was taken from the literature [29]. First of all, iron oleate complex was synthesized and this compound reacted with oleic acid in the presence of a high boiling solvent to obtain oleic acid coated monodisperse iron oxide nanoparticles.

3.4. Synthesis of Dopamine Modified Chain Transfer Agent (CTA)

3.4.1. Synthesis of 2-(((dodecylthio)carbonothioyl)thio)-2-methylpropanoic acid (CTA)

The chain transfer agent (CTA) that was intended to be modified with dopamine was synthesized according to the literature [61].

3.4.2. Synthesis of 2,5-dioxopyrrolidin-1-yl 2-(((dodecylthio)carbonothioyl)thio)-2-methylpropanoate (CTA-NHS)

CTA-Succinimide ester (CTA-NHS) was synthesized according to the literature example [52].

3.4.3. Synthesis of 1-((3,4-dihydroxyphenethyl)amino)-2-methyl-1-oxopropan-2-yl dodecyl carbonotrithioate (CTA-Dopa)

Dopamine modified CTA (CTA-Dopa) was prepared according to previously reported procedure [52]. The product was purified by column chromatography using ethyl acetate (40 %) / hexane (60 %) (328 mg, 38% yield). The characterization of product was done by ^{1}H NMR spectroscopy.

3.5. Synthesis of Disulfide Containing Chain Transfer Agent

3.5.1. Synthesis of 2-((2-hydroxyethyl)disulfaneyl)ethyl 2-(((dodecylthio)carbonothioyl)thio)-2-methylpropanoate (CTA-SS-OH)

CTA-SS-OH was obtained by the esterification reaction between CTA and 2,2'-disulfanediyldiethanol. CTA (2-(((dodecylthio)carbonothioyl)thio)-2-methylpropanoic acid) (1 g, 2.74 mmol) was dissolved in 5 mL of dry CH_2Cl_2 and the solution was kept cold in an ice bath. DCC (678 mg, 3.29 mmol) was dissolved in 3 mL of CH_2Cl_2. Then, this solution was added to CTA solution. The resulting mixture was stirred for 10 minutes. After that, 2,2'-disulfanediyldiethanol (423 mg, 2.74 mmol) was added to the mixture dropwise. Finally, DMAP (34 mg, 0.274 mmol) which was dissolved in 1 mL of EtOAc was added to final mixture. The temperature of this mixture was allowed to come to room temperature. Then, it was stirred at room temperature for 24 hours. After the reaction, the white solid (DCU) which is a by-product of this reaction was removed by filtration. Then, in order to purify the compound, the mixture was extracted with 20 mL of 0.1 M HCl and brine twice. Then, the organic part was dried over Na_2SO_4. The solvent was evaporated by rotary evaporation. Obtained yellow viscous liquid was purified by column chromatography using ethyl acetate (15 %) / hexane (85 %) (823 mg, 60% yield). ^{1}H NMR ($CDCl_3$) δ (ppm): 4.38 (t, 2H), 3.89 (q, 2H), 3.27 (t, 2H), 2.94 (t, 2H), 2.90 (t, 2H), 1.66 (m, 8H), 1.33 (m, 18H), 0.88 (t, 3H).

3.5.2. Synthesis of 2- ((2- ((((2,5-dioxopyrrolidin-1-yl)oxy)carbonyl)oxy)ethyl) disulfaneyl)ethyl 2-(((dodecylthio) carbonothioylthio)-2-methylpropanoate (CTA-SS-DSC)

CTA-SS-DSC compound was synthesized using CTA-SS-OH and DSC molecule to get activated carboxylic acid for the next amine conjugation. For this synthesis, CTA-SS-OH (400 mg, 0.799 mmol) and DSC (368 mg, 1.438 mmol) and TEA (81 mg, 0.799 mmol) were mixed in 10 mL of dry CH_2Cl_2. The reaction mixture was stirred continuously and kept at room temperature for 24 hours. In order to purify this compound, the mixture was

extracted with 20 mL of saturated $NaHCO_3$ and brine twice. Organic part was dried over Na_2SO_4. The solvent was removed by rotary evaporation.

3.5.3. Synthesis of 2- ((2- (((3,4- dihydroxyphenethyl)carbamoyl)oxy)ethyl) disulfaneyl)ethyl 2- (((dodecylthio)carbonothioyl)thio)-2-methylpropanoate (CTA-SS-Dopa)

CTA-SS-Dopa compound was synthesized using CTA-SS-DSC and dopamine hydrochloride. CTA-SS-DSC (250 mg, 0.389 mmol) was dissolved in 5 mL of dry DMF. Then, dopamine hydrochloride (77.5 mg, 0.409 mmol) was dissolved in 1.5 mL of dry DMF and it was added to previous solution drop by drop for 15 minutes. After this step, TEA (79 mg, 0.778 mmol) was added to final mixture slowly. The mixture was stirred at room temperature for 48 hours in the dark. The solvent was partially evaporated. Then, 20 mL of 1N HCl was added to the concentrated solution. The reaction mixture was extracted with 10 mL of EtOAc twice. Organic part was dried over Na_2SO_4. The solvent was removed by rotary evaporation. Obtained yellow solid was purified by column chromatography using ethyl acetate (20 %) / hexane (80%) (111 mg, 42% yield). ^{1}H NMR ($CDCl_3$) δ (ppm): 6.80 (s, 1H), 6.72 (s, 1H), 6.61 (d, 1H), 4.85 (s, 1H), 4.39 (t, 2H), 4.29 (t, 2H) 3.40 (t, 2H), 3.26 (t, 2H), 2.90 (t, 4H), 2.70 (t, 2H) 1.66 (m, 8H), 1.33 (m, 18H), 0.88 (t, 3H).

3.6. Place Exchange Reaction between Oleic Acid-Coated Nanoparticle and Chain Transfer Agent

3.6.1. Place Exchange Reaction between Fe_3O_4@OA and CTA-Dopa (Fe_3O_4@Dopa-CTA)

The ligand exchange reaction procedure was done according to the previously mentioned literature example [52]. For this synthesis, oleic acid stabilized Fe_3O_4 nanoparticles (Fe_3O_4@OA) (30 mg) was dissolved in 4 mL of chloroform. Then, Dopa-CTA (90 mg) was added to this solution. The final mixture was allowed to stir at 40 ^oC for 48 hours under a nitrogen blanked. After the reaction, the solvent was partially removed by

rotary evaporation. In order to purify this compound, 30 mL of methanol was added to this mixture to precipitate the desired product (Fe_3O_4@Dopa-CTA) until all free dopamine modified CTA was removed. After that, the product was kept in chloroform to prevent aggregation.

3.6.2. Place Exchange Reaction between Fe_3O_4@OA and CTA-SS-Dopa (Fe_3O_4@Dopa-SS-CTA)

CTA-SS-Dopa molecule was immobilized into the iron oxide nanoparticles by ligand exchange reaction. For this reaction, CTA-SS-Dopa (90 mg) was mixed with oleic acid stabilized iron oxide nanoparticles (30 mg) in chloroform (4 mL). The resulting mixture was stirred at 40 °C for 48 hours under a nitrogen blanket. After the reaction, the solvent was partially evaporated. Then, this viscous solution was precipitated in methanol (30 mL). The methanol-chloroform mixture was centrifuged (7000 rpm, 10 minutes) and wash was repeated until all unreacted CTA-SS-Dopa was removed. Finally, thus obtained black product was stored in $CHCl_3$ until further use.

3.7. RAFT Polymerization of PEGMEA from the Surface of Fe_3O_4 Nanoparticles

3.7.1. Synthesis of Polymer-Coated Fe_3O_4 Nanoparticles (Fe_3O_4 @Dopa-PEGMEA)

The procedure for surface-initiated RAFT polymerization of PEGMEA was taken from the same literature where the ligand exchange reaction was done [52]. For this polymerization, Fe_3O_4@Dopa-CTA (10 mg), PEGMEA (500 mg, 1.04 mmol) and AIBN (0.68 mg, 0.004 mmol) were dissolved in toluene (3 mL). The reaction mixture was purged with N_2 for 20 minutes to remove O_2 from the reaction environment. Then, reaction mixture was allowed to stir at 75 °C for 24 hours. After polymerization, the solvent was removed by rotary evaporation. Then, the polymers were precipitated in cold diethyl ether (3 times) to remove unreacted monomers. Finally, a black viscous product was obtained.

3.7.2. Synthesis of Degradable Polymer-Coated Fe_3O_4 Nanoparticles (Fe_3O_4 @Dopa-SS-PEGMEA)

RAFT polymerization was done on the surface of iron oxide nanoparticles by using PEGMEA as the monomer. For this reason, 10 mg of Fe_3O_4@Dopa-SS-CTA was mixed with PEGMEA (500 mg, 1.04 mmol) and AIBN (0.68 mg, 0.004 mmol). The obtained mixture was dissolved in toluene (3 mL). This mixture was purged with N_2 for 20 minutes to remove O_2 gas from the reaction mixture. Finally, the reaction was stirred at 75 °C for 2, 4, 8, 16 and 24 hours in order to measure the molecular weights of the polymers grown from the surface depending on time. This polymerization process was repeated 3 times for 2, 4, 8, 16 and 24 hours. After the reaction, solvent was removed by rotary evaporation. The obtained black viscous product was precipitated in cold diethyl ether to remove unreacted monomers.

3.8. Reductive Cleavage of PEGMEA Polymers from Fe_3O_4 Nanoparticles

DTT was used in order to cleave the disulfide bond that builds a bridge between and nanoparticles and polymers. For this cleavage reaction, 15 mg of Fe_3O_4@Dopa-SS-PEGMEA and DTT (1.54 mg, 0.01 mmol) were dissolved in 1 mL of pH=8.0 phosphate buffer solution. Resulting mixture was stirred at room temperature for 2 hours. To separate iron oxide nanoparticles and polymers, reaction mixture was added into water (6 mL) and the solution was centrifuged at 9000 rpm for 20 minutes. Iron oxide nanoparticles precipitated because they lost water dispersibility. However, hydrophilic PEG based polymers dissolved in water and could be obtained through lyophilization.

3.9. RAFT Polymerization of PEGMEA from the Surface of Fe_3O_4 Nanoparticles (Fe_3O_4@Dopa-SS-PEGMEA) and Free CTA (Dopa-SS-PEGMEA)

RAFT polymerization was done on the surface of iron oxide nanoparticles by using PEGMEA as the monomer. For this reason, 10 mg of Fe_3O_4@Dopa-SS-CTA was mixed with PEGMEA (500 mg, 1.04 mmol) and AIBN (0.68 mg, 0.004 mmol). However, in this case free CTA was added (2 mg, 0.005 mmol) to the mixture. The obtained mixture was dissolved in toluene (3 mL). The mixture was purged with N_2 for 20 minutes to remove O_2 gas from the reaction mixture. The reaction was stirred at 75 °C for 24 hours. After the reaction, solvent was removed by rotary evaporation. The obtained black viscous product was precipitated in cold diethyl ether to remove unreacted monomers. Finally, polymer-coated nanoparticles (Fe_3O_4@Dopa-SS-PEGMEA) and free polymers (Dopa-SS-PEGMEA) were obtained. These compounds were separated by dialysis system.

3.10. Synthesis of BODIPY Dye Monomer

3.10.1. Synthesis of BODIPY Bromide (BODIPY-Br)

The fluorescent dye (BODIPY-Br) that was intended to be modified to BODIPY acetate was synthesized according to the literature [62]. Obtained dark green solid was purified by column chromatography using ethyl acetate (10 %) / hexane (90%) (809 mg, 46% yield). Obtained product was characterized by ^{1}H NMR spectroscopy.

3.10.2. Synthesis of BODIPY Acetate (BODIPY-OAc)

The synthesis of BODIPY acetate that was intended to be modified to BODIPY alcohol was taken from the same literature where the previous synthesis was done [62]. Dark red solid was obtained (250 mg, 92% yield). The characterization of product was done by ^{1}H NMR spectroscopy.

3.10.3. Synthesis of BODIPY Alcohol (BODIPY-OH)

BODIPY alcohol that was intended to be modified to BODIPY monomer was synthesized according to the literature example [62]. Obtained dark red solid was purified by column chromatography using ethyl acetate (8 %) / hexane (92%). Then, column chromatography was repeated using ethyl acetate (10 %) / hexane (90%) (190 mg, 84% yield). The synthesized product was characterized by ^{1}H NMR spectroscopy.

3.10.4. Synthesis of BODIPY Acrylate Monomer

BODIPY acrylate monomer was synthesized to use it as monomer with PEGMEA monomer to do copolymer brushes on the surface of iron oxide nanoparticles by RAFT polymerization. Firstly, BODIPY-OH (25 mg, 0.055 mmol) was dissolved in of anhydrous CH_2Cl_2 (1.5 mL) and the solution was kept cold in an ice bath. Acryloyl chloride (10 mg, 0.010 mmol) was dissolved in 1 mL of dry CH_2Cl_2. Then, this solution was added to BODIPY-OH solution which was still kept cold in an ice bath very slowly. The resulting mixture was stirred for 10 minutes. After that, TEA (39 mg, 0.387 mmol) was added to the mixture dropwise. Then, it was stirred at 0 °C for 16 hours in an ice bath. Thereafter, the mixture was extracted with 20 mL of deionized water and 20 mL brine twice. Then, the organic part was dried over Na_2SO_4. The solvent was vacuumed by rotary evaporation. Obtained dark red solid was purified by column chromatography using ethyl acetate (1 %) / hexane (99 %) (16 mg, 57% yield). ^{1}H NMR ($CDCl_3$) δ (ppm): 6.39 (d, 1H), 6.16-6.06 (m, 1H), 5.81 (d,1H), 4.15 (t, 2H), 3.02-2.91 (m, 2H), 2.49 (s, 6H), 2.40 (q, 4H), 2.33 (s, 6H), 1.94 (s, 3H), 1.70-1.27 (m, 16H), 1.05 (t, 6H).

3.11. RAFT Copolymerization of PEGMEA and BODIPY Acrylate from the Surface of Fe_3O_4 Nanoparticles (Fe_3O_4@Dopa-SS-PEGMEA-r-BODIPY)

RAFT copolymerization was done on the surface of iron oxide nanoparticles by using PEGMEA and BODIPY acrylate as the monomer. For this reason, 10 mg of Fe_3O_4@Dopa-SS-CTA was mixed with PEGMEA (500 mg, 1.04 mmol), BODIPY acrylate (3.13 mg, 0.006

mmol) and AIBN (0.68, 0.004 mmol). The obtained mixture was dissolved in 3 mL of toluene. This mixture was purged with N_2 for 20 minutes to remove O_2 gas from the reaction mixture. Finally, the reaction was stirred at 75 °C for 24 hours. This polymerization process was repeated 3 times. After the reaction, solvent was removed by rotary evaporation. The obtained greenish viscous product was precipitated in cold diethyl ether to get rid of unreacted monomers.

3.12. Reductive Cleavage of PEGMEA and BODIPY Copolymer Brushes from Fe_3O_4 Nanoparticles

DTT was used in order to cleave the disulfide bond that builds a bridge between and nanoparticles and polymers. For this cleavage reaction, 15 mg of Fe_3O_4@Dopa-SS-PEGMEA-r-BODIPY and DTT (1.54 mg, 0.01 mmol) were dissolved in pH=8.0 phosphate buffer (1 mL) solution. Resulting mixture was stirred at room temperature for 4 hours. In order to separate iron oxide nanoparticles and polymers, reaction mixture was added into water (9 mL) and the solution was centrifuged at 9000 rpm for 15 minutes. Iron oxide nanoparticles precipitated since they were no longer dispersible in water. However, hydrophilic mostly PEG, slightly dye based copolymer brushes dissolved in water and could be obtained through lyophilization.

3.13. End Group Modification of Polymer-Coated Fe_3O_4 Nanoparticles

3.13.1. Synthesis of (E)-bis(2,5-dioxopyrrolidin-1-yl) 4,4'-(diazene-1,2-diyl)bis(4-cyanopentanoate) (NHS-ACVA)

This compound was synthesized according to the literature [63]. For this synthesis, V501 (500 mg, 1.78 mmol), NHS (548 mg, 4.76 mmol) were dissolved in 5 mL of dry DMF. On the other hand, EDCI (913 mg, 4.76 mmol) which was dissolved in 4 mL of dry DMF was added to previously prepared solution at 0 °C for 1 hour. Then, the reaction mixture was allowed to stir at room temperature for 36 hours. In order to purify this NHS-ACVA, the

reaction mixture was precipitated into 400 mL of distilled water. White solid precipitate was collected by filtration method. The product was lyophilized for 24 hours to get rid of water. Finally, white solid product was obtained (640 mg, 76% yield).

3.13.2. End Group Modification of Degradable Polymer-Coated Fe_3O_4 Nanoparticles with NHS activated Carboxylic Acid Containing Azo Initiator (Fe_3O_4@Dopa-SS-PEGMEA-NHS)

NHS-activated Carboxylic Acid functionalized azo initiator (NHS-ACVA) (14.2 mg, 0.03 mmol) and polymer-coated Fe_3O_4 nanoparticles (30 mg) were dissolved in 2 mL of dry DMF. Then, the mixture was purged with N_2 for 20 minutes. After that, it was allowed to stir at 75 ^oC for 16 hours. To purify obtained compound, the reaction mixture was dialyzed against 250 mL of acetonitrile using dialysis membrane (molecular weight cutoff 3500 Da) for 24 hours. Finally, the solvent was removed by rotary evaporation.

4. RESULTS AND DISCUSSIONS

4.1. Synthesis of Fe_3O_4 Nanoparticles and Characterizations

Magnetic iron oxide nanoparticles were synthesized by thermal decomposition method which provides very good size and polydispersity control. There are two steps to synthesize magnetic nanoparticles. The first step is the synthesis of iron oleate complex by using iron (III) chloride and sodium oleate salt as precursors (Figure 4.1).

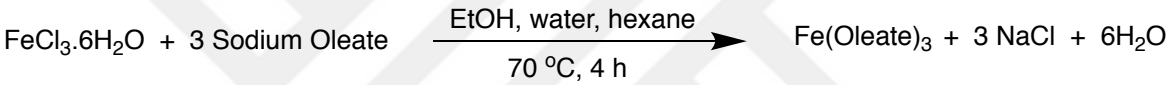

Figure 4.1. The synthesis of iron oleate complex.

Thereafter, oleic acid coated nanoparticles were synthesized using iron oleate complex and oleic acid in the presence of a high boiling solvent 1-octadecene (Figure 4.2). Oleic acid coating prevents iron oxide nanoparticles from agglomeration.

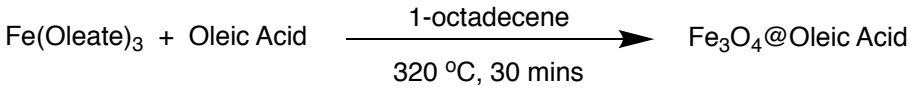

Figure 4.2. Synthesis of iron oxide nanoparticles.

The characterization of these oleic acid-coated magnetic nanoparticles was done by using FT-IR spectroscopy and dynamic light scattering (DLS) (Figure 4.3). The peaks at 2923 and 2851 cm^{-1} indicate that the symmetric and asymmetric $–CH_2-$, correspondingly. The peak at 590 cm^{-1} comes from the Fe-O bonds of iron oxide molecules. Their average sizes determined using DLS were around 10 nm (diameter).

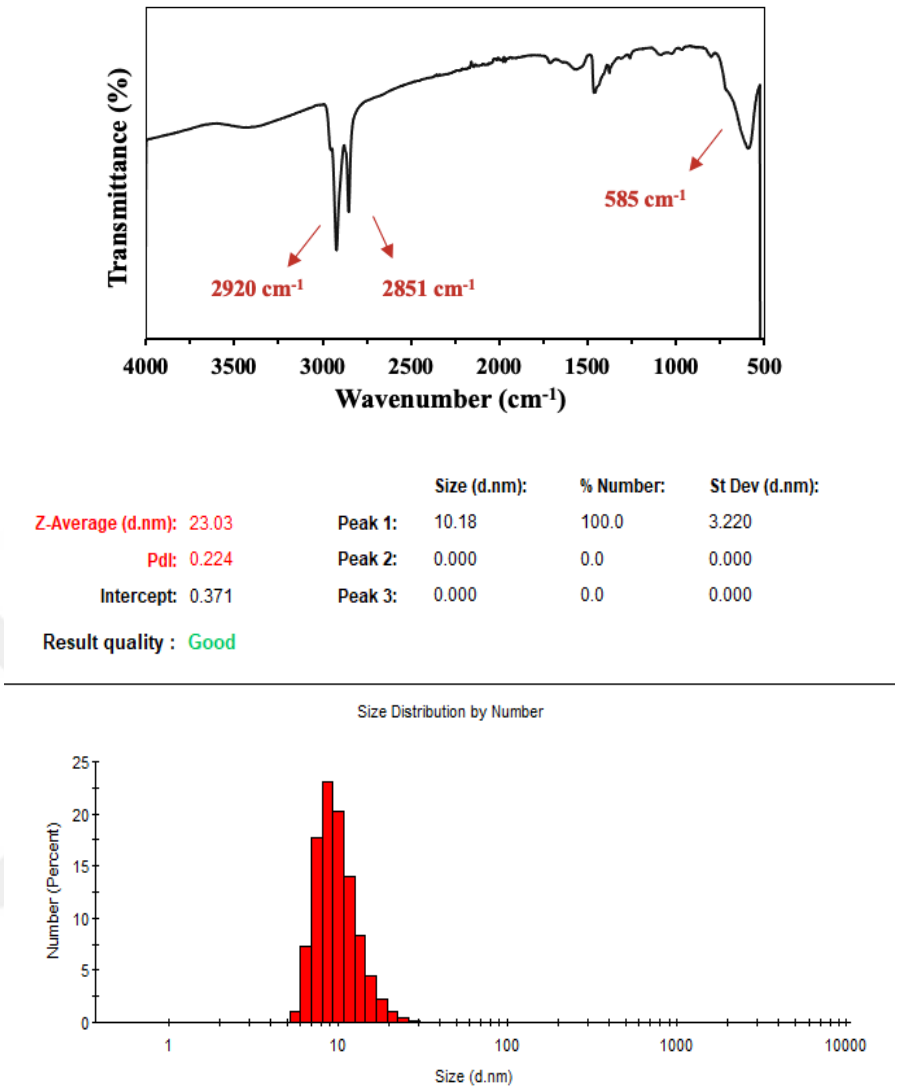

Figure 4.3. FT-IR spectrum (top) and DLS analysis (bottom) of Fe_3O_4@OA.

4.2. Synthesis of Dopamine Modified Chain Transfer Agent (CTA) and Characterizations

4.2.1. Synthesis of 2-(((dodecylthio)carbonothioyl)thio)-2-methylpropanoic acid (CTA)

A chain transfer agent (CTA) was synthesized in order to coat surface of magnetic iron oxide particles so polymers can grow from the surface. Since the chain transfer agent has trithiocarbonate group in its structure, it can be used for RAFT polymerization (Figure

4.4). It was synthesized according to the literature example [61]. In addition, this trithiocarbonate group can be modified to functional groups by radical exchange reactions.

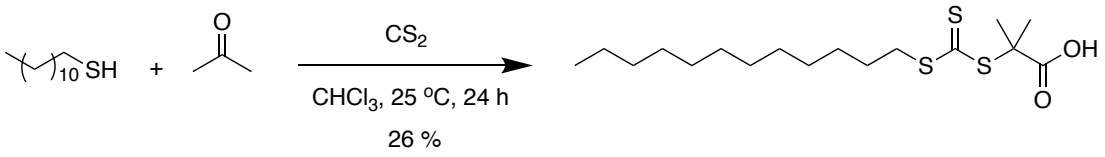

Figure 4.4. Synthesis of chain transfer agent (CTA).

4.2.2. Synthesis of Dopamine Modified Chain Transfer Agent (CTA-Dopa)

An anchoring group is required for binding the chain transfer agent to surface of iron oxide nanoparticles. For that purpose, dopamine was chosen as the anchoring group which can be bind to nanoparticle easily and remain stable on it. Dopamine modified chain transfer agent (CTA-Dopa) was prepared according to previously reported procedure (Figure 4.5) [52]. The characterization of this compound was done with ^{1}H NMR and was determined to be similar to previously reported ^{1}H NMR spectrum of this compound.

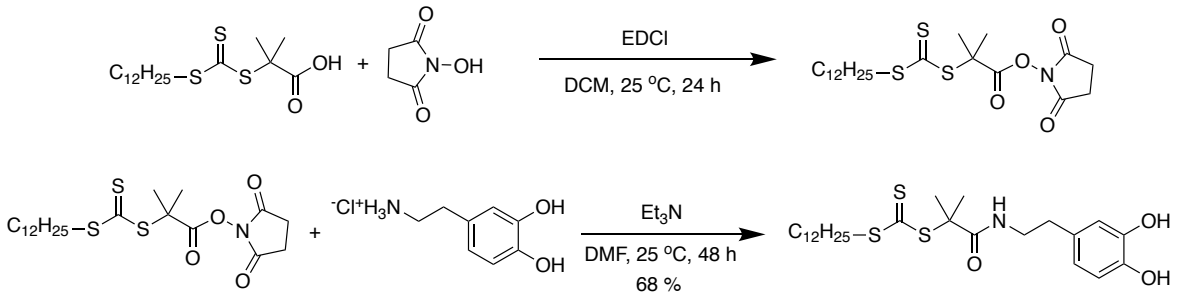

Figure 4.5. Synthetic pathway of dopamine modified chain transfer agent (Dopa-CTA).

4.3. Synthesis of Disulfide Containing Dopamine Modified Chain Transfer Agent (CTA) and Characterizations

4.3.1. Synthesis of Chain Transfer Agent Alcohol (CTA-SS-OH)

In order to obtain cleavable chain transfer agent, which is sensitive to redox media, previously synthesized CTA was modified with alcohol which has a disulfide bond. Carboxylic acid containing CTA was converted into alcohol by using 2,2'-disulfanediyldiethanol which is a diol (Figure 4.6). The reaction is an esterification reaction in the presence of DCC, DMAP and CH_2Cl_2 as the solvent. The yield of this reaction was calculated as 60 %. Characterization of this compound was done with ^1H NMR (Figure 4.7). The presence of the characteristic peak at 4.38 ppm belonging to the protons adjacent to the carbon oxygen bond between the CTA and diol indicates successful conjugation.

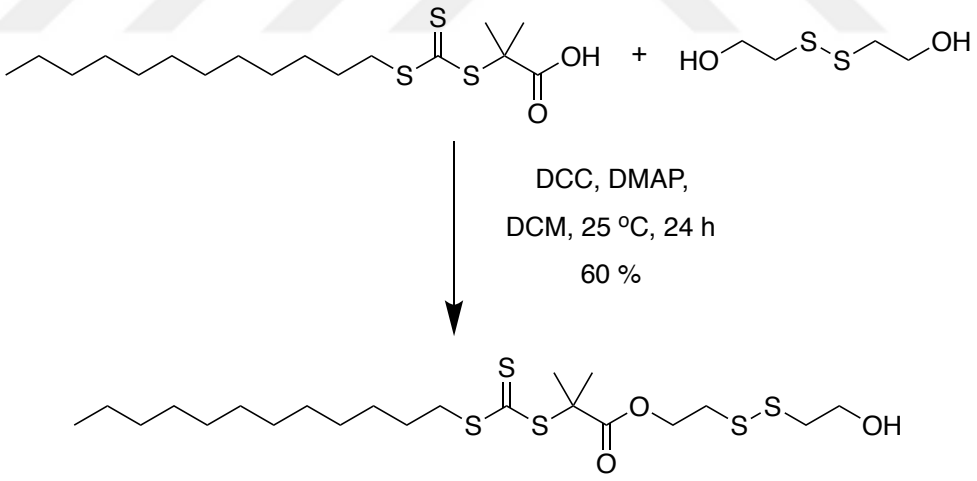

Figure 4.6. Synthesis of CTA-SS-OH.

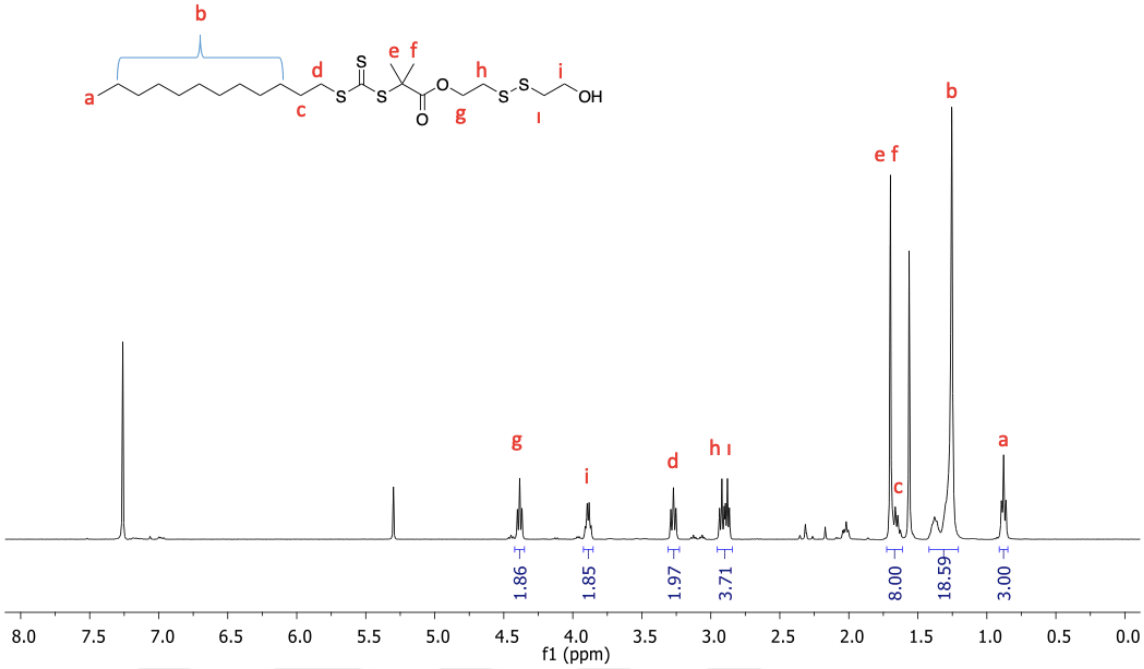

Figure 4.7. ^{1}H NMR spectrum of CTA-SS-OH.

4.3.2. Synthesis of DSC Activated Chain Transfer Agent (CTA-SS-DSC)

CTA alcohol should be activated by DSC, before the conjugation of dopamine. DSC is attached to the CTA alcohol in the presence of TEA. For this reaction, previously synthesized CTA-SS-OH and DSC were used in the presence of TEA and dry DCM as the solvent (Figure 4.8). Finally, there was need for installation of an activated carbonate group in the CTA structure, so the CTA-SS-OH molecule was activated by DSC.

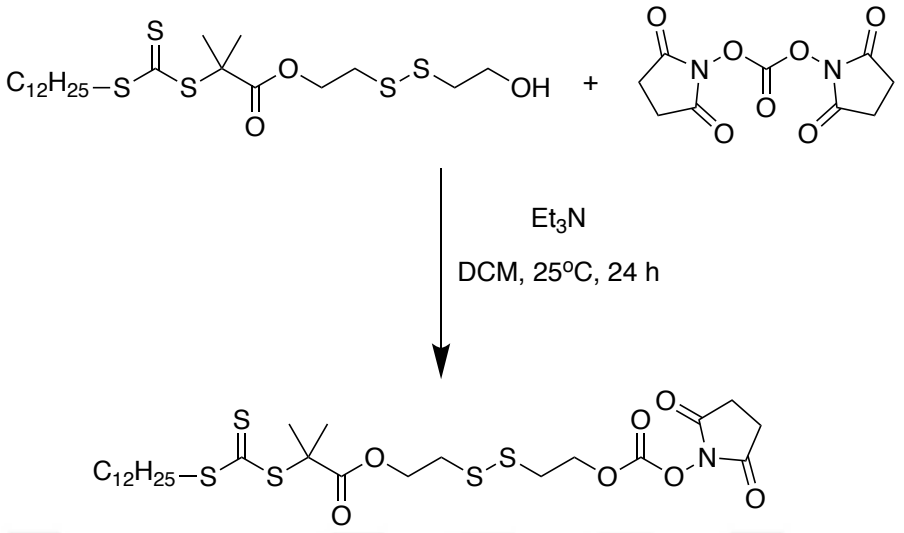

Figure 4.8. Synthesis of CTA-SS-DSC.

4.3.3. Synthesis of Dopamine Modified Disulfide Containing Chain Transfer Agent (CTA-SS-Dopa)

In order to bind cleavable chain transfer agent to the surface of iron oxide nanoparticles, anchoring group is attached to the CTA. Dopamine is a strong and stable anchoring group for iron oxide surfaces, so previously synthesized DSC activated CTA is modified with dopamine group. For this reaction, CTA-SS-DSC and dopamine hydrochloride were used in the presence of TEA and DMF as the solvent (Figure 4.9). The yield of this reaction was calculated as 42 %. Characterization of this compound was done with ^{1}H NMR (Figure 4.10). The presence of the characteristic peaks at 6.80, 6.72, 6.61 ppm belonging to the protons of dopamine and they indicate attachment of dopamine to CTA. In addition, the presence of the characteristic peak at 4.29 ppm belonging to the protons adjacent to the carbamate indicates successful conjugation.

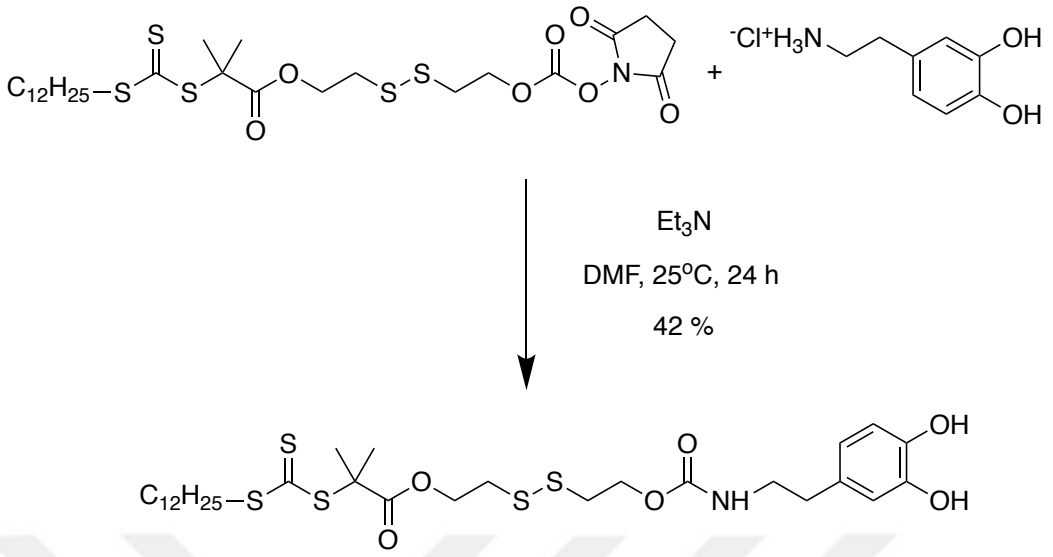

Figure 4.9. Synthesis of CTA-SS-Dopa.

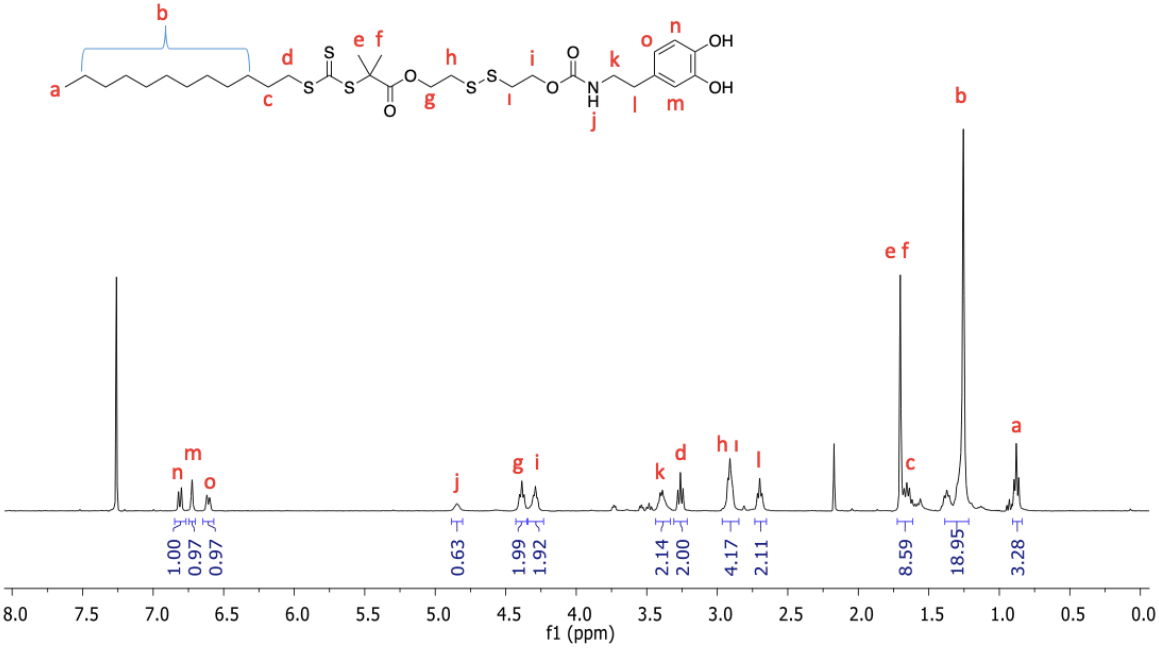

Figure 4.10. ^{1}H NMR spectrum of CTA-SS-Dopa.

4.4. Immobilization of Chain Transfer Agent onto Fe_3O_4 Nanoparticles by Ligand Exchange Reaction and Characterizations

4.4.1. Immobilization of CTA-Dopa onto Fe_3O_4 Nanoparticles (Fe_3O_4@Dopa-CTA)

To be able to grow polymeric brushes from the surface of magnetic iron oxide nanoparticles, immobilization of chain transfer agent is necessary. For this purpose, dopamine modified CTA (CTA-Dopa) was coated to iron oxide nanoparticle surface by ligand exchange reaction. This molecule is synthesized using oleic acid coated iron oxide nanoparticle (Fe_3O_4@OA) and excess amount of CTA-Dopa in the presence of CH_2Cl_2 at 40 °C under a N_2 blanket (Figure 4.11). After the reaction, Fe_3O_4@Dopa-CTA was precipitated in methanol until all free chain transfer agent is removed. Finally, the product was kept in chloroform to prevent them from aggregation.

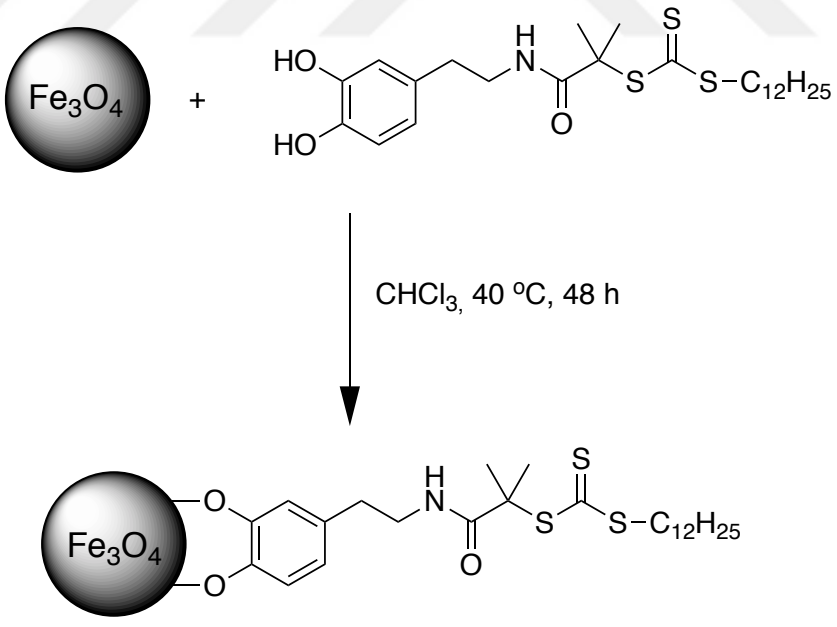

Figure 4.11. Synthesis of Fe_3O_4@Dopa-CTA.

The characterization of this material was done by FT-IR, UV spectroscopy and DLS. The characteristic peak of amide carbonyl group of CTA-Dopa was observed at 1644 cm^{-1} and the peak at 590 cm^{-1} comes from Fe-O bond. FT-IR indicates the place exchange reaction between oleic acid and chain transfer agent is successful. Then, UV spectroscopy was used to see the existence of CTA-Dopa. The immobilized molecule gives a shoulder-like peak at 320 nm which does not exist in spectrum of oleic acid coated nanoparticle and iron oxide gives a sharp peak at 250 nm. These also indicates that CTA-Dopa molecule was successfully attached to iron oxide molecule (Figure 4.12). According to DLS results, Fe_3O_4@Dopa-CTA nanoparticles have a diameter of 11.8 nm.

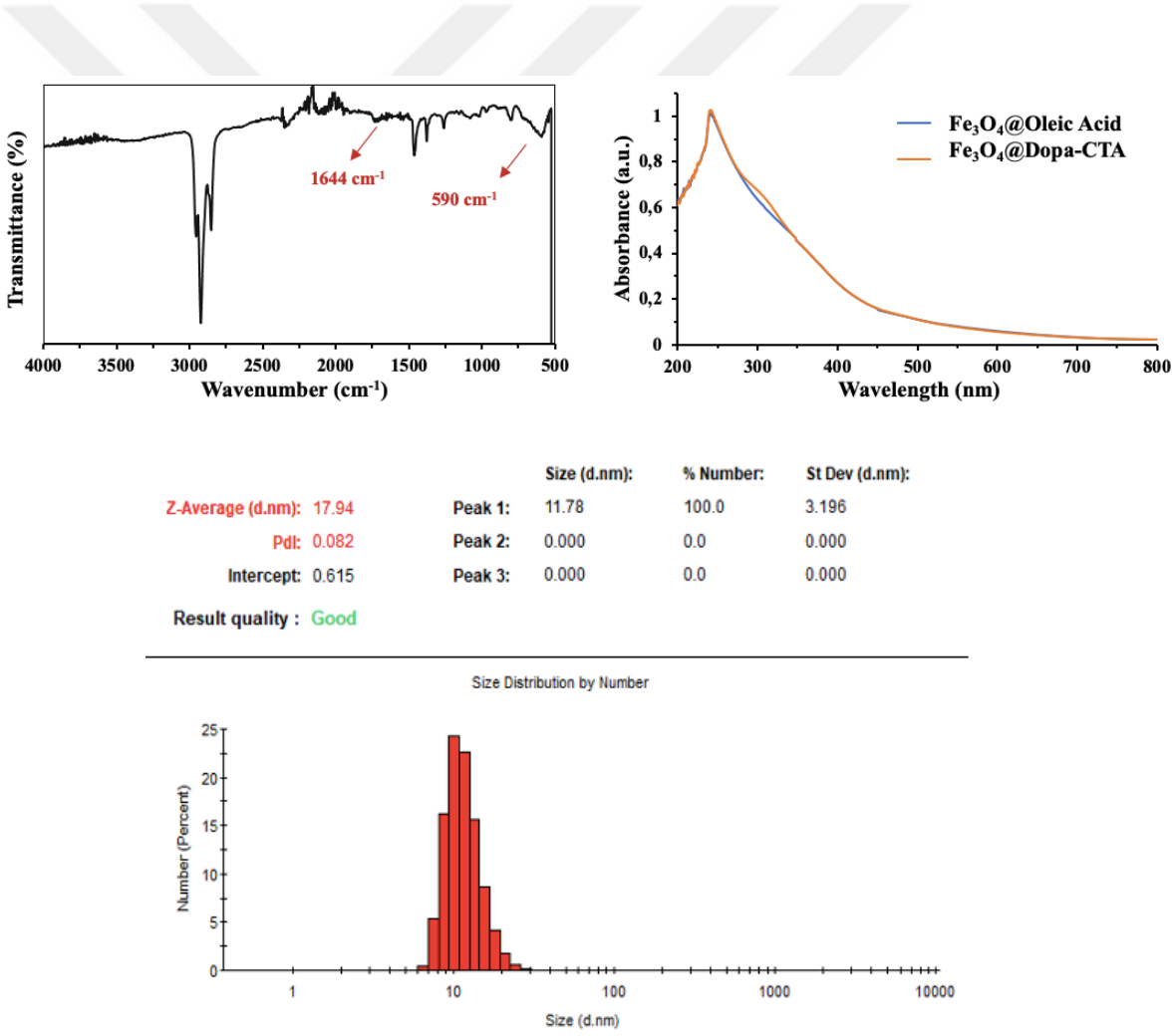

Figure 4.12. FT-IR spectrum (top left), UV spectroscopy (top right) and DLS analysis (bottom) of Fe_3O_4@Dopa-CTA.

4.4.2. Immobilization of CTA-SS-Dopa onto Fe_3O_4 Nanoparticles (Fe_3O_4@Dopa-SS-CTA)

CTA-SS-Dopa molecule was immobilized onto iron oxide nanoparticles by ligand exchange reaction (Figure 4.13). Disulfide containing dopamine modified CTA was attached to iron oxide nanoparticles for polymers to be grown from the surface. This molecule was synthesized using oleic acid stabilized iron oxide nanoparticles and excess amount of CTA-SS-Dopa molecule. After the reaction, reaction mixture was precipitated in methanol to remove excess amount of CTA-SS-Dopa. The obtained product was stored in $CHCl_3$ to eliminate the aggregation of nanoparticles.

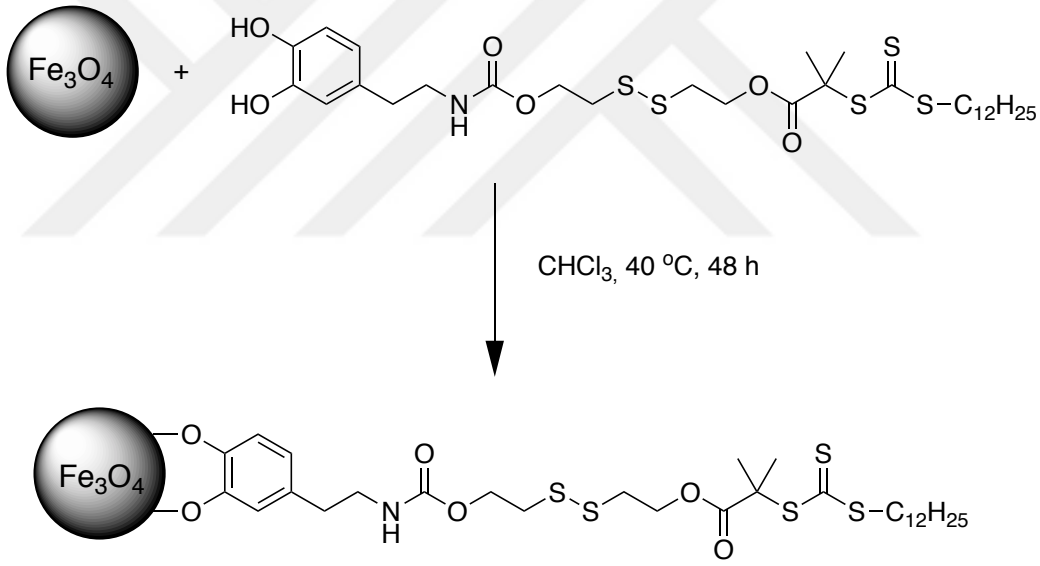

Figure 4.13. Ligand exchange reaction between Fe_3O_4@OA and CTA-SS-Dopa.

Characterization of this molecule was achieved using FT-IR, DLS and UV spectroscopy. The new shoulder like peak at 280 nm originates from the surface immobilized chain transfer agent. In FT-IR, the peak at 1641 cm^{-1} belongs to the amide carbonyl group. In addition, the peak at 550 cm^{-1} belongs to the Fe-O bond (Figure 4.14). This information shows that the conjugation of chain transfer agent to iron oxide nanoparticles is successful. According to DLS results, Fe_3O_4@Dopa-SS-CTA molecule has the diameter of 10.3 nm.

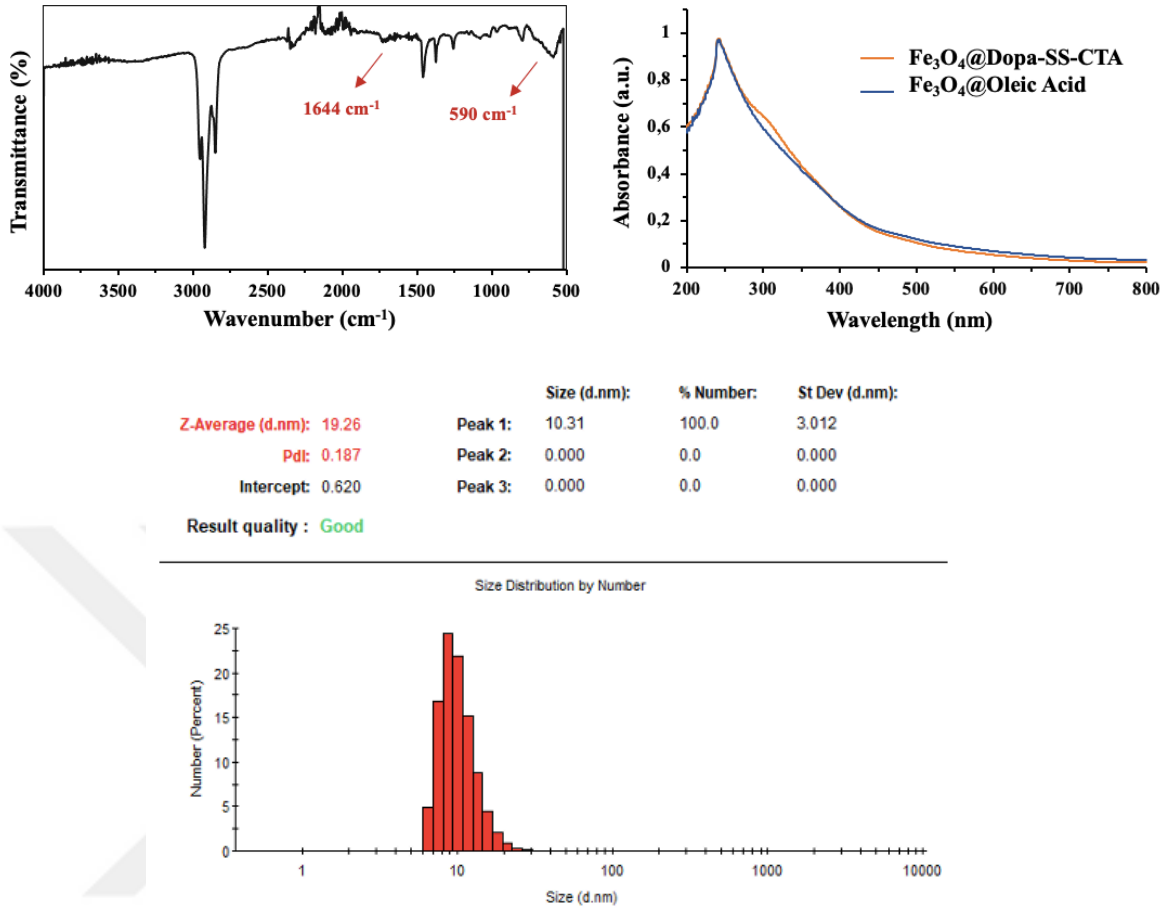

Figure 4.14. UV spectroscopy (top left), FT-IR spectrum (top right), and DLS analysis (bottom) of Fe_3O_4@Dopa-SS-CTA.

4.5. Surface Initiated RAFT Polymerization of PEGMEA from the Surface of Fe_3O_4 Nanoparticles and Characterizations

4.5.1. Synthesis of Polymer-Coated Fe_3O_4 Nanoparticles (Fe_3O_4@Dopa-PEGMEA)

Once the chain transfer agent is immobilized onto iron oxide nanoparticles, RAFT polymerization of PEGMEA was carried out. The PEGMEA was used as the monomer because when it polymerizes it provides an anti-biofouling and biocompatible coating and by this monomer, compound gains hydrophilic property. Polymers were grown from the surface of nanoparticles by grafting-from approach. For this synthesis, Fe_3O_4@Dopa-CTA, PEGMEA monomers and AIBN as the initiator were used and toluene was used as a solvent.

The reaction mixture was purged with N_2 and stirred at 75 °C for 24 hours (Figure 4.15). Then, the reaction mixture was precipitated in cold diethyl ether. This precipitation showed successful polymerization however there could be some unreacted monomers, so this step was continued until all monomers were removed.

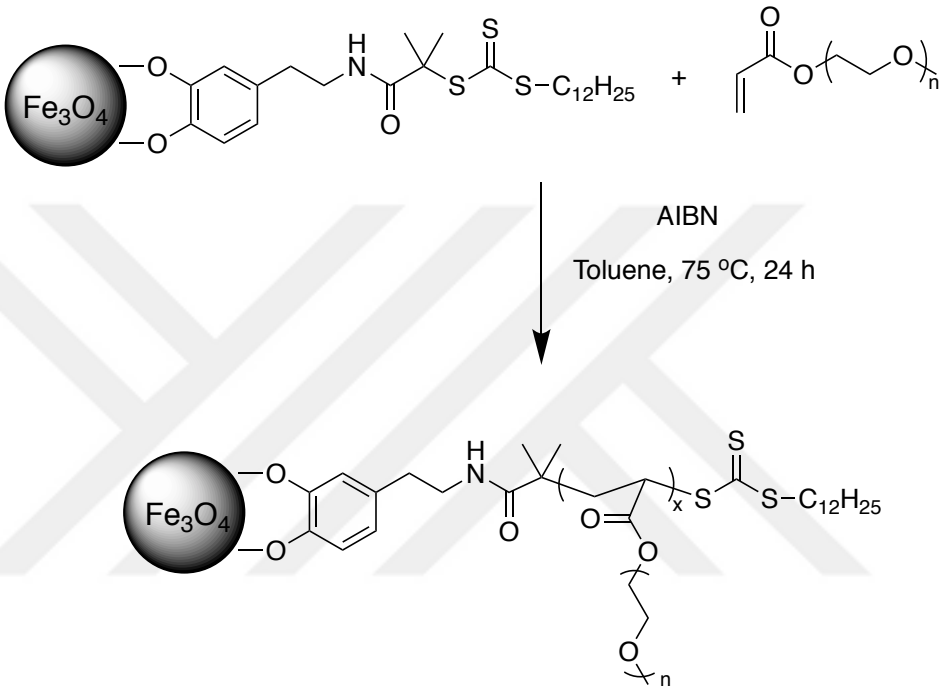

Figure 4.15. Surface initiated RAFT polymerization of PEGMEA.

Characterization of surface-initiated polymers was carried out with FT-IR, UV spectroscopy and DLS. From FT-IR spectrum, the strong peak at 1731 cm^{-1} which corresponds to carbonyl groups of PEGMEA, indicates polymerization. The peak at 1093 cm^{-1} originates from the C-O-C ether stretch. These peaks show that successfully grown polymeric brushes from the surface of iron oxide nanoparticles. In UV spectroscopy, the shoulder like peak at 308 nm that corresponds to trithiocarbonate group of chain transfer agent, so end group remains after the RAFT polymerization (Figure 4.16). From DLS results, the diameter of polymer-coated iron oxide nanoparticles was calculated as 22.2 nm. After the polymerization, size of magnetic nanoparticle increases as expected. In addition, as a physical characterization, a solubility test was done. A small amount of polymer-coated iron oxide nanoparticles was added into water. Then, it was observed that it was dispersible in

water, whereas the initial CTA immobilized iron oxide nanoparticles were not dispersible in water, so by polymerization nanoparticles gained hydrophilic property.

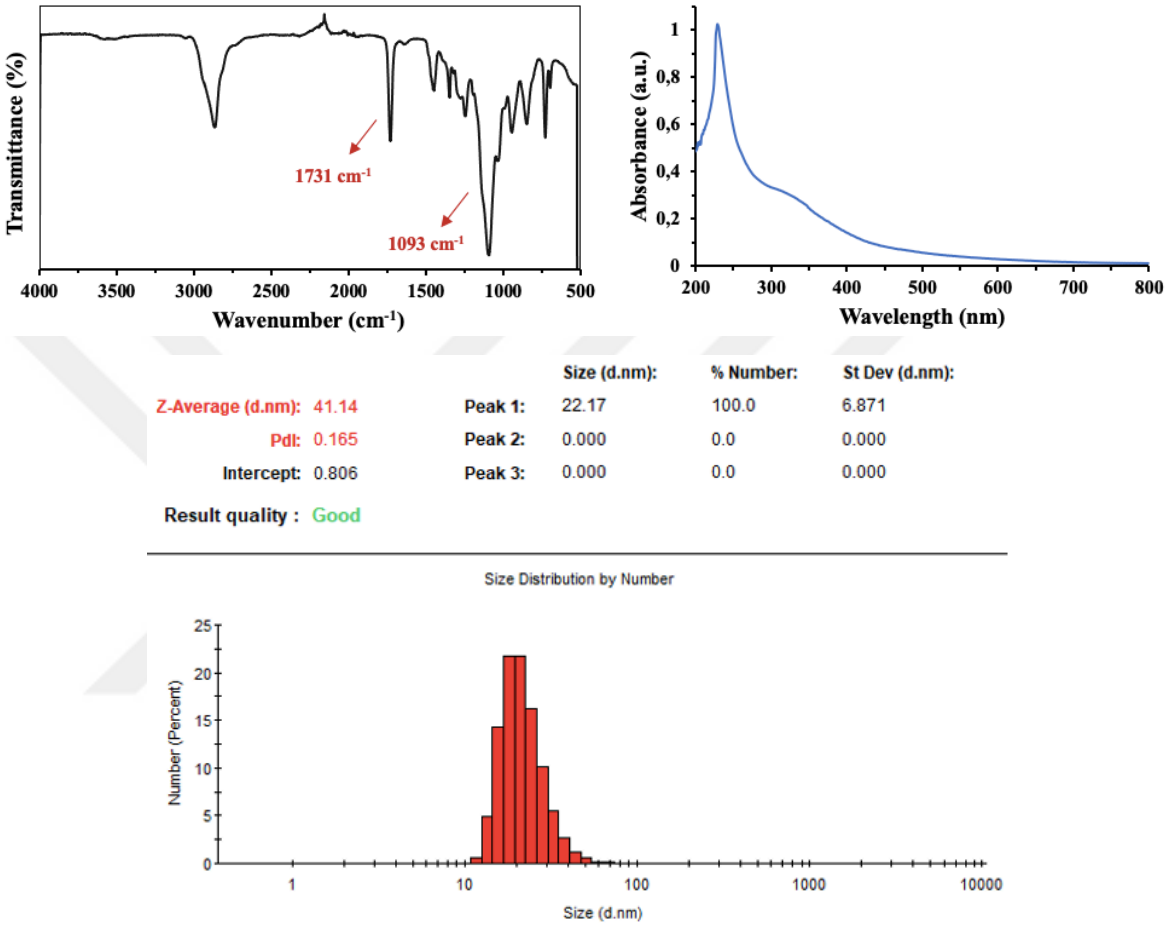

Figure 4.16. FT-IR spectrum (top left) and UV-Vis spectroscopy (top right) and DLS analysis (bottom) of Fe_3O_4@Dopa-PEGMEA.

4.5.2. Synthesis of Degradable Polymer-Coated Fe_3O_4 Nanoparticles (Fe_3O_4@Dopa-SS-PEGMEA)

After successful conjugation of dopamine modified CTA to iron oxide nanoparticles, RAFT polymerization of PEGMEA was done by grafting-from method in the presence of AIBN and toluene (Figure 4.17). The reaction mixture was purged with N_2 for 20 minutes. Then, it was stirred at 75 °C for 2, 4, 8, 16 and 24 hours to see the molecular weight

difference upon increase in time. After the polymerization reaction, black viscous liquid was precipitated in cold diethyl ether until removal of unreacted monomers.

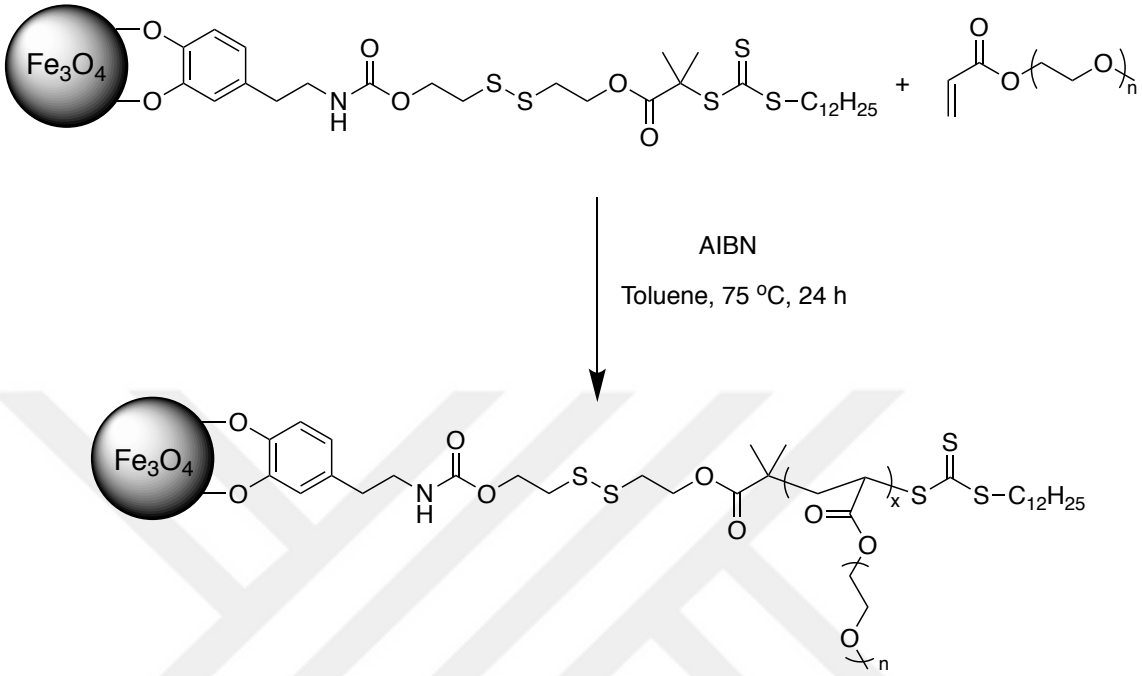

Figure 4.17. Synthesis of Fe_3O_4@Dopa-SS-PEGMEA by RAFT polymerization.

The characterization of grafted polymers was undertaken using UV spectroscopy, DLS and FT-IR spectrum shown in Figure 4.18. In FT-IR spectrum, the strong peak at 1731 cm^{-1} comes from the carbonyl groups of PEGMEA and the peak at 1094 cm^{-1} belongs to the ether groups of the polymers. In addition, the peak at 320 nm in UV spectroscopy indicates the presence of the trithiocarbonate groups at the chain end of the polymers. These indications combined demonstrate that polymerization reaction occurred successfully. According to DLS results, Fe_3O_4@Dopa-SS-PEGMEA molecule possessed a diameter of 31.6 nm. As expected, when polymeric brushes are grown from the surface, size of magnetic nanoparticle increases.

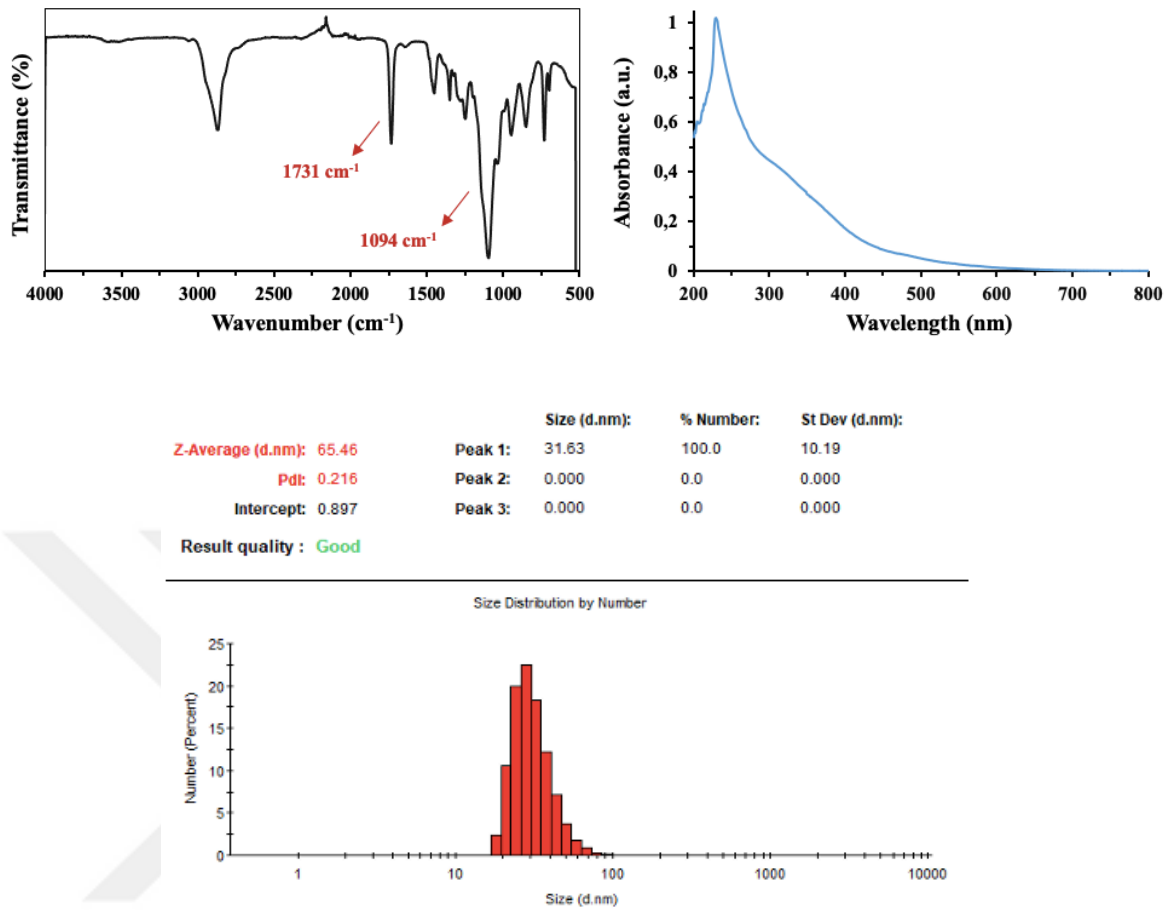

Figure 4.18. FT-IR spectrum (top left), UV spectroscopy (top right) and DLS analysis (bottom) and of Fe_3O_4@Dopa-SS-PEGMEA.

After the polymerization of PEGMEA from the surface of iron oxide nanoparticles, polymer coated magnetic nanoparticles (Fe_3O_4@Dopa-SS-PEGMEA) were soluble in water even though CTA coated magnetic nanoparticles (Fe_3O_4@Dopa-SS-CTA) were not soluble in water (Figure 4.19). Because of the presence of hydrophilic p(PEGMEA) polymeric brushes on the nanoparticle surface, compound becomes dispersible in water.

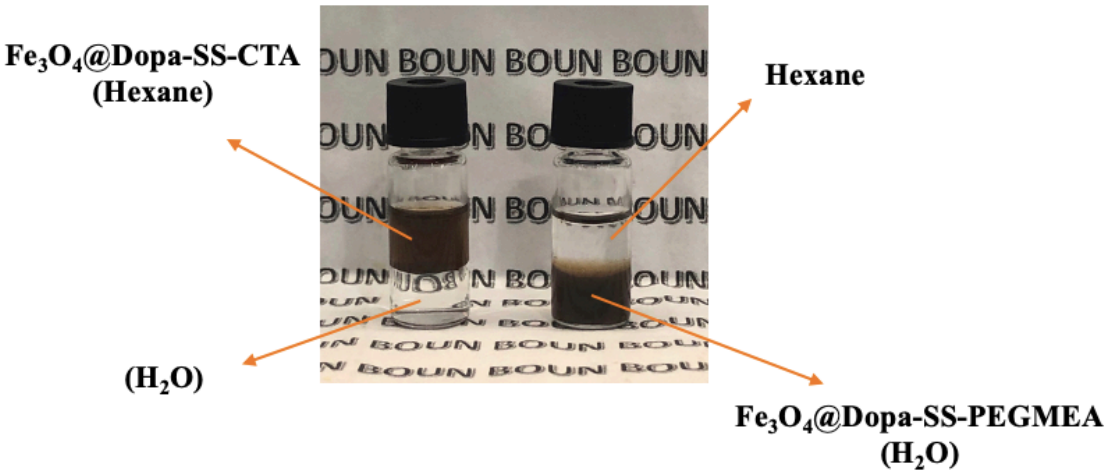

Figure 4.19. Dispersibility difference of Fe_3O_4@Dopa-SS-CTA (left) and Fe_3O_4@Dopa-SS-PEGMEA nanoparticles.

4.6. Degradation of PEGMEA Polymeric Brushes from the Surface of Fe_3O_4 Nanoparticles and Characterizations

4.6.1. Reductive Cleavage of PEGMEA Polymers from Fe_3O_4 Nanoparticles

The molecular weights and polydispersity indexes of polymeric brushes, which are grown from the surface of iron oxide nanoparticles, cannot be calculated. However, the system that were created in this project provides us to calculate molecular weight and PDI values of polymeric brushes by GPC. In this project, magnetic nanoparticles were coated with disulfide containing chain transfer agent and then, polymeric brushes were grown from the nanoparticle surfaces. These disulfide bonds are sensitive to redox media and they can be cleaved by thiol containing materials like DTT and glutathione. So, magnetic nanoparticle and polymeric brushes are easily separated under mild conditions and polymeric brushes can be analyzed. Polymer-coated iron oxide nanoparticles and DTT were dissolved in phosphate buffer solution and stirred at room temperature for 2 hours (Figure 4.20). Then, polymers and nanoparticles were centrifuged to separate from each other by solubility difference. Polymer coated iron oxide nanoparticles were gained water dispersibility by PEG based polymeric brushes and they lost their magnetic strength because of polymer coating.

However, when iron oxide nanoparticles were separated from polymeric brushes, they gained magnetic strength again but lost their water dispersibility (Figure 4.21).

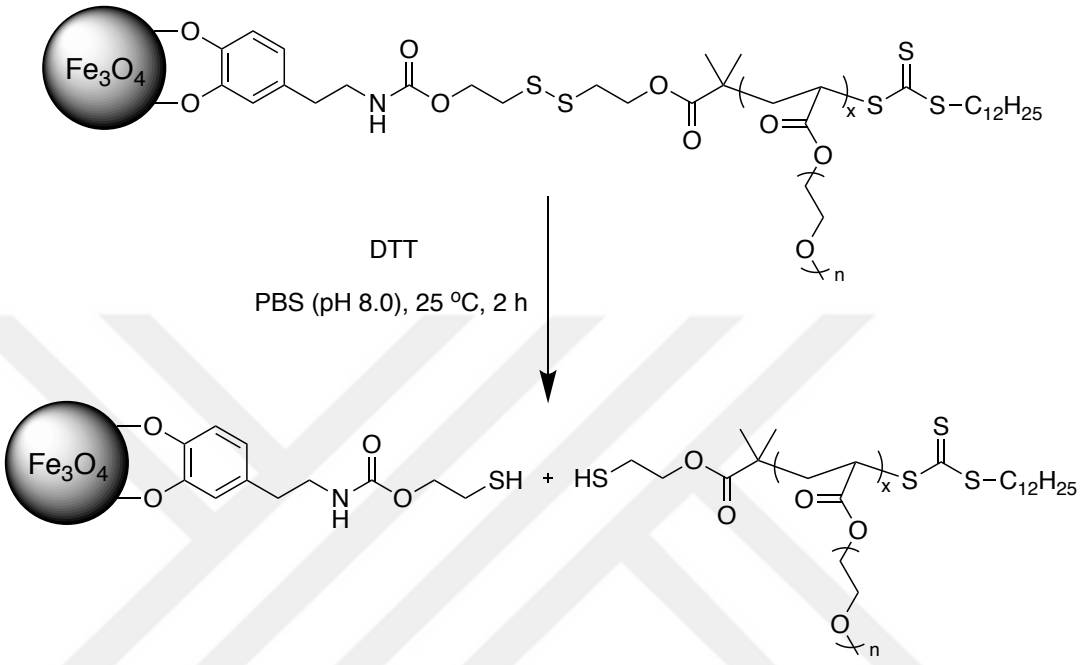

Figure 4.20. Cleavage of disulfide bond in polymer-coated nanoparticles by DTT.



Figure 4.21. Dispersibility of Fe_3O_4@Dopa-SS-PEGMEA in water (left), after treatment with DTT and centrifugation.

Characterization of these separated molecules was done by Ellman's analysis. When Ellman's reagent was added to cleaved iron oxide nanoparticles and polymers, the color of the solution turned into yellow. That was a positive test for this analysis. In addition, in UV-Vis spectroscopy, peak at 412 nm was observed for both nanoparticles and polymers (Figure 4.22). This indicates that nanoparticles and polymers have free thiol group in their structures. Ellman analysis was also applied to Fe_3O_4@Dopa-SS-PEGMEA molecule as the control group. There was no peak at 412 nm in UV spectroscopy. As expected, there was no free thiol group in the structure of polymer-coated iron oxide nanoparticles, so the test was negative.

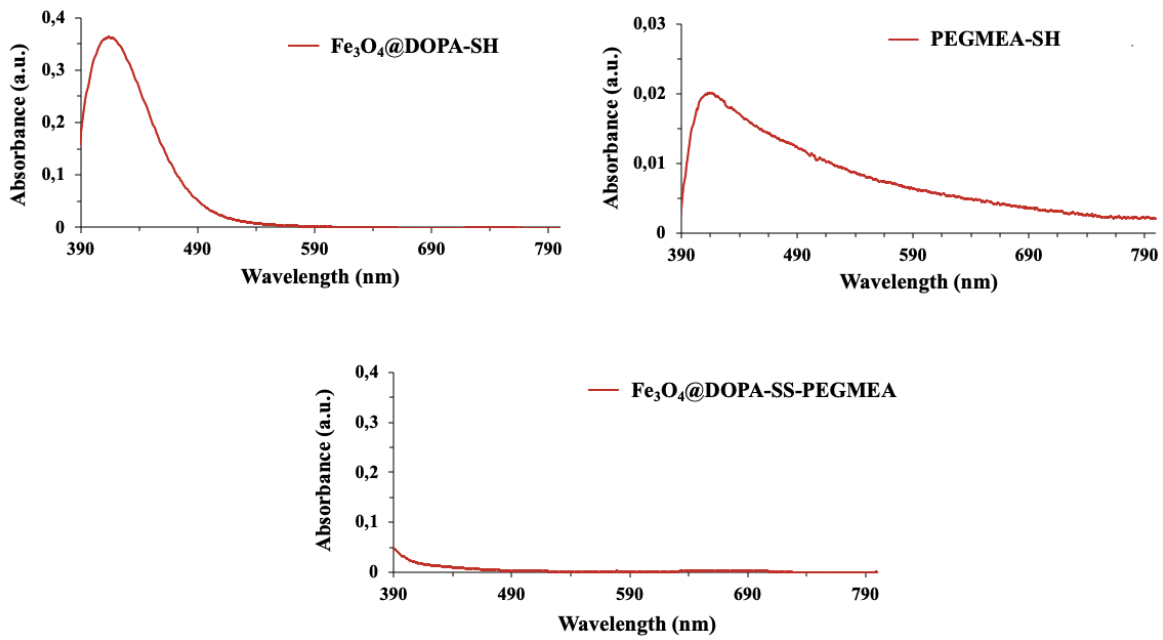

Figure 4.22. UV-Vis spectra of cleaved iron oxide nanoparticles (upper-left), polymeric brushes (upper-right) and Fe_3O_4@Dopa-SS-PEGMEA (without DTT exposure) upon treatment with Ellman's reagent.

4.6.2. Molecular Weight and PDI Analysis of Cleaved Polymeric Brushes

The molecular weights of the polymeric brushes that were cleaved from the surface of iron oxide nanoparticles were analyzed by gel permeation chromatography (GPC) (Table 4.1). Polymerization reaction was set up for 2, 4, 8, 16, 24 hours under the same conditions for three times to determine how molecular weights were changing with time.

Table 4.1. Molecular weights and PDI values of polymer-coated iron oxide nanoparticles having different time polymerizations.

Fe_3O_4@Dopa-SS-PEGMEA	Molecular Weight	Polydispersity Index (PDI)	Average Yield
2 hour	15 kDa	1.68	16%
	13 kDa	1.61	
	12 kDa	1.58	
4 hour	20 kDa	1.66	22%
	14 kDa	1.57	
	16 kDa	1.60	
8 hour	16 kDa	1.59	57%
	16 kDa	1.61	
	16 kDa	1.49	
16 hour	13 kDa	1.58	79%
	15 kDa	1.61	
	16 kDa	1.65	
24 hour	16 kDa	1.63	92%
	14 kDa	1.66	
	16 kDa	1.69	

According to GPC results, it was obviously realized that molecular weights of 4, 8, 16- and 24-hour polymers were close to one another. The molecular weights of 2- and 4-hour polymers were not decreased by time but the yield of 2 and 4-hour polymers was slightly low. Therefore, the polymerization reactions that was done for 8 hours because it is enough to reach desired molecular weights.

4.6.3. Polymerization of PEGMEA From the Surface of Nanoparticle (Fe_3O@Dopa-SS-PEGMEA) and From the Free CTA (Dopa-SS-PEGMEA)

After successful conjugation of dopamine modified CTA to iron oxide nanoparticles, RAFT polymerization of PEGMEA was done by grafting-from method in the presence of AIBN, free CTA and toluene (Figure 4.23). The reaction mixture was purged with N_2 for 20 minutes. Then, it was stirred at 75 °C for 24 hours. After the polymerization reaction, black viscous liquid was precipitated in cold diethyl ether until removal of unreacted monomers.

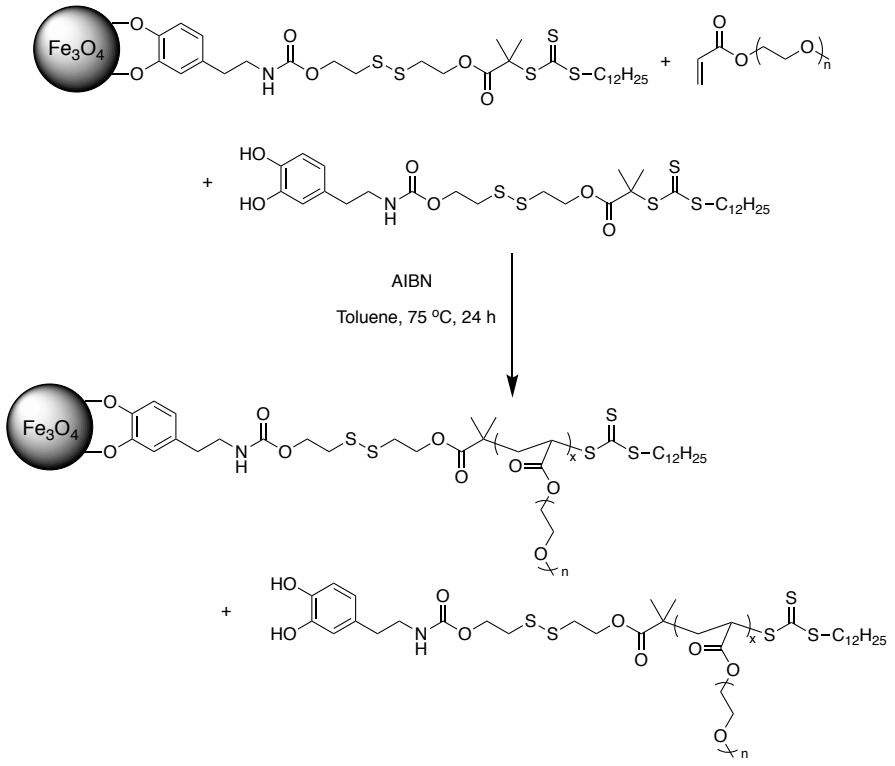

Figure 4.23. Synthesis of Fe_3O_4@Dopa-SS-PEGMEA by RAFT polymerization with free CTA.

4.6.4. Polymerization of PEGMEA From the Surface of Nanoparticle (Fe_3O@Dopa-SS-PEGMEA) at Different Conditions

In this project, iron oxide nanoparticles were coated by cleavable polymeric brushes. The molecular weights of the polymeric brushes that were cleaved from the surface of iron oxide nanoparticles were determined by GPC. Polydispersity index (PDI) of these polymeric brushes are also analyzed by GPC. However, measured PDI values of polymeric brushes were little bit high (Table 4.1). Therefore, polymerization of PEGMEA from the surface of iron oxide nanoparticles were repeated at different conditions to decrease polydispersity index of polymers. In order to obtain low PDI value, free CTA was added to the media. It is very effective way in RAFT polymerization, so it became successful (Table 4.2). So, in the rest of project, polymerizations were done by adding free CTA.

Molecular weight control of polymeric brushes is also important. It was intended to control molecular weight by changing conditions, such as, change in volume of solvent, concentration of initiator and concentration of monomer. As seen in the Table 4.2 below, volume of solvent and initiator concentration were not effective that much. However, increase in concentration of monomer by 4 times is very effective. With this change, molecular weights of polymers were increased by 2 times.

Table 4.2. Molecular weights and PDI values of polymer-coated iron oxide nanoparticles having different conditions.

Change in Condition	Molecular Weight	Polydispersity Index (PDI)
Adding free CTA	19 kDa	1.39
Decrease in volume of solvent (1/2)	20 kDa	1.43
Increase in volume of solvent (x2)	18 kDa	1.47
Decrease in concentration of initiator (1/2)	15 kDa	1.39
Increase in concentration of initiator (x2)	18 kDa	1.40
Decrease in concentration of monomer (1/2)	16 kDa	1.42
Increase in concentration of monomer(x2)	20 kDa	1.46
Increase in concentration of monomer (x4)	50 kDa	1.56

4.7. Synthesis of BODIPY Dye Monomer

The aim of synthesizing BODIPY monomer is to polymerize it from the surface of iron oxide nanoparticle with PEG based monomer. By grafting from approach, copolymeric brushes which consist of BODIPY and PEGMEA, were grown from the surface of magnetic nanoparticles. BODIPY is a hydrophobic molecule as many drugs so it can be use as drug model. It is a fluorescent dye having characteristic peak at UV-vis spectroscopy, so it facilitates release studies of polymer conjugated magnetic nanoparticles. There are a few steps to synthesize BODIPY acrylate monomer.

4.7.1. Synthesis of BODIPY Bromide (BODIPY-Br)

First of all, BODIPY bromide was synthesized intended to be modified to BODIPY acetate according to previously reported procedure [62]. 11-Bromoundecanoic acid, oxalyl chloride, 3-ethyl-2,4-dimetylpyrrole and boron trifluoride dimethyl etherate were used in the presence of TEA and DCM/Toluene as the solvent (Figure 4.24). The yield of reaction was calculated as 46% and dark green solid was obtained. The chemical composition of the obtained compound was confirmed to be identical to previously reported one since the ^{1}H NMR spectra was in agreement with one reported in literature.

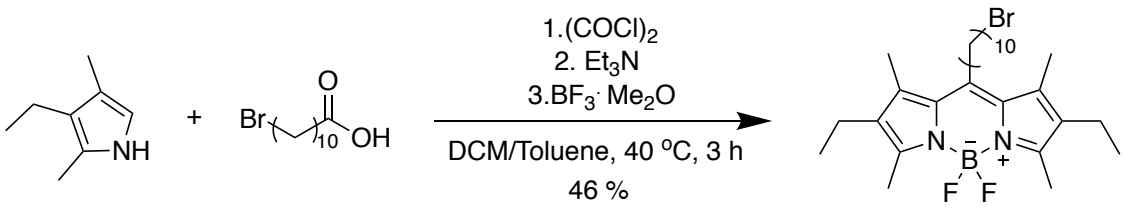

Figure 4.24. Synthesis of BODIPY bromide (BODIPY-Br).

4.7.2. Synthesis of BODIPY Acetate (BODIPY-OAc)

BODIPY acetate that was intended to be modified to BODIPY alcohol was prepared according to the literature [62]. For this reaction, previously synthesized BODIPY-Br and potassium acetate were used and they were dissolved in DMF (Figure 4.25). 250 mg, red solid product was obtained with 92% yield. Characterization of this compound was done with ^{1}H NMR and the spectrum of obtained product was in agreement with one reported in literature.

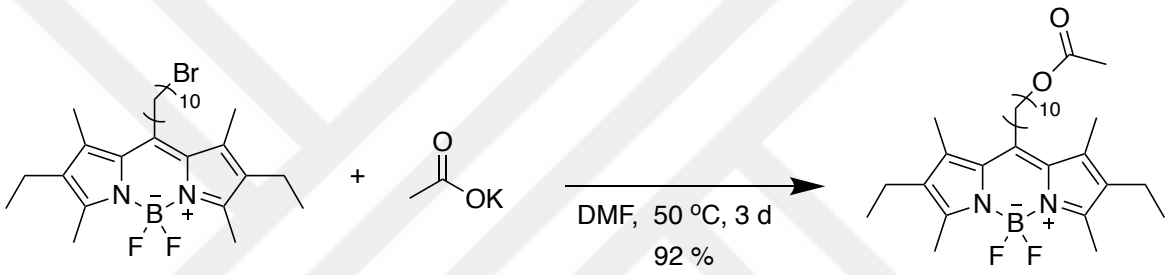

Figure 4.25. Synthesis of BODIPY acetate (BODIPY-OAc).

4.7.3. Synthesis of BODIPY Alcohol (BODIPY-OH)

BODIPY alcohol that was intended to be modified to BODIPY monomer was synthesized according to the literature [62]. Previously synthesized BODIPY-OAc and lithium hydroxide were used in the presence of THF/MeOH mixture (Figure 4.26). The yield of reaction was calculated as 84% and dark red solid was obtained. The characterization of bodipy alcohol was done with ^{1}H NMR and was determined to be similar to previously reported ^{1}H NMR spectrum of this compound.

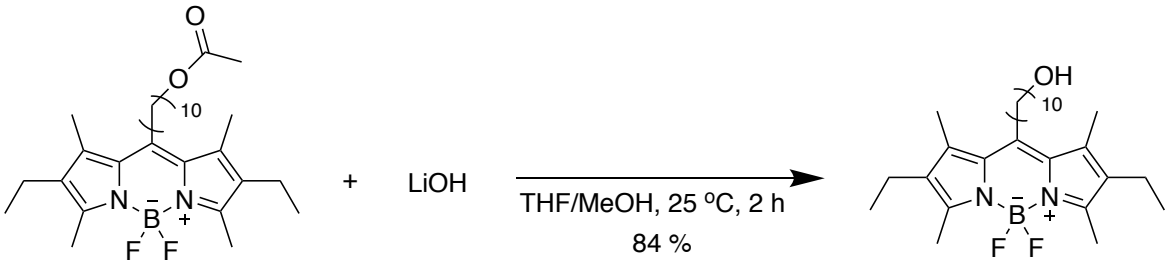

Figure 4.26. Synthesis of BODIPY alcohol (BODIPY-OH).

4.7.4. Synthesis of BODIPY Acrylate Monomer

BODIPY acrylate monomer was synthesized to use it as monomer with PEGMEA monomer to do copolymer brushes on the surface of iron oxide nanoparticles by RAFT polymerization. For this reaction, previously synthesized BODIPY Alcohol and acryloyl chloride were used in the presence of TEA and DCM as the solvent (Figure 4.27). The yield of reaction was calculated as 57% and 16 mg dark red solid was obtained. Characterization of this compound was done with ^{1}H NMR (Figure 4.28). The peak at 1.70-1.27 ppm comes from the alkyl chain of dye. The peaks at 6.39, 6.16-6.06, 5.81 ppm come from the acrylate group of monomers. In addition, the presence of characteristic peak at 4.15 ppm comes from the protons adjacent to the acrylate group. BODIPY-OH had a characteristic peak at 3.64, in this case it shifted to 4.15 ppm, so it indicates that BODIPY-OH was successfully modified to BODIPY acrylate monomer.

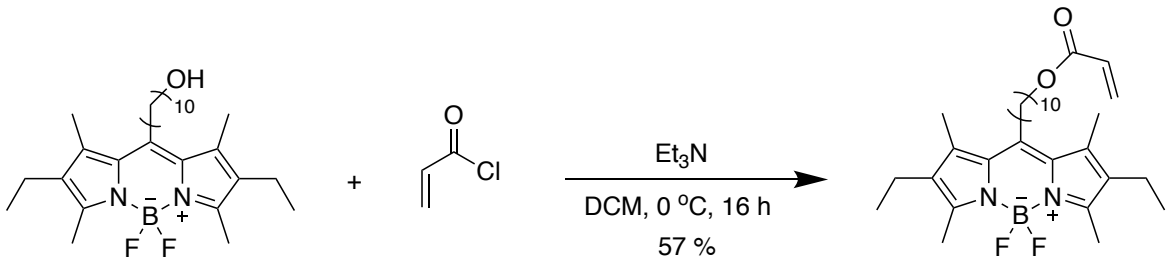

Figure 4.27. Synthesis of BODIPY acrylate monomer.

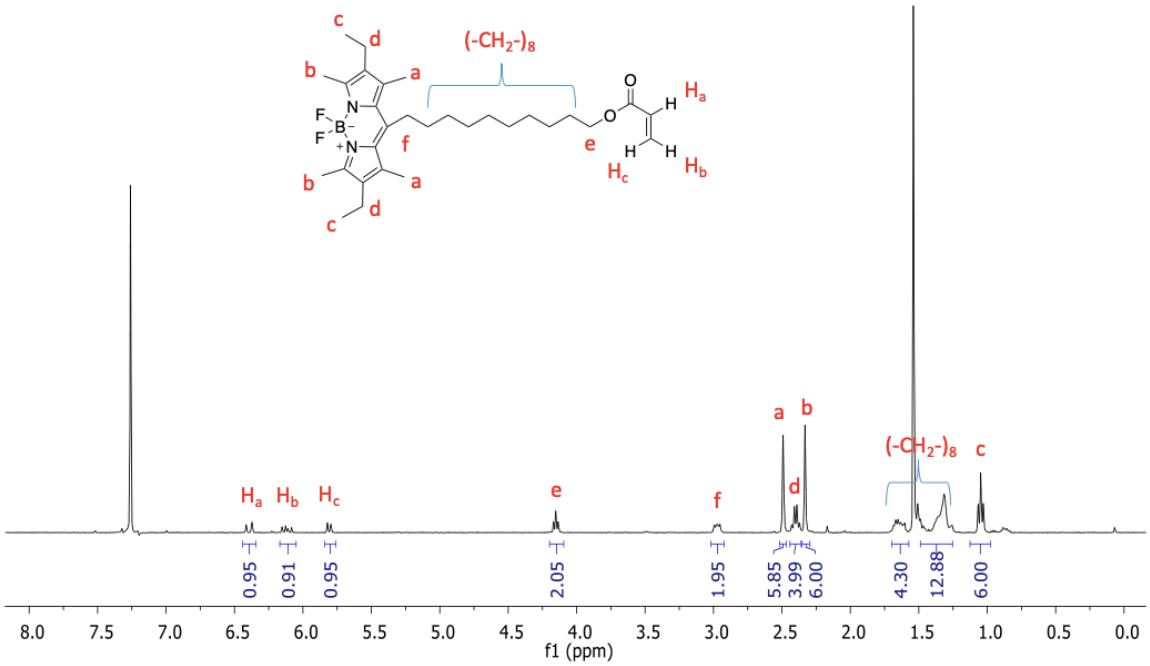

Figure 4.28. ^{1}H NMR spectrum of BODIPY acrylate monomer.

4.8. RAFT Copolymerization of PEGMEA and BODIPY Acrylate from the Surface of Fe_3O_4 Nanoparticles (Fe_3O_4@Dopa-SS-PEGMEA-r-BODIPY)

RAFT copolymerization of PEG and fluorescent dye based polymeric brushes was done by grafting-from method on the surface of iron oxide nanoparticles by using PEGMEA and BODIPY acrylate as monomer. For this reason, cleavable chain transfer agent coated iron oxide nanoparticles (Fe_3O_4@Dopa-SS-CTA), PEGMEA and previously synthesized BODIPY acrylate was used. AIBN was used as the initiator and toluene was used as a solvent (Figure 4.29). After the polymerization, greenish viscous product was obtained.

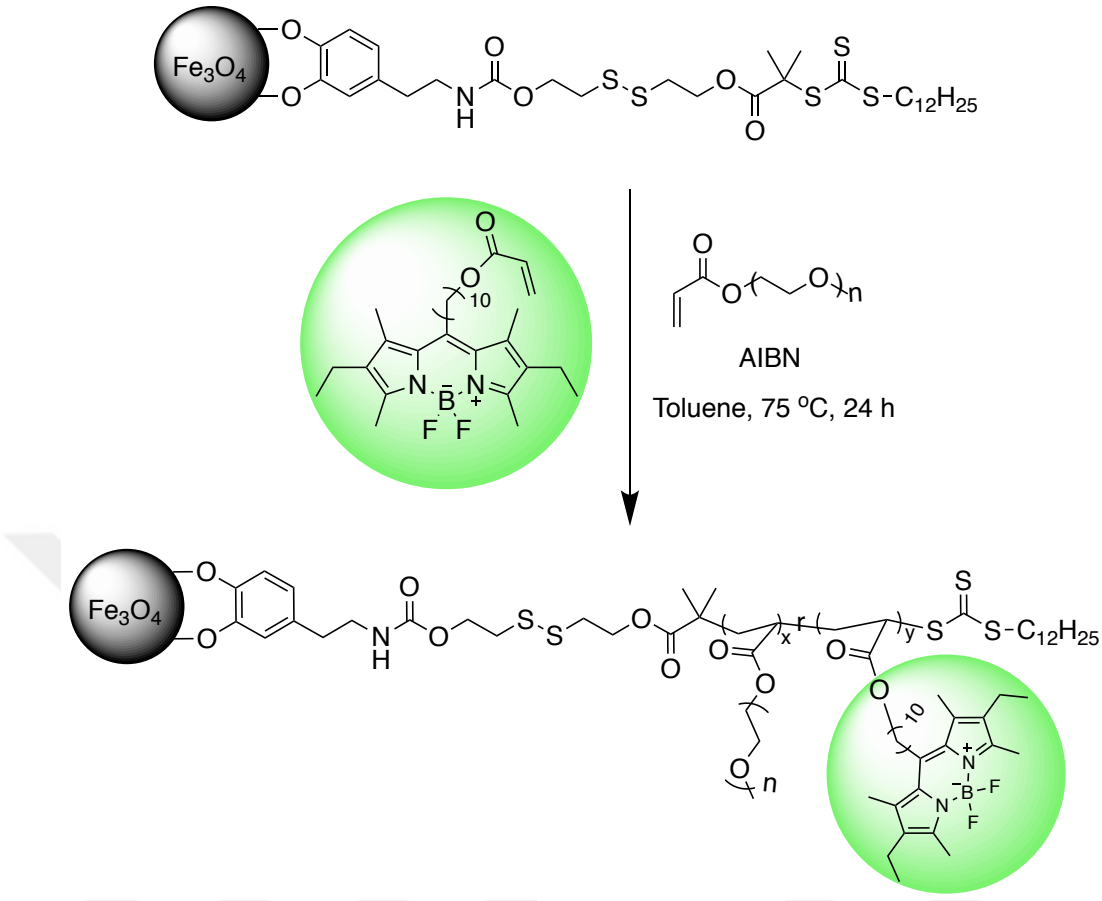

Figure 4.29. Synthesis of Fe_3O_4@Dopa-SS-PEGMEA-r-BODIPY by RAFT polymerization.

Characterization of surface-initiated polymers was carried out with UV-vis spectroscopy. BODIPY is a fluorescent dye molecule, so it has a characteristic strong peak at 520 nm in UV spectroscopy. On the other hand, the shoulder like peak at 308 nm that corresponds to trithiocarbonate group of chain transfer agent, so end groups remain stable after the RAFT copolymerization (Figure 4.30).

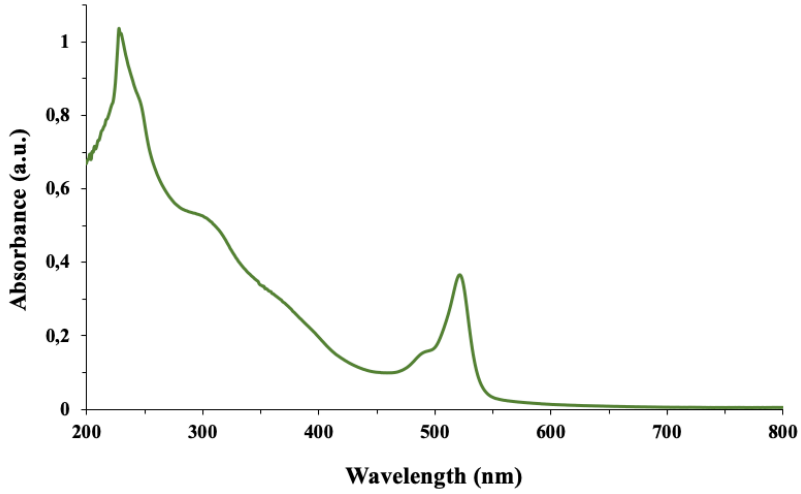

Figure 4.30. UV-vis Spectrum of Fe_3O_4@Dopa-SS-PEGMEA-r-BODIPY.

In addition, BODIPY is a hydrophobic dye molecule so it is not soluble in water. However, BODIPY acrylate monomer was synthesized and it was polymerized from the surface of magnetic nanoparticles with PEG based PEGMEA monomer. PEG is very hydrophilic and its percentage in polymer-coated nanoparticle is higher than BODIPY, so it provided water dispersibility both of magnetic nanoparticle and BODIPY fluorescent dye (Figure 4.31).

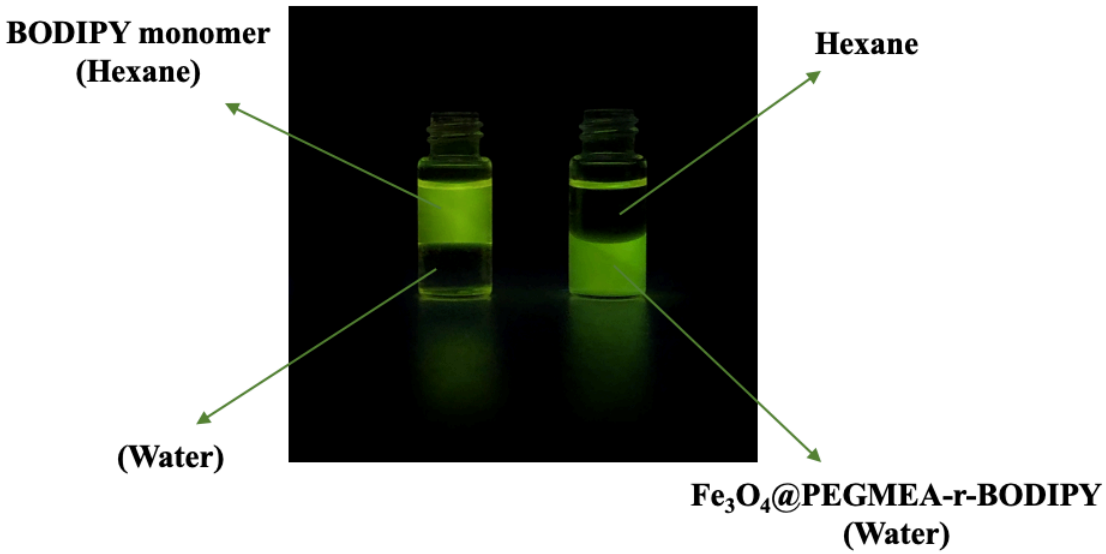

Figure 4.31. Dispersibility difference of BODIPY monomer (left) and Fe_3O_4@PEGMEA-r-BODIPY nanoparticles.

4.9. Reductive Cleavage of PEGMEA and BODIPY Copolymer Brushes from Fe_3O_4 Nanoparticles

DTT was used in order to cleave the disulfide bond that builds a bridge between and nanoparticles and polymers. For this cleavage reaction, 15 mg of Fe_3O_4@Dopa-SS-PEGMEA-r-BODIPY and DTT (1.54 mg, 0.01 mmol) were dissolved in pH=8.0 phosphate buffer (1 mL) solution. Resulting mixture was stirred at room temperature for 4 hours (Figure 4.32). In order to separate iron oxide nanoparticles and polymers, reaction mixture was added into water (6 mL) and the solution was centrifuged at 9000 rpm for 15 minutes. Iron oxide nanoparticles without polymer coating were not dispersible in aqueous media. However, hydrophilic mostly PEG, slightly dye based copolymer brushes dissolved in water and could be obtained through lyophilization. This is shown in Figure 4.33.

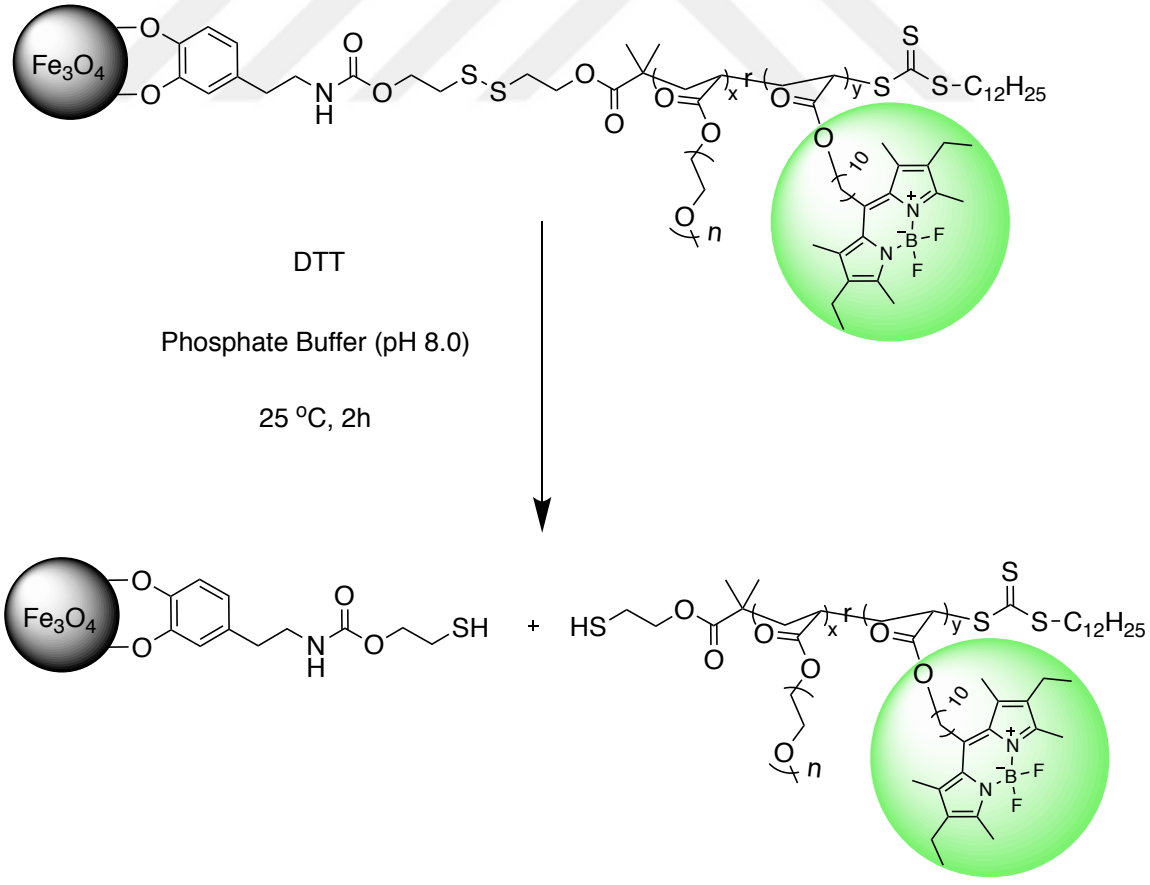

Figure 4.32. Cleavage of disulfide bond in copolymer-coated nanoparticles by DTT.



Figure 4.33 Dispersibility of Fe_3O_4@Dopa-SS-PEGMEA-r-BODIPY in water (left), after treatment with DTT and centrifugation.

4.10. Release Study of PEGMEA and BODIPY Copolymer Brushes from Fe_3O_4 Nanoparticles by Glutathione

First of all, release behavior of PEGMEA and BODIPY copolymer brushes were analyzed in the medium which had Glutathione in it. For this study, Fe_3O_4@Dopa-SS-PEGMEA-r-BODIPY and 10 mM glutathione solution were used. 10 mM glutathione solution was prepared in pH 7.4 phosphate buffer solution. In 50 kDa dialysis membrane, PEGMEA-r-BODIPY copolymer brushes started to cleave from the surface of Fe_3O_4 nanoparticles by glutathione so they started to get out of dialysis bag. Cumulative release was done by taking samples at different times from the outer solution. Copolymer brushes have BODIPY fluorescent dye in their structure and this dye has a characteristic signal at 525 nm, so released dye concentration was analyzed by UV-vis spectroscopy. As expected, absorbance of dye increased, so dye concentration increased by time (Figure 4.34) Unfortunately, the release of dye containing polymeric brushes were continued until it reached a plateau around 60 %. These release studies will need further optimization in the future to enable higher degree of release.

On the other hand, release behavior of PEGMEA and BODIPY copolymer brushes were analyzed without glutathione. So, the effect of glutathione on copolymer-coated

nanoparticles were analyzed. As expected, there was a little concentration of dye release because ester bonds in the compound can be hydrolyzed by the phosphate buffer solution.

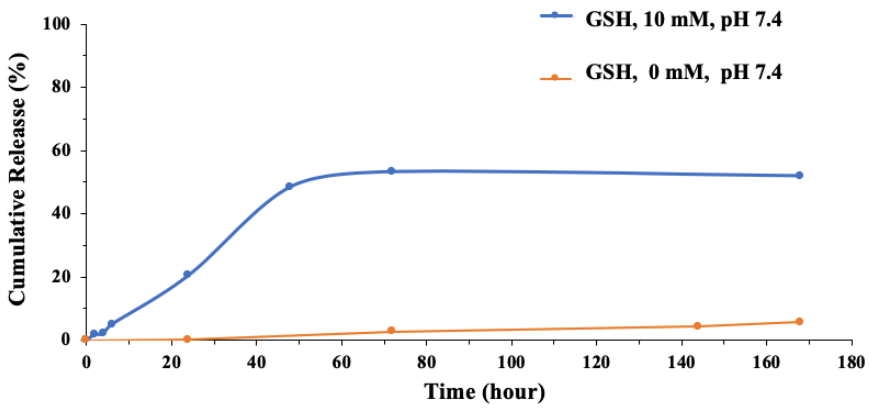

Figure 4.34. Release of Fe_3O_4-Dopa-SS-PEGMEA-r-BODIPY by glutathione.

4.11. Functionalization of Polymer-Coated Fe_3O_4 Nanoparticles by End Group Modifications

4.11.1. Synthesis of NHS Containing Carboxylic Acid Functionalized V-501 Azo Initiator (NHS-ACVA)

The aim of synthesizing this molecule is to modify the trithiocarbonate groups of the polymer brushes as NHS-activated carboxylic acid groups using radical exchange reaction. The NHS-activated carboxylic acid containing azo-initiator was synthesized according to literature report [63]. NHS-ACVA is the product of esterification reaction V-501 azo-initiator and NHS in the presence of EDCI and DMF (Figure 4.35). The reaction was carried out at room temperature and the yield of reaction was 76 %. NHS-ACVA molecule was precipitated in excess amount of water to get rid of impurities. The characterization of this compound was done with ^{1}H NMR and it was similar to spectrum of previously reported product.

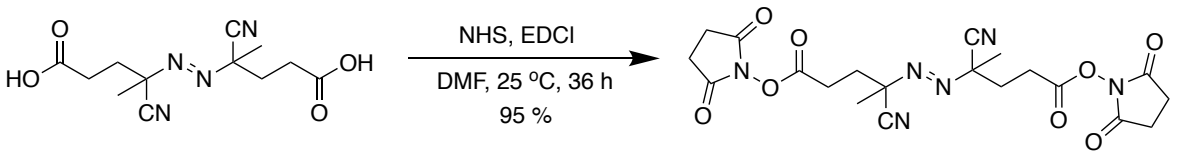

Figure 4.35. Synthesis of NHS-ACVA radical initiator.

4.11.2. End Group Modification of Polymer-Coated Fe_3O_4 Nanoparticles by NHS Activated Carboxylic Acid Containing Azo Initiator

The end groups of polymer-coated iron oxide nanoparticles were modified with NHS-activated carboxylic acid group. This modification provides the attachment of any biomolecules to the ends of polymer brushes. The radical exchange reaction took place between end group of polymer-coated nanoparticles and NHS-ACVA. For this purpose, Fe_3O_4@Dopa-SS-PEGMEA and excess amount of NHS-ACVA were dissolved in DMF. Then, the reaction mixture was stirred for 16 hours at 75 °C under a nitrogen blanket to remove oxygen (Figure 4.36). After the reaction, the mixture was dialyzed against acetonitrile to get rid of impurities.

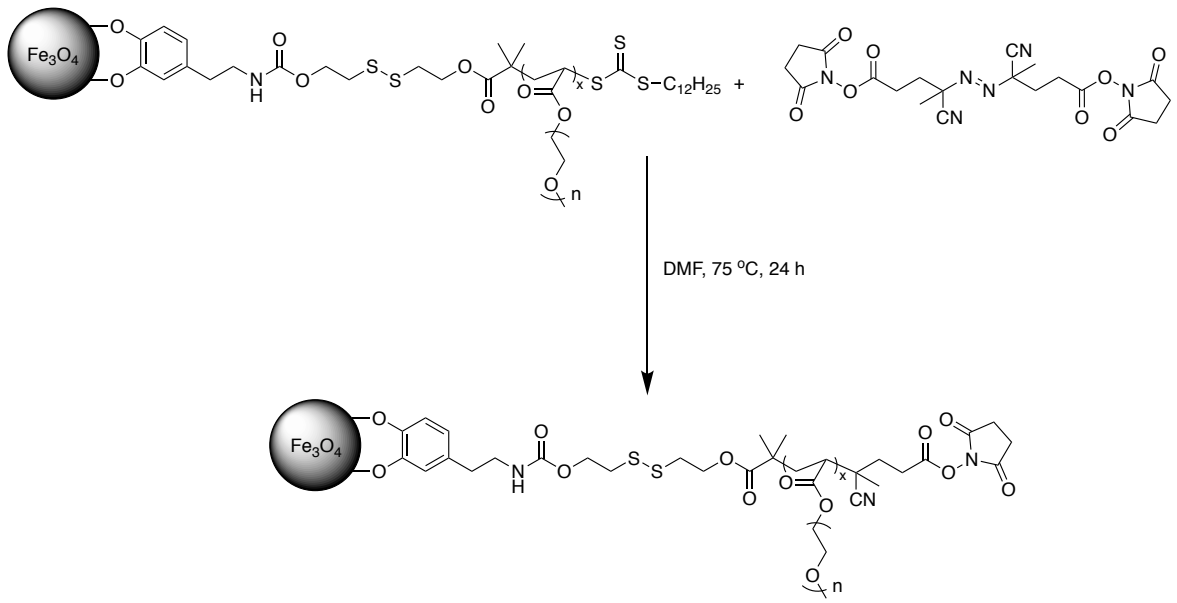

Figure 4.36. End group modification of polymer-coated iron oxide nanoparticles by NHS-activated carboxylic acid group.

Characterization of this transformation was carried out with FT-IR spectroscopy. The characteristic peaks at 1750 and 1778 cm^{-1} in FT-IR comes from the NHS group. In addition, from UV-Vis spectroscopy, the characteristic peak of trithiocarbonate group which is observed at 308 nm before post-polymerization modification, disappeared (Figure 4.37). This UV spectrum indicates that the end group modification of polymer coated iron oxide nanoparticles by radical exchange reaction was successful.

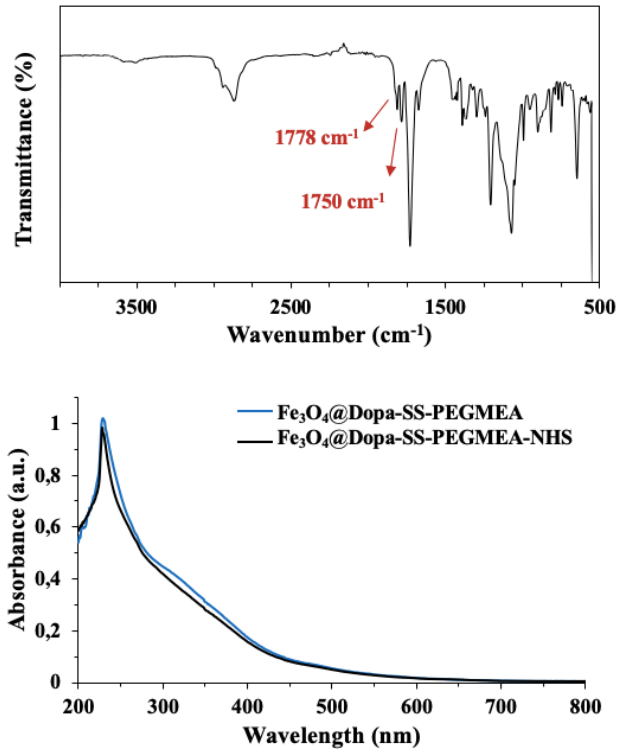

Figure 4.37. FT-IR spectrum (top) and UV-Vis spectra (bottom) of Fe_3O_4@Dopa-SS-PEGMEA-NHS nanoparticles.

5. CONCLUSION

In this project, iron oxide nanoparticles coated with polymeric brushes were synthesized by surface-initiated RAFT polymerization. A redox-responsive disulfide based cleavable linkage was integrated between the nanoparticle surface and the polymer brush. This allows for facile cleavage of polymer brushes which are 'grafted-from' the nanoparticle surface. Development of such a cleavable system has several advantages. Firstly, it solves the difficulties associated with determination of composition and molecular weight of the polymer brushes that was fabricated using the 'grafting-from' approach. As a control, in this thesis, polymer-coated iron oxide nanoparticle without the disulfide linkage were also synthesized.

Monodisperse iron oxide nanoparticles were synthesized by thermal decomposition method. A novel disulfide-containing RAFT polymerization CTA bearing a dopamine group was synthesized. Using place exchange reaction, the novel CTA was anchored onto the surface of the magnetic nanoparticles. Using RAFT polymerization and using the 'grafting-from' approach, PEGMEA based polymer brushes were grown from the nanoparticle surfaces. As synthesized polymer-coated nanoparticles possessed good water dispersibility. The surface tethered polymers were cleaved in the presence of reducing agents such as glutathione and DTT. This enable facile analysis of the molecular weights and PDI values of the polymeric brushes.

To understand the cleavage kinetics of the polymer brushes from the nanoparticle surface, a fluorescent dye based monomer was synthesized. BODIPY was chosen as a model dye due to its high fluorescence and an acrylate based monomer was synthesized. Furthermore, since BODIPY is a very hydrophobic molecule, it also acts as a model of a hydrophobic drug, and thus demonstrates solubilization of a drug can be achieved using this water dispersible magnetic nanoparticle. While the dye-conjugated polymers did not cleave from the surface, exposure to redox-environment led to their cleavage as deduced from UV-vis spectrophotometry. Finally, to demonstrate that the end groups of these brushes can be modified with a reactive group, an NHS-containing activated ester bearing azo initiator was synthesized and end group modification of grafted copolymers was achieved through radical exchange reaction.

REFERENCES

1. Gavard, J., Hanini, Schmitt, Kacem, Chau, Ammar, and J. Gavard, "Evaluation Of Iron Oxide Nanoparticle Biocompatibility", *International Journal of Nanomedicine*, pp. 787, 2011.

2. Mahmoudi, M., M.A. Sahraian, M.A. Shokrgozar, and S. Laurent, "Superparamagnetic Iron Oxide Nanoparticles: Promises For Diagnosis And Treatment Of Multiple Sclerosis", *ACS Chemical Neuroscience*, Vol. 2, pp. 118–140, 2011.

3. Park, J., K. An, Y. Hwang, J.E.G. Park, H.J. Noh, J.Y. Kim, J.H. Park, N.M. Hwang, and T. Hyeon, "Ultra-Large-Scale Syntheses Of Monodisperse Nanocrystals", *Nature Materials*, Vol. 3, pp. 891–895, 2004.

4. Laurent, S., D. Forge, M. Port, A. Roch, C. Robic, L. Vander Elst, and R.N. Muller, "Magnetic Iron Oxide Nanoparticles: Synthesis, Stabilization, Vectorization, Physicochemical Characterizations, And Biological Applications", *Chemical Reviews*, Vol. 108, pp. 2064–2110, 2008.

5. Quan, Q., J. Xie, H. Gao, M. Yang, F. Zhang, G. Liu, X. Lin, A. Wang, H.S. Eden, S. Lee, G. Zhang, and X. Chen, "HSA Coated Iron Oxide Nanoparticles As Drug Delivery Vehicles For Cancer Therapy", *Molecular Pharmaceutics*, Vol. 8, pp. 1669–1676, 2011.

6. Thomas, G., J. Boudon, L. Maurizi, M. Moreau, P. Walker, I. Severin, A. Oudot, C. Goze, S. Poty, J.M. Vrigneaud, F. Demoisson, F. Denat, F. Brunotte, and N. Millot, "Innovative Magnetic Nanoparticles For PET/MRI Bimodal Imaging", *ACS Omega*, Vol. 4, pp. 2637–2648, 2019.

7. Oz, Y., Y. Abdouni, G. Yilmaz, C.R. Becer, and A. Sanyal, "Magnetic Glyconanoparticles For Selective Lectin Separation And Purification", *Polymer Chemistry*, Vol. 10, pp. 3351–3361, 2019.

8. Albarqi, H.A., L.H. Wong, C. Schumann, F.Y. Sabei, T. Korzun, X. Li, M.N. Hansen, P. Dhagat, A.S. Moses, Olena Taratula, and Oleh Taratula, "Biocompatible Nanoclusters With High Heating Efficiency For Systemically Delivered Magnetic Hyperthermia", *ACS*

Nano, Vol. 13, pp. 6383–6395, 2019.

9. Qiao, R., L. Esser, C. Fu, C. Zhang, J. Hu, P. Ramírez-Arcía, Y. Li, J.F. Quinn, M.R. Whittaker, A.K. Whittaker, and T.P. Davis, "Bioconjugation And Fluorescence Labeling Of Iron Oxide Nanoparticles Grafted With Bromomaleimide-Terminal Polymers", *Biomacromolecules*, Vol. 19, pp. 4423–4429, 2018.

10. Mohammadi Ziarani, G., M. Malmir, N. Lashgari, and A. Badiei, "The Role Of Hollow Magnetic Nanoparticles In Drug Delivery", *RSC Advances*, Vol. 9, pp. 25094–25106, 2019.

11. Akbarzadeh, A., S. Mohamad, and D. Soodabeh, "Magnetic Nanoparticles: Preparation, Physical Properties, And Applications In Biomedicine", *Nanoscale Research Letters*, Vol. 7, pp. 1–14, 2012.

12. Wu, W., C.Z. Jiang, and V.A.L. Roy, "Designed Synthesis And Surface Engineering Strategies Of Magnetic Iron Oxide Nanoparticles For Biomedical Applications", *Nanoscale*, Vol. 8, pp. 19421–19474, 2016.

13. Dar, M.I., and S.A. Shivashankar, "Single Crystalline Magnetite, Maghemite, And Hematite Nanoparticles With Rich Coercivity", *RSC Advances*, Vol. 4, pp. 4105–4113, 2014.

14. Mohammed, L., H.G. Gomaa, D. Ragab, and J. Zhu, "Magnetic Nanoparticles For Environmental And Biomedical Applications: A Review", *Particuology*, Vol. 30, pp. 1–14, 2017.

15. Kalubowilage, M., K. Janik, and S.H. Bossmann, "Magnetic Nanomaterials For Magnetically-Aided Drug Delivery And Hyperthermia", *Applied Sciences*, Vol. 9, pp. 2927, 2019.

16. Basuki, J.S., A. Jacquemin, L. Esser, Y. Li, C. Boyer, and T.P. Davis, "A Block Copolymer-Stabilized Co-Precipitation Approach To Magnetic Iron Oxide Nanoparticles For Potential Use As MRI Contrast Agents", *Polymer Chemistry*, Vol. 5, pp. 2611–2620, 2014.

17. Herranz, F., B. Salinas, H. Groult, J. Pellico, A. V. Lechuga-Vieco, R. Bhavesh, and J. Ruiz-Cabello, "Superparamagnetic Nanoparticles For Atherosclerosis Imaging",

Nanomaterials, Vol. 4, pp. 408–438, 2014.

18. Dai, Z., F. Meiser, and H. Möhwald, "Nanoengineering Of Iron Oxide And Iron Oxide/Silica Hollow Spheres By Sequential Layering Combined With A Sol–Gel Process", *Journal of Colloid and Interface Science*, Vol. 288, pp. 298–300, 2005.

19. Jensen, K.M.Ø., H.L. Andersen, C. Tyrsted, E.D. Bøjesen, A.-C. Dippel, N. Lock, S.J.L. Billinge, B.B. Iversen, and M. Christensen, "Mechanisms For Iron Oxide Formation Under Hydrothermal Conditions: An In Situ Total Scattering Study", *ACS Nano*, Vol. 8, pp. 10704–10714, 2014.

20. Kurzhals, S., R. Zirbs, and E. Reimhult, "Synthesis And Magneto-Thermal Actuation Of Iron Oxide Core-PNIPAM Shell Nanoparticles", *ACS Applied Materials and Interfaces*, Vol. 7, pp. 19342–19352, 2015.

21. Lee, S.-J., J.-R. Jeong, S.-C. Shin, J.-C. Kim, and J.-D. Kim, "Synthesis And Characterization Of Superparamagnetic Maghemite Nanoparticles Prepared By Coprecipitation Technique", *Journal of Magnetism and Magnetic Materials*, Vol. 282, pp. 147–150, 2004.

22. Karaagac, O., H. Kockar, S. Beyaz, and T. Tanrisever, "A Simple Way To Synthesize Superparamagnetic Iron Oxide Nanoparticles In Air Atmosphere: Iron Ion Concentration Effect", *IEEE Transactions on Magnetics*, Vol. 46, pp. 3978–3983, 2010.

23. Chin, A.B., and I.I. Yaacob, "Synthesis And Characterization Of Magnetic Iron Oxide Nanoparticles Via W/O Microemulsion And Massart's Procedure", *Journal of Materials Processing Technology*, Vol. 191, pp. 235–237, 2007.

24. Cui, H., and W. Ren, "Low Temperature And Size Controlled Synthesis Of Monodispersed γ-Fe2O3 Nanoparticles By An Epoxide Assisted Sol-Gel Route", *Journal of Sol-Gel Science and Technology*, Vol. 47, pp. 81–84, 2008.

25. Wang, J., J. Sun, Q. Sun, and Q. Chen, "One-Step Hydrothermal Process To Prepare Highly Crystalline Fe3O4 Nanoparticles With Improved Magnetic Properties", *Materials Research Bulletin*, Vol. 38, pp. 1113–1118, 2003.

26. Mao, B., Z. Kang, E. Wang, S. Lian, L. Gao, C. Tian, and C. Wang, "Synthesis Of Magnetite Octahedrons From Iron Powders Through A Mild Hydrothermal Method",

Materials Research Bulletin, Vol. 41, pp. 2226–2231, 2006.

27. Sun, S., and H. Zeng, "Size-Controlled Synthesis Of Magnetite Nanoparticles", *Journal of the American Chemical Society*, Vol. 124, pp. 8204–8205, 2002.

28. Lassenberger, A., T.A. Grünewald, P.D.J. Van Oostrum, H. Rennhofer, H. Amenitsch, R. Zirbs, H.C. Lichtenegger, and E. Reimhult, "Monodisperse Iron Oxide Nanoparticles By Thermal Decomposition: Elucidating Particle Formation By Second-Resolved In Situ Small-Angle X-Ray Scattering", *Chemistry of Materials*, Vol. 29, pp. 4511–4522, 2017.

29. Park, J., K. An, Y. Hwang, J.-G. Park, H.-J. Noh, J.-Y. Kim, J.-H. Park, N.-M. Hwang, and T. Hyeon, "Ultra-Large-Scale Syntheses Of Monodisperse Nanocrystals", *Nature Materials*, Vol. 3, pp. 891–895, 2004.

30. Guardia, P., J. Pérez-Juste, A. Labarta, X. Batlle, and L.M. Liz-Marzán, "Heating Rate Influence On The Synthesis Of Iron Oxide Nanoparticles: The Case Of Decanoic Acid", *Chemical Communications*, Vol. 46, pp. 6108–6110, 2010.

31. Jun, Y.W., Y.M. Huh, J.S. Choi, J.H. Lee, H.T. Song, S. Kim, S. Yoon, K.S. Kim, J.S. Shin, J.S. Suh, and J. Cheon, "Nanoscale Size Effect Of Magnetic Nanocrystals And Their Utilization For Cancer Diagnosis Via Magnetic Resonance Imaging", *Journal of the American Chemical Society*, Vol. 127, pp. 5732–5733, 2005.

32. Lu, C., L.R. Bhatt, H.Y. Jun, S.H. Park, and K.Y. Chai, "Carboxyl-Polyethylene Glycol-Phosphoric Acid: A Ligand For Highly Stabilized Iron Oxide Nanoparticles", *Journal of Materials Chemistry*, Vol. 22, pp. 19806–19811, 2012.

33. Larsen, E.K.U., T. Nielsen, T. Wittenborn, H. Birkedal, T. Vorup-Jensen, M.H. Jakobsen, L. Østergaard, M.R. Horsman, F. Besenbacher, K.A. Howard, and J. Kjems, "Size-Dependent Accumulation Of PEGylated Silane-Coated Magnetic Iron Oxide Nanoparticles In Murine Tumors", *ACS Nano*, Vol. 3, pp. 1947–1951, 2009.

34. Xu, C., K. Xu, H. Gu, R. Zheng, H. Liu, X. Zhang, Z. Guo, and B. Xu, "Dopamine As A Robust Anchor To Immobilize Functional Molecules On The Iron Oxide Shell Of Magnetic Nanoparticles", *Journal of the American Chemical Society*, Vol. 126, pp. 9938–9939, 2004.

35. Quan, W.Y., Z. Hu, H.Z. Liu, Q.Q. Ouyang, D.Y. Zhang, S.D. Li, P.W. Li, and Z.M. Yang, "Mussel-Inspired Catechol-Functionalized Hydrogels And Their Medical Applications", *Molecules*, Vol. 24, pp. 1–27, 2019.

36. Shultz, M.D., J. Ulises Reveles, S.N. Khanna, and E.E. Carpenter, "Reactive Nature Of Dopamine As A Surface Functionalization Agent In Iron Oxide Nanoparticles", *Journal of the American Chemical Society*, Vol. 129, pp. 2482–2487, 2007.

37. Rajh, T., M.C. Thurnauer, P. Thiyagarajan, and D.M. Tiede, "Structural Characterization Of Self-Organized TiO 2 Nanoclusters Studied By Small Angle Neutron Scattering", *The Journal of Physical Chemistry B*, Vol. 103, pp. 2172–2177, 1999.

38. Velusamy, P., S. Chia-Hung, A. Shritama, G.V. Kumar, V. Jeyanthi, and K. Pandian, "Synthesis Of Oleic Acid Coated Iron Oxide Nanoparticles And Its Role In Anti-Biofilm Activity Against Clinical Isolates Of Bacterial Pathogens", *Journal of the Taiwan Institute of Chemical Engineers*, Vol. 59, pp. 450–456, 2016.

39. Hofmann, A., S. Thierbach, A. Semisch, A. Hartwig, M. Taupitz, E. Rühl, and C. Graf, "Highly Monodisperse Water-Dispersable Iron Oxide Nanoparticles For Biomedical Applications", *Journal of Materials Chemistry*, Vol. 20, pp. 7842–7853, 2010.

40. Jain, T.K., J. Richey, M. Strand, D.L. Leslie-Pelecky, C.A. Flask, and V. Labhasetwar, "Magnetic Nanoparticles With Dual Functional Properties: Drug Delivery And Magnetic Resonance Imaging", *Biomaterials*, Vol. 29, pp. 4012–4021, 2008.

41. Naha, P.C., Y. Liu, G. Hwang, Y. Huang, S. Gubara, V. Jonnakuti, A. Simon-Soro, D. Kim, L. Gao, H. Koo, and D.P. Cormode, "Dextran-Coated Iron Oxide Nanoparticles As Biomimetic Catalysts For Localized And PH-Activated Biofilm Disruption", *ACS Nano*, Vol. 13, pp. 4960–4971, 2019.

42. Chang, P.R., J. Yu, X. Ma, and D.P. Anderson, "Polysaccharides As Stabilizers For The Synthesis Of Magnetic Nanoparticles", *Carbohydrate Polymers*, Vol. 83, pp. 640–644, 2011.

43. Gaihre, B., M.S. Khil, D.R. Lee, and H.Y. Kim, "Gelatin-Coated Magnetic Iron Oxide Nanoparticles As Carrier System: Drug Loading And In Vitro Drug Release Study", *International Journal of Pharmaceutics*, Vol. 365, pp. 180–189, 2009.

44. Tyukova, I.S., A.P. Safronov, A.P. Kotel'Nikova, and D.Y. Agalakova, "Electrostatic And Steric Mechanisms Of Iron Oxide Nanoparticle Sol Stabilization By Chitosan", *Polymer Science - Series A*, Vol. 56, pp. 498–504, 2014.

45. Khandhar, A.P., P. Keselman, S.J. Kemp, R.M. Ferguson, P.W. Goodwill, S.M. Conolly, and K.M. Krishnan, "Evaluation Of PEG-Coated Iron Oxide Nanoparticles As Blood Pool Tracers For Preclinical Magnetic Particle Imaging", *Nanoscale*, Vol. 9, pp. 1299–1306, 2017.

46. Arsianti, M., M. Lim, C.P. Marquis, and R. Amal, "Assembly Of Polyethylenimine-Based Magnetic Iron Oxide Vectors: Insights Into Gene Delivery", *Langmuir*, Vol. 26, pp. 7314–7326, 2010.

47. Walker, M., I. Will, A. Pratt, V. Chechik, P. Genever, and D. Ungar, "Magnetically Triggered Release Of Entrapped Bioactive Proteins From Thermally Responsive Polymer-Coated Iron Oxide Nanoparticles For Stem-Cell Proliferation", *ACS Applied Nano Materials*, Vol. 3, pp. 5008–5013, 2020.

48. Matsumura, S., A.R. Hlil, C. Lepiller, J. Gaudet, D. Guay, Z. Shi, S. Holdcroft, and A.S. Hay, "Stability And Utility Of Pyridyl Disulfide Functionality In RAFT And Conventional Radical Polymerizations", *Journal of Polymer Science: Part A: Polymer Chemistry*, Vol. 46, pp. 7207–7224, 2008.

49. Padwal, P., R. Bandyopadhyaya, and S. Mehra, "Polyacrylic Acid-Coated Iron Oxide Nanoparticles For Targeting Drug Resistance In Mycobacteria", *Langmuir*, Vol. 30, pp. 15266–15276, 2014.

50. Nosrati, H., M. Salehiabar, M. Fridoni, M.A. Abdollahifar, H. Kheiri Manjili, S. Davaran, and H. Danafar, "New Insight About Biocompatibility And Biodegradability Of Iron Oxide Magnetic Nanoparticles: Stereological And In Vivo MRI Monitor", *Scientific Reports*, Vol. 9, pp. 1–10, 2019.

51. Arslan, M., T.N. Gevrek, J. Lyskawa, S. Szunerits, R. Boukherroub, R. Sanyal, P. Woisel, and A. Sanyal, "Bioinspired Anchorable Thiol-Reactive Polymers: Synthesis And Applications Toward Surface Functionalization Of Magnetic Nanoparticles", *Macromolecules*, Vol. 47, pp. 5124–5134, 2014.

52. Oz, Y., M. Arslan, T.N. Gevrek, R. Sanyal, and A. Sanyal, "Modular Fabrication Of

Polymer Brush Coated Magnetic Nanoparticles: Engineering The Interface For Targeted Cellular Imaging", *ACS Applied Materials & Interfaces*, Vol. 8, pp. 19813–19826, 2016.

53. Perrier, S., "50th Anniversary Perspective: RAFT Polymerization - A User Guide", *Macromolecules*, Vol. 50, pp. 7433–7447, 2017.

54. Moad, G., "RAFT Polymerization To Form Stimuli-Responsive Polymers", *Polymer Chemistry*, Vol. 8, pp. 177–219, 2017.

55. Willcock, H., and R.K. O'Reilly, "End Group Removal And Modification Of RAFT Polymers", *Polymer Chemistry*, Vol. 1, pp. 149–157, 2010.

56. Moad, G., E. Rizzardo, and S.H. Thang, "Radical Addition-Fragmentation Chemistry In Polymer Synthesis", *Polymer*, Vol. 49, pp. 1079–1131, 2008.

57. Bulmus, V., "RAFT Polymerization Mediated Bioconjugation Strategies", *Polymer Chemistry*, Vol. 2, pp. 1463–1472, 2011.

58. Scales, S.J., S.P. Tsai, N. Zacharias, J. Dela Cruz-Chuh, G. Bullen, E. Velasquez, J. Chang, E. Bruguera, K.R. Kozak, and J. Sadowsky, "Development Of A Cysteine-Conjugatable Disulfide FRET Probe: Influence Of Charge On Linker Cleavage And Payload Trafficking For An Anti-HER2 Antibody Conjugate", *Bioconjugate Chemistry*, Vol. 30, pp. 3046–3056, 2019.

59. Cui, Y., H. Dong, X. Cai, D. Wang, and Y. Li, "Mesoporous Silica Nanoparticles Capped With Disulfide-Linked PEG Gatekeepers For Glutathione-Mediated Controlled Release", *ACS Applied Materials and Interfaces*, Vol. 4, pp. 3177–3183, 2012.

60. Gamcsik, M.P., M.S. Kasibhatla, S.D. Teeter, and O.M. Colvin, "Glutathione Levels In Human Tumors", *Biomarkers*, Vol. 17, pp. 671–691, 2012.

61. Rezaee Shirin-Abadi, A., and M. Zafarghandi, "Preparation Of Microencapsulated Phase Change Materials (MPCMs) By Using RAFT Synthesized Well-Defined Surfactants", *Polymer*, Vol. 190, pp. 122215, 2020.

62. Amat-Guerri, F., M. Liras, M. Luisa Carrascoso, and R. Sastre, "Methacrylate-Tethered Analogs Of The Laser Dye PM567—Synthesis, Copolymerization With Methyl Methacrylate And Photostability Of The Copolymers", *Photochemistry and*

Photobiology, Vol. 77, pp. 577, 2003.

63. Wang, H., Z. Chen, L. Xin, J. Cui, S. Zhao, and Y. Yan, “Synthesis Of Pyrene-Capped Polystyrene By Free Radical Polymerization And Its Application In Direct Exfoliation Of Graphite Into Graphene Nanosheets”, *Journal of Polymer Science Part A: Polymer Chemistry*, Vol. 53, pp. 2175–2185, 2015.

APPENDIX A: COPYRIGHT NOTICES

Copyrights that belong to figures and chapters which were taken from literature articles can be found here.

RE: Permission Request Form: Nora
1 mesaj

CONTRACTS-COPYRIGHT (shared) <Contracts-Copyright@rsc.org> 19 Ağustos 2020 11:07
Alıcı: "noraejderyan@gmail.com" <noraejderyan@gmail.com>

Many thanks for sending the permissions request below. The Royal Society of Chemistry hereby grants permission for the use of the material specified below in your thesis.

Please note that if the material specified below or any part of it appears with credit or acknowledgement to a third party then you must also secure permission from that third party before reproducing that material.

Please ensure that the published article carries a credit to The Royal Society of Chemistry in the following format:

[Original citation] – Reproduced by permission of The Royal Society of Chemistry

and that any electronic version of the work includes a hyperlink to the article on the Royal Society of Chemistry website.

Best wishes,

Chloe Szebrat
Contracts and Copyright Executive
Royal Society of Chemistry
Thomas Graham House
Science Park, Milton Road
Cambridge, CB4 0WF, UK

www.rsc.org

From: noraejderyan@gmail.com <noraejderyan@gmail.com>
Sent: 19 August 2020 09:02
To: CONTRACTS-COPYRIGHT (shared) <Contracts-Copyright@rsc.org>
Subject: Permission Request Form: Nora

Name: Nora

Institution: Boğaziçi University

Email: noraejderyan@gmail.com

Address:

Bogazici University Kuzey Kampus Sarıyer

Istanbul
34342
Turkey

I am preparing the following work for publication:

Article/chapter title: Fabrication of Degradable Polymer Coated Nanoparticles
Journal/book title: Thesis
Editor/author(s): Nora Ejderyan
Publisher: Amitav Sanyal
Is this request for a thesis?: Yes

I would very much appreciate your permission to use the following material:

Journal/book title: Designed synthesis and surface engineering strategies of magnetic iron oxide nanoparticles for biomedical applications
Editor/author(s): Wei Wu, Chang Zhong Jiang and Vellaisamy A. L. Roy
ISBN/DOI: 10.1039/c6nr07542h
Year of publication: 2016
Page(s): 19421-19474
Type of material: Figure
Figure/image number (if relevant): 1

Any additional comments:

Agree to terms: I agree

Figure A.1. Copyright license of [12].

RightsLink Printable License 19.08.2020 11:28

ELSEVIER LICENSE
TERMS AND CONDITIONS

Aug 19, 2020

This Agreement between Nora Ejderyan ("You") and Elsevier ("Elsevier") consists of your license details and the terms and conditions provided by Elsevier and Copyright Clearance Center.

License Number	4891360977945
License date	Aug 17, 2020
Licensed Content Publisher	Elsevier
Licensed Content Publication	Particuology
Licensed Content Title	Magnetic nanoparticles for environmental and biomedical applications: A review
Licensed Content Author	Leena Mohammed,Hassan G. Gomaa,Doaa Ragab,Jesse Zhu
Licensed Content Date	Feb 1, 2017
Licensed Content Volume	30
Licensed Content Issue	n/a
Licensed Content Pages	14
Start Page	1

Figure A.2. Copyright license of [14].

Open Access Review

Magnetic Nanomaterials for Magnetically-Aided Drug Delivery and Hyperthermia

by Madumali Kalubowilage, Katharine Janik and Stefan H. Bossmann *

Department of Chemistry, Kansas State University, 201 CBC Building, Manhattan, KS 66506-0401, USA

* Author to whom correspondence should be addressed.

Appl. Sci. **2019**, *9*(14), 2927; https://doi.org/10.3390/app9142927

Received: 31 May 2019 / Revised: 2 July 2019 / Accepted: 11 July 2019 / Published: 22 July 2019

(This article belongs to the Special Issue Magnetic Nanomaterials for Drug Delivery and Therapy)

Permissions

No special permission is required to reuse all or part of article published by MDPI, including figures and tables. For articles published under an open access Creative Common CC BY license, any part of the article may be reused without permission provided that the original article is clearly cited. Reuse of an article does not imply endorsement by the authors or MDPI.

Figure A.3. Copyright license of [15].

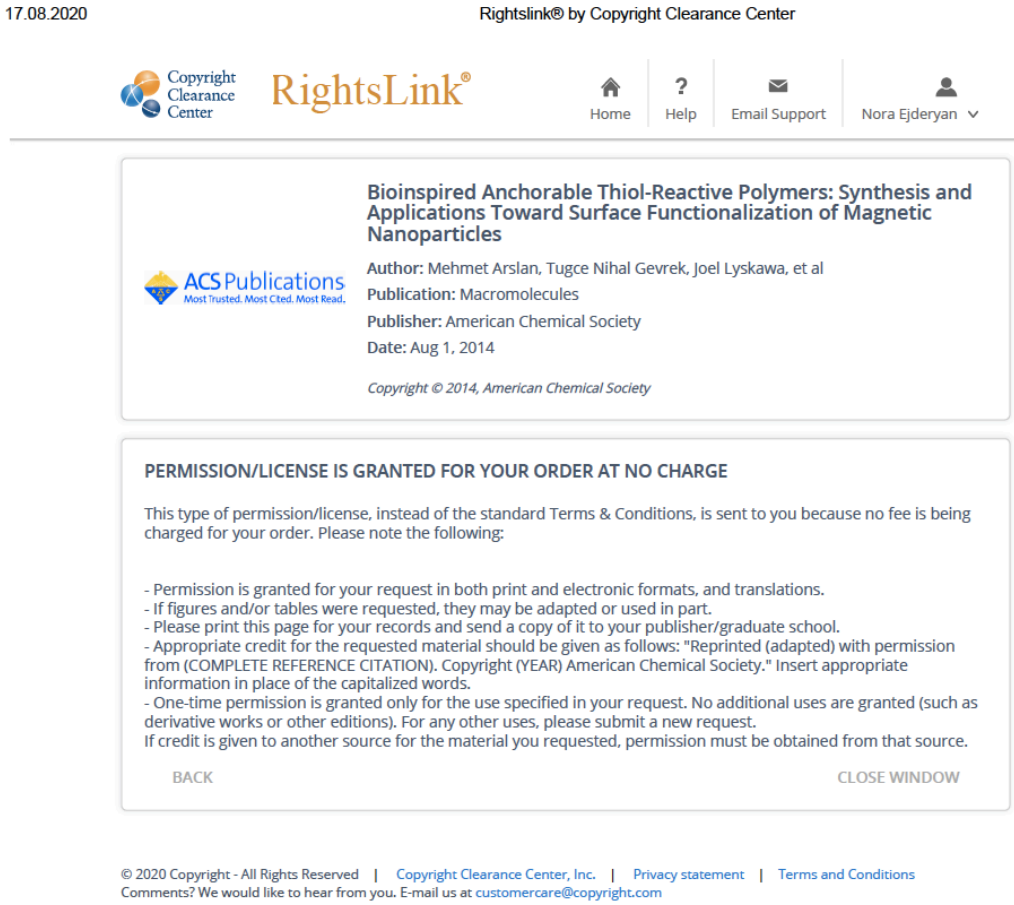

Figure A.4. Copyright license of [51].



Figure A.5. Copyright license of [52].

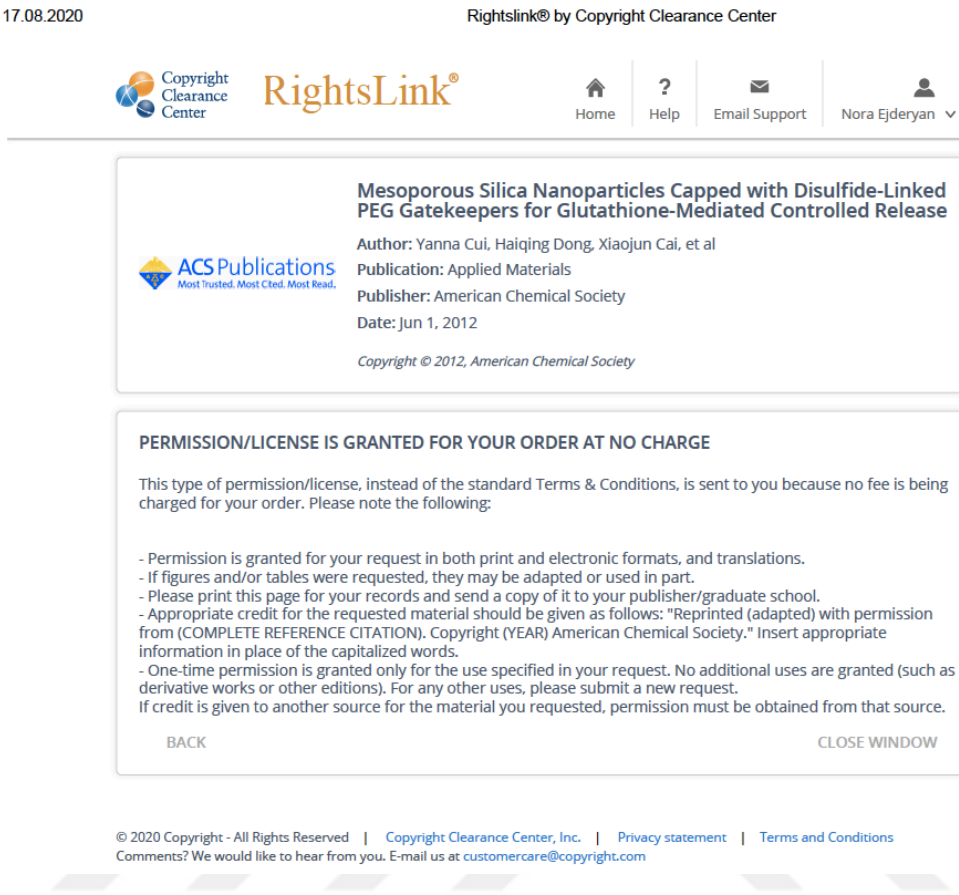

Figure A.6. Copyright license of [59].